AD_____

Award Number: DAMD17-03-1-0179

TITLE: 2-Methoxyestradiol as a Chemotherapeutic for Prostate Cancer

PRINCIPAL INVESTIGATOR: Carlos Perez-Stable, Ph.D.

CONTRACTING ORGANIZATION: University of Miami
Miami, FL 33101

REPORT DATE: April 2006

TYPE OF REPORT: Annual

PREPARED FOR: U.S. Army Medical Research and Materiel Command
Fort Detrick, Maryland 21702-5012

REPORT DOCUMENTATION PAGE

Form Approved
OMB No. 0704-0188

1. REPORT DATE *(DD-MM-YYYY)*	**2. REPORT TYPE**	**3. DATES COVERED** *(From - To)*
01-04-2006	Annual	1 APR 2005 - 31 MAR 2006

4. TITLE AND SUBTITLE
2-Methoxyestradiol as a Chemotherapeutic for Prostate Cancer

5a. CONTRACT NUMBER

5b. GRANT NUMBER
DAMD17-03-1-0179

5c. PROGRAM ELEMENT NUMBER

6. AUTHOR(S)
Carlos Perez-Stable, Ph.D.

E-mail: cperez@med.miami.edu

5d. PROJECT NUMBER

5e. TASK NUMBER

5f. WORK UNIT NUMBER

7. PERFORMING ORGANIZATION NAME(S) AND ADDRESS(ES)

University of Miami
Miami, FL 33101

8. PERFORMING ORGANIZATION REPORT NUMBER

9. SPONSORING / MONITORING AGENCY NAME(S) AND ADDRESS(ES)
U.S. Army Medical Research and Materiel Command
Fort Detrick, Maryland 21702-5012

10. SPONSOR/MONITOR'S ACRONYM(S)

11. SPONSOR/MONITOR'S REPORT NUMBER(S)

12. DISTRIBUTION / AVAILABILITY STATEMENT
Approved for Public Release; Distribution Unlimited

13. SUPPLEMENTARY NOTES
Original contains color plates: All DTIC reproductions will be in black and white.

14. ABSTRACT

2-Methoxyestradiol (2-ME) is an endogenous metabolite of estradiol with promise for cancer chemotherapy, including advanced prostate cancer. Our hypothesis is one of the cancer-specific mechanisms whereby 2-ME exerts its anti-prostate cancer activity is the deregulated activation of cyclin B1/cdk1 kinase during the cell cycle, which results in the induction of apoptotic cell death. Several experimental results support this hypothesis: 1) there is a positive correlation between the levels of cyclin B1 protein and the ability of 2-ME to increase G2/M cell cycle arrest and apoptosis in prostate cancer cells; 2) inhibition of cdk1 activity lowers 2-ME-mediated apoptosis while overexpression of cyclin B1 increases 2-ME-mediated apoptosis; 3) low doses of 2-ME and docetaxel can increase G2/M cell cycle arrest and apoptosis in prostate cancer cell lines and in the Gγ/T transgenic mouse model of prostate cancer greater than either drug alone. We conclude that 2-ME can increase apoptosis in prostate cancer cells because of the expression of cyclin B1 protein, which is minimally expressed in normal cells.

15. SUBJECT TERMS
Estrogen metabolite; mitotic cell cycle arrest; apoptosis

16. SECURITY CLASSIFICATION OF:			**17. LIMITATION OF ABSTRACT**	**18. NUMBER OF PAGES**	**19a. NAME OF RESPONSIBLE PERSON**
					USAMRMC
a. REPORT	**b. ABSTRACT**	**c. THIS PAGE**			**19b. TELEPHONE NUMBER** *(include area code)*
U	U	U	UU	58	

Table of Contents

INTRODUCTION

One of the more promising emerging chemotherapeutic agents is 2-methoxyestradiol (2-ME), an endogenous metabolite of estradiol [1-3]. 2-ME can inhibit the growth of a variety of cancer cells, including advanced androgen-independent prostate cancer (AI-PC) [4,5] utilizing a remarkable number of diverse mechanisms that include mitotic cell cycle arrest and induction of apoptosis [1-3]. 2-ME=s anti-prostate cancer activity, however, is poorly understood. A better understanding of the mechanisms of 2-ME=s anti-prostate cancer effects will be helpful to better evaluate its clinical potential in managing AI-PC. 2-ME may be an example of a chemotherapeutic agent that takes advantage of the molecular and biochemical differences between cancer and normal cells. One such difference may be the requirement for cell cycle proteins like cyclins and cyclin-dependent kinases. Our hypothesis is that one of the cancer-specific mechanisms whereby 2-ME exerts its anti-prostate cancer activity is the deregulated activation of cyclin B1/cdc2 kinase during the cell cycle, which results in the induction of apoptotic cell death. The purpose and scope of this research proposal is to (1) determine the molecular mechanisms of the 2-ME-mediated G2/M cell cycle arrest in prostate cancer cell lines; (2) determine whether activation of cyclin B1/cdc2 kinase by 2-ME is required for induction of apoptosis in prostate cancer and non-transformed normal cells; and (3) identify synergisms and mechanisms of interaction between 2-ME and other clinically relevant chemotherapeutic drugs. In this annual report, we present our accomplishments in the third year of the proposal.

BODY

To better understand 2-ME=s anti-prostate cancer action, we have focused on events related to mitotic cell cycle arrest (G2/M) and induction of apoptosis in LNCaP, DU 145, and PC-3 human prostate cancer cell lines. A manuscript entitled A2-Methoxyestradiol and paclitaxel have similar effects on the cell cycle and induction of apoptosis in prostate cancer cells@ published in *Cancer Letters* summarizes some of our results and is included in the appendix [6]. Blocking the 2-ME and paclitaxel increase in cyclin B1/cdk activity with the potent cdk inhibitors purvalanol A and alsterpaullone resulted in decreased apoptosis. These results suggest that 2-ME and paclitaxel-mediated increase in cyclin B1-dependent kinase activity is required for induction of apoptosis in prostate cancer cells.

The following sections report our findings from May 2005 to the present associated with each task in the approved statement of work.

Specific Aim 1: Determine the molecular mechanisms of the 2-ME/2-EE-mediated G2/M cell cycle arrest in prostate cancer cell lines (months 1-30).

1. Determine the effect of 2-ME/2-EE on the cdc2 phosphorylation status of thr-14 and thr-161positions in the human prostate cancer cell lines LNCaP, DU 145, and PC-3 using quantitative Western blot (months 1-4).

Completed and presented in the 2004 annual report.

2. Identify quantitative differences in the total levels of cdc25C, myt1, wee1, and CAK proteins in 2-ME/2-EE treated prostate cancer cell lines using quantitative Western blot (months 1-4).

Completed and presented in the 2004 annual report.

3. Determine the effect of the novel anti-cancer cdc25C inhibitor MX7174 and the wee1 inhibitorPD0166285 on 2-ME/2-EE-mediated G2/M cell cycle arrest in prostate cancer cell lines using quantitative Western blot and flow cytometry (months 2-6).

We have not pursued this task because we have focused on other mechanisms.

4. Determine the effect of 2-ME/2-EE on the subcellular localization of cyclin B1 and the other regulators of cdc2 kinase using Western blot and immunocytochemistry (months 2-6).

We presented data for this task in the 2005 annual report.

5. Develop and characterize stable LNCaP, DU 145, and PC-3 Tet-Off inducible cell lines containing the dn-cdc2, cdc2-AF, and cyclin B1-AS genes regulated by the addition (off) or removal (on) of dox in the media (months 4-24).

We cloned the dominant negative (dn)-cdk1 cDNA into the pTRE-Tight vector from Clontech and have co-transfected this plasmid with the pTK-Hyg hygromycin selection plasmid into the LNCaP-Tet-Off cell line (from Kerry Burnstein). Unfortunately, we have been unable to obtain a satisfactory clone that can induce the expression of dn-cdk1. Instead, we isolated stable LN-AI (androgen-independent variant of LNCaP; ref. 7) overexpressing dn-cdk1 (**Fig. 1A**) and tested whether there is an effect on 2-ME-mediated apoptosis. The results show that there is less cleaved PARP (correlates with less apoptosis) in dn-cdk1 clones 8 and 13 compared to negative control clone when treated with 2 μM 2-ME for 72 hours (**Fig. 1B**). This result suggests that inhibition of cdk1 activity lowers 2-ME-mediated apoptosis and supports the hypothesis.

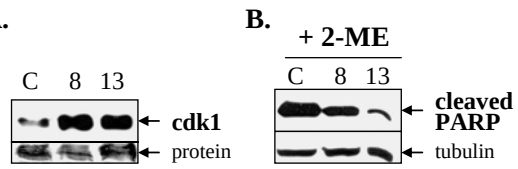

Fig. 1. Expression of dn-cdk1 inhibits 2-ME-mediated cleavage of PARP. A. Western blot analysis showing higher expression of cdk1 in dn-cdk1 stable clones 8 and 13 compared to negative control (C). **B.** Western blot analysis showing less cleaved PARP in dn-cdk1 clones 8 and 13 compared to control treated with 2-ME (2 μM) for 72h.

6. Determine the effect of expressing dn-cdc2, cdc2-AF, and cyclin B1-AS on 2-ME/2-EE-mediated G2/M arrest in LNCaP, DU 145, and PC-3 Tet-Off inducible cell lines using flow cytometry (months 8-30).

We suggest that prostate cancer cells that express higher levels of cyclin B1 are more sensitive to lower doses of 2-ME due to increased G2/M cell cycle arrest. LN-AI cells express the highest levels of cyclinB1 compared to all other prostate cancer cell lines (see Fig. 3). LNCaP, LN-AI, and PC-3 cells were treated with 2 μM 2-ME for 24 hours, analyzed by flow cytometry, and compared to control treated cells. Results show that only in LN-AI cells is there a G2/M block with 2 μM 2-ME, suggesting that higher cyclin B1 protein levels allows lower doses of 2-ME to increase G2/M cell cycle block.

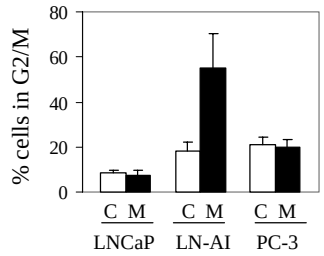

Fig. 2. Flow cytometric analysis showing that 2 μM 2-ME can increase G2/M in LN-AI but not LNCaP or PC-3 cells.

<u>Specific aim 2:</u> Determine whether activation of cyclin B1/cdc2 kinase by 2-ME/2-EE is required for induction of apoptosis in the Tet-Off inducible prostate cancer cell lines and in stably transfected non-transformed normal cells (months 1-30).

1. Determine whether 2-ME/2-EE treatment of the non-transformed/normal cell lines (BPH-1, NRP-152, primary prostate, CD34+ bone marrow progenitor) results in G2/M arrest and apoptosis (flow cytometry), and correlate with the expression levels of cyclin B1 protein (quantitative Western blot) (months 1-24).

We compared the levels of cyclin B1 protein in LNCaP, LN-AI, LN-AI/CSS (LN-AI cells grown in charcoal-stripped serum or androgen ablation conditions), DU 145, PC-3, and MSC cells by Western blot analysis (**Fig. 3A**). The results show higher cyclin B1 protein in LN-AI followed by LNCaP, LN-AI/CSS, DU 145, and PC-3. Cyclin B1 was below the level of detection in MSC cells. Interestingly, there appears to be a correlation with the level of G2/M cell cycle arrest by treatment with 5 μM 2-ME for 24 hours and the levels of cyclin B1 protein (**Fig. 3B**). Finally, there is a correlation with the amount of apoptosis stimulated by 5 μM 2-ME for 72 hours and the levels of cyclin B1 (**Fig. 3C**). These results suggest that higher cyclin B1 protein sensitizes prostate cancer cells to 2-ME-mediated G2/M cell cycle arrest and apoptosis. Very low levels of cyclin B1 in normal MSC cells may protect them from 2-ME-mediated apoptosis, perhaps explaining why 2-ME is cancer-specific and does not harm normal cells.

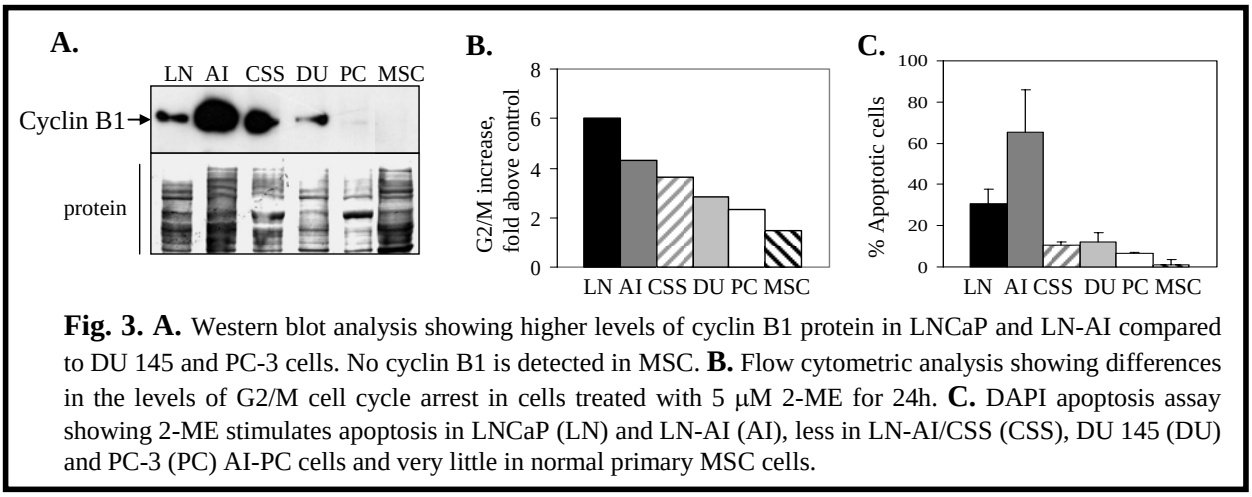

Fig. 3. A. Western blot analysis showing higher levels of cyclin B1 protein in LNCaP and LN-AI compared to DU 145 and PC-3 cells. No cyclin B1 is detected in MSC. **B.** Flow cytometric analysis showing differences in the levels of G2/M cell cycle arrest in cells treated with 5 μM 2-ME for 24h. **C.** DAPI apoptosis assay showing 2-ME stimulates apoptosis in LNCaP (LN) and LN-AI (AI), less in LN-AI/CSS (CSS), DU 145 (DU) and PC-3 (PC) AI-PC cells and very little in normal primary MSC cells.

2. Use Tet-Off inducible prostate cancer cell lines to determine if inhibition of cdc2 kinase with dn-cdc2, cyclin B1-AS, and MX7174 will decrease 2-ME/2-EE-mediated apoptosis (months 8-30).

See the data presented above in Fig. 1.

3. Use Tet-Off inducible prostate cancer cell lines to determine if further activation of cdc2 kinase with cdc2-AF and PD0166285 will increase 2-ME/2-EE-mediated apoptosis (months 8-30).

To determine if overexpression of cyclin B1 has an effect on 2-ME-mediated apoptosis, we isolated LNCaP clones stably overexpressing cyclin B1 protein using the pCMX/cyclin B1 expression plasmid obtained from J. Pines (co-transfected with pCMVneo plasmid for G418 resistance). We isolated three stable LNCaP clones overexpressing cyclin B1 and compared results to Neo negative control not overexpressing cyclin B1 (similar to parental LNCaP cells) (**Fig. 4A**). There was significantly greater induction of apoptosis in the LN/B1-23 clone compared to the Neo negative control when treated with 2-ME, as determined by PARP cleavage and DAPI analysis (**Fig. 4B, C**). These results suggest that higher cyclin B1 protein levels can sensitize prostate cancer cells to 2-ME-mediated apoptosis. Similar results were obtained in stable PC-3 clones overexpressing cyclin B1 protein (not shown). These results also support the hypothesis of this grant.

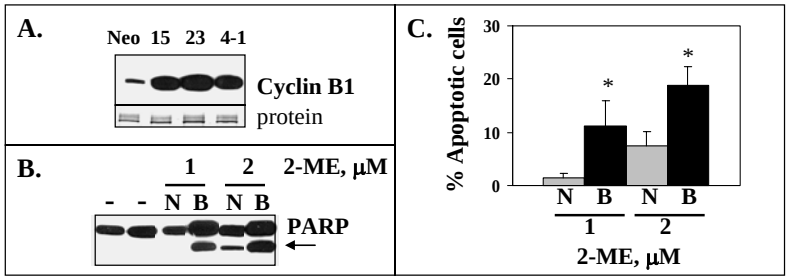

Fig 4. Overexpression of cyclin B1 sensitizes LNCaP cells to 2-ME-mediated apoptosis. A. Western blot showing three LNCaP clones stably overexpressing cyclin B1 compared to negative control Neo clone. **B.** Western blot showing greater cleavage of PARP in LN/B1-23 clone compared to Neo clone when treated with 2-ME (1, 2 μM) for 72h. **C.** DAPI showing greater number of apoptotic cells in LN/B1-23 compared to Neo clone. * $P<0.004$, two-tailed Student's *t*-test; n=5, three independent experiments.

4. Determine whether stable expression of cyclin B1 in NRP-152 and MSC sensitizes them to 2-ME/2-EE-mediated apoptosis (months 4-24).

Our efforts to transfect cyclin B1 protein into NRP-152 cells have failed. We have successfully transfected NRP-152 cells with plasmids expressing green fluorescence protein (GFP) using Lipofectamine 2000 so our problem is not because of poor transfection efficiency. However, when we transfect NRP-152 cells with the pCMX/cyclin B1 expression plasmid (see Fig. 3), we can never detect cyclin B1 protein by Western blot analysis. One possibility is that the levels of cyclin B1 are tightly regulated in normal cells, thus preventing its overexpression. This may be addressed by incubating recombinant cyclin B1 protein (ProSci, Inc) in NRP-152

protein extracts and compare with prostate cancer extracts. A prediction would be that cyclin B1 is rapidly degraded in NRP-152 but not in prostate cancer cells.

5. Determine whether stable expression of cyclin B1-AS in BPH-1 will reduce cyclin B1 protein levels and decrease 2-ME/2-EE-mediated apoptosis (months 4-24).

We presented data in the 2005 annual report using siRNA SMARTpool specific for cyclin B1 that reduction of cyclin B1 protein lowered 2-ME-mediated cleavage of PARP protein. However, transient transfection of cyclin B1 siRNA presents some technical problems. We are now in the process of analyzing stable LNCaP cell clones that express siRNA specific for cyclin B1 (pKD-Cyclin B1 siRNA plasmid, Upstate Biotechnologies), resulting in lower levels of cyclin B1 compared to negative control clones (pKD-NegCon plasmid, Upstate). Our expectation is that clones that have less cyclin B1 protein will be less sensitive to 2-ME-mediated apoptosis.

<u>Specific aim 3</u>: Identify synergisms and mechanisms of interaction between 2-ME/2-EE and other clinically relevant chemotherapeutic drugs (months 8-36).

1. Identify the in vitro growth condition (multicellular spheroids using polyhema) whereby prostate cancer cells are in a non-proliferative state and determine if 2-ME/2-EE will induce G2/M arrest and apoptosis (months 8-10).

LNCaP cells were grown in growth media containing 0.1% fetal bovine serum (FBS) for 24, 48, and 72 hours. Flow cytometry showed a decrease in S phase from 18% in media with 5% FBS to 7% in 0.1% FBS after 24 hours. This low proliferation is similar to human prostate cancer in situ [8]. Western blot analysis showed a decrease in cyclin B1 protein in control treated cells grown in 0.1% FBS at 48 and 72 hours. However, treatment with 5 μM 2-ME still resulted in an increase in cyclin B1 protein (**Fig. 5**) and increase in G2/M cell cycle arrest (not shown). We have not yet determined if 2-ME can also increase apoptosis in low-proliferating LNCaP cells.

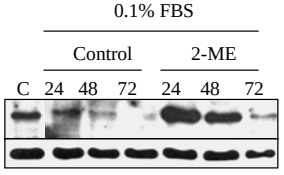

Fig. 5. Western blot analysis showing decrease in cyclin B1 protein when LNCaP cells are grown in 0.1% FBS. Treatment with 2-ME still increases cyclin B1 protein in 0.1% FBS.

2. Correlate the levels of cyclin B1 protein in the non-proliferation condition with the ability of 2-ME/2-EE to increase cdc2 kinase activity and induce G2/M arrest and apoptosis (8-10).

We have not yet determined if 2-ME can also increase apoptosis in low-proliferating LNCaP cells.

3. Determine the IC_{50} dose and the effect on the cell cycle for docetaxel (taxotere), R-roscovitine, and etoposide in prostate cancer cell lines (months 10-14).

We presented data for docetaxel (Doc) inhibition of prostate cancer cell lines in the 2004 annual report.

4. Use isobolograph analysis of cell growth assays to determine if docetaxel, R-roscovitine, and etoposide can synergize with 2-ME/2-EE to inhibit prostate cancer cells in proliferating and non-proliferating in vitro conditions (months 14-18).

We determined in proliferation growth conditions whether the combination of 2-ME and Doc can inhibit prostate cancer cells greater than additive over the growth inhibition with single drugs. Using previously described methods [6], results show that the combination of 2-ME and Doc can inhibit the growth of LN-AI and LN-AI/CSS cells greater than additive over the growth inhibition of the single drugs (Fig. 6). However, in DU 145 and PC-3 cells, we have not yet found a greater than additive growth inhibition effect with the combination of 2-ME and Doc. These results suggest that the combination of 2-ME and Doc may offer a therapeutic benefit against prostate cancer.

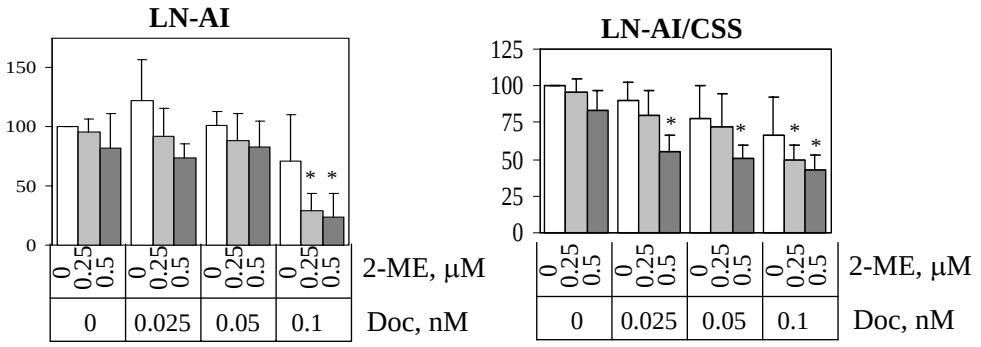

Fig. 6. Cell growth assays showing a greater than additive inhibition of cell growth with the combination of 2-ME and docetaxel (Doc) in LN-AI and LN-AI/CSS. *, $P<0.05$.

5. Determine whether the drug that can act synergistically with 2-ME/2-EE to inhibit prostate cancer cell growth also has a synergistic effect on the cell cycle and apoptosis (months 16-20).

We determined in LN-AI cells whether the combination of 2-ME and docetaxel has an effect on the cell cycle and apoptosis. LN-AI cells were treated with 0.5 μM 2-ME, 0.1 nM Doc, and their combinations and compared with control treated cells. After 24 hours, the 2-ME/Doc combination results in G2/M block in the cell cycle whereas 2-ME and Doc (low dose) alone did not result in any difference in G2/M compared to control cells (**Fig. 7A**). After 72 hours, the 2-ME/Doc combination results in a significant increase in apoptosis over that of each single drug and control cells (**Fig. 7B**). These results suggest that lower doses of 2-ME and Doc can be used in combination to obtain the G2/M cell cycle block and increase in apoptosis.

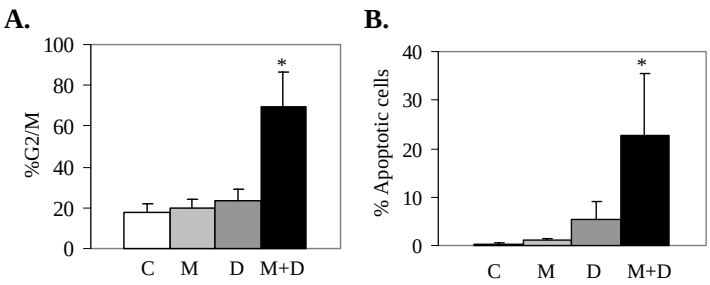

Fig. 7. A. Flow cytometry showing the combination of 0.5 μM 2-ME and 0.1 nM Doc can increase G2/M cell cycle block whereas either drug alone can not. **B.** DAPI apoptosis assay showing greater apoptosis in combination over single drugs. *, $P<0.01$ compared to either drug alone.

6. Using the most promising drug combination identified in vitro, test the in vivo anti-prostate cancer efficacy in the Gγ/T-15 and TRAMP transgenic mice (10 mice per group x 6 groups = 60 Gγ/T-15 and 60 TRAMP transgenic male mice) (months 20-36).

Our in vitro experiments showed that 2-ME and paclitaxel block prostate cancer cells in the G2/M phase of the cell cycle [6]. We sought to determine if a similar G2/M block is observed in 2-ME and Doc treated Gγ/T prostate tumors. Mice with palpable prostate tumors were injected i.p. with 2-ME (150 mg/kg), Doc (5 mg/kg), a combination of 2-ME and Doc, and vehicle controls for 1 and 2 days. Prostate tumors were removed and a small piece minced in 2 ml of PI staining solution (0.1% sodium citrate, 0.03% NP40, and 50 μg/ml PI), filtered through a 40 μM nylon mesh, and DNA distribution histograms generated by analysis of 10,000 nuclei in a Coulter XL flow cytometer. The percentage of cells in the G1, S, and G2/M DNA content were determined by the ModFit program (Verity Software House) from 5 prostate tumor samples from each treatment group. Results show that treatment with 2-ME and Doc for two consecutive

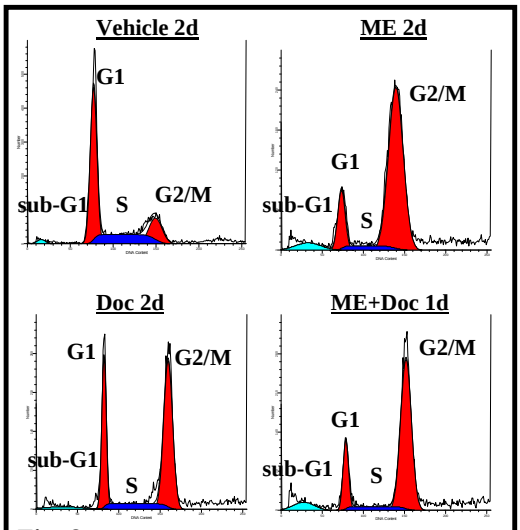

Fig. 8. Combination of 2-ME plus Doc results in G2/M block earlier than each drug alone in Gγ/T prostate tumors.

days was required for G2/M block (**Fig. 8**). There was no difference in the cell cycle between vehicle controls and 2-ME and Doc treatments for 1 day (not shown). In contrast, the combination of 2-ME and Doc for 1 day resulted in G2/M block (**Fig. 8**). These results suggest that the combination of 2-ME and Doc blocked Gγ/T prostate tumors in the G2/M phase of the cell cycle more rapidly than each drug alone.

We next investigated the anti-prostate cancer efficacy of the 2-ME and Doc combination in the Gγ/T mice. Mice with palpable prostate tumors were injected i.p. 11 times over 14 days with 2-ME (M, 30, 75, and 150 mg/kg; n=10 each dose), every 3 days with Doc (D, 2.5 and 5 mg/kg; n=10 each dose), low dose combination of 2-ME and Doc (M 75 + D 2.5 mg/kg; n=9), high dose combination of 2-ME and Doc (M, 150 + D, 5 mg/kg; n=11), or vehicle controls (n=29). We used the new nanocrystal colloidal dispersion liquid formulation developed by EntreMed for 2-ME. 2-ME-NCD has been shown to significantly increase bioavailability and is now being tested in Phase II clinical trials. Primary prostate tumors and visible lymph node metastases were removed and weights determined. Results show that as single drugs, only the 150 mg/kg dose of 2-ME and the 5mg/kg dose of Doc significantly inhibited primary tumors by 32% (P<0.05) and 39% (P<0.02), respectively compared to control treated mice (**Fig. 9**). Interestingly, the low dose combination of 2-ME and Doc (75 + 2.5 mg/kg) significantly inhibited primary prostate tumors by 42% (P<0.02), despite each dose of the drug by itself having no significant effect (**Fig. 9**). The high dose combination of 2-ME and Doc (150 + 5 mg/kg) significantly inhibited primary prostate tumors by 50% (P<0.002), although the effect does not appear to be additive over the single drugs. Both the low and high dose 2-ME and Doc combinations inhibited metastatic prostate tumors by 68% (P=0.14) and 79% (P=0.06) better than any 2-ME or Doc dose alone (3-59%; P>0.18). Overall, these results suggest that lower doses of 2-ME and Doc can be used in combination to inhibit primary and metastatic androgen-independent prostate cancer. We are currently investigating if this effect is due to greater apoptosis and less angiogenesis.

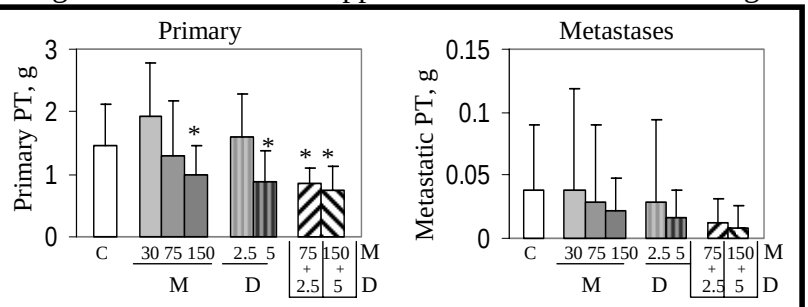

Fig. 9. Combination of 2-ME (M) and Doc (D) inhibits primary and metastatic prostate tumors in Gγ/T transgenic mice. *, P<0.05; n=9-10 for each treatment.

KEY RESEARCH ACCOMPLISHMENTS

- Stable LN-AI clones that overexpress dominant negative cdk1 lower 2-ME-mediated apoptosis compared to the negative control clone (Fig. 1).
- Prostate cancer cell lines like LN-AI that express the highest levels of cyclin B1 protein undergo G2/M block with lower doses of 2-ME compared to cell lines like LNCaP and PC-3 that express less cyclin B1 (Fig. 2).
- In prostate cancer and primary non-cancer MSC cells, there is a positive correlation with the levels of cyclin B1 and the ability of 2-ME to increase G2/M cell cycle block and apoptosis (Fig. 3).
- Stable LNCaP clones that overexpress cyclin B1 protein are more sensitive to 2-ME-mediated apoptosis compared to the negative control clone (Fig. 4).
- LNCaP cells growing in non-proliferating conditions are still sensitive to 2-ME increase in cyclin B1 and G2/M cell cycle block (Fig. 5).
- Combination of low doses of 2-ME and Doc can inhibit the growth of LN-AI and LN-AI/CSS cells greater than additive compared to single drugs (Fig. 6).
- Combination of low doses of 2-ME and Doc can increase G2/M cell cycle arrest and apoptosis whereas the single low doses have no effect (Fig. 7).
- Combination of 2-ME and Doc blocked Gγ/T prostate tumors in the G2/M phase of the cell cycle more rapidly than each drug alone (Fig. 8).

- Lower doses of 2-ME and Doc can be used in combination to inhibit primary and metastatic androgen-independent prostate cancer in Gγ/T transgenic mice (Fig. 9).

REPORTABLE OUTCOMES

Publications

1. **Perez-Stable CM**. 2006. 2-Methoxyestradiol and paclitaxel have similar effects on the cell cycle and induction of apoptosis in prostate cancer cells. Cancer Letters, 231:49-64. **Appended manuscript.**
2. Gomez A, de las Pozas A, **Perez-Stable C.** 2006. Sequential combination of flavopiridol and docetaxel reduces the levels of XIAP and AKT proteins and stimulates apoptosis in human LNCaP prostate cancer cells. Mol. Cancer Therapeutics, in press. **Appended manuscript.**
3. Reiner T, de las Pozas A, **Perez-Stable C**. 2006. Sequential combinations of flavopiridol and docetaxel inhibit prostate tumors, induce apoptosis, and decreases angiogenesis in the Gγ/T-15 transgenic mouse model of prostate cancer. The Prostate, in press. **Appended manuscript**

CONCLUSIONS

Our data supports the hypothesis that one of the cancer-specific mechanisms whereby 2-ME exerts its anti-prostate cancer activity is the deregulated activation of cyclin B1/cdc2 kinase during the cell cycle, which results in the induction of apoptotic cell death. First, dominant negative cdk1 lowered 2-ME-mediated apoptosis in LN-AI cells. Second, overexpression of cyclin B1 increases 2-ME-mediated apoptosis in LNCaP cells. Third, there is a positive correlation between the levels of cyclin B1 protein and the ability of 2-ME to increase G2/M cell cycle arrest and apoptosis in prostate cancer cells. Cyclin B1 protein levels is lowest in non-cancer MSC cells and this correlates with the smallest increase in G2/M and apoptosis by 2-ME. Fourth, low doses of 2-ME and Doc can increase G2/M arrest and apoptosis in combination but not as single drugs in LN-AI cells. This suggests that lower doses of 2-ME and Doc can be used in combination chemotherapy against prostate cancer. Fifth, the combination of 2-ME and Doc can increase G2/M arrest in Gγ/T prostate tumors better than the single drugs. In addition, the low dose combination of 2-ME and Doc inhibited primary prostate tumor growth whereas the single doses had no effect. Therefore, our data suggests the combination of 2-ME and Doc will be an effective chemotherapy regimen against prostate tumor.

REFERENCES

1. Zhu BT, Conney AH. Is 2-methoxyestradiol an endogenous estrogen metabolite that inhibits mammary carcinogenesis? Cancer Res 1998;58:2269-77.
2. Pribluda VS, Gubish ER, LaValle TM, Treston A, Swartz GM, Green SJ. 2-Methoxyestradiol: an endogenous antiangiogenic and antiproliferative drug candidate. Cancer Met Rev 2000;19:173-9.
3. Mooberry SL. Mechanism of action of 2-methoxyestradiol: new developments. Drug Resist Updat. 2003; 6:355-61.
4. Qadan LR, Perez-Stable CM, Anderson C, D'Ippolito G, Herron A, Howard GA, Roos BA. 2-Methoxyestradiol induces G2/M arrest and apoptosis in prostate cancer. Biochem Biophys Res Commun 2001;285:1259-66.
5. Kumar AP, Garcia GE, Slaga TH. 2-methoxyestradiol blocks cell-cycle progression at G(2)/M phase and inhibits growth of human prostate cancer cells. Mol Carcinog 2001;31:111-24.
6. Perez-Stable C. 2-Methoxyestradiol and paclitaxel have similar effects on the cell cycle and induction of apoptosis in prostate cancer cells. Cancer Lett. 2006; 231:49-64.
7. Perez-Stable CM, Schwartz GG, Farinas A, Finegold M, Binderup L, Ηοωαρδ ΓΑ, Ροοσ ΒΑ. Τηε Γγ/Τ-15 transgenic mouse model of androgen-independent prostate cancer: target cells of carcinogenesis and the effect of the vitamin D analog EB 1089. Cancer Epi. Bio. Prev. 2002; 11: 555-563.

8. Berges RR, Vukanovic J, Epstein JI, CarMichel M, Cisek L, Johnson DE, Veltri RW, Walsh PC, Isaacs JT. 1995. Implication of cell kinetic changes during the progression of human prostatic cancer. Clin. Cancer Res. 1:473-480.

Available online at www.sciencedirect.com
SCIENCE DIRECT
Cancer Letters 231 (2006) 49–64
CANCER Letters
www.elsevier.com/locate/canlet

2-Methoxyestradiol and paclitaxel have similar effects on the cell cycle and induction of apoptosis in prostate cancer cells

Carlos Perez-Stable[a,b,*]

[a]*Geriatric Research, Education, and Clinical Center and Research Service, Veterans Affairs Medical Center, GRECC (11-GRC), 1201 NW 16 Street, Miami, FL 33125, USA*
[b]*Department of Medicine and Sylvester Comprehensive Cancer Center, University of Miami School of Medicine, Miami, FL 33101, USA*

Received 29 July 2004; received in revised form 12 October 2004; accepted 14 January 2005

Abstract

2-Methoxyestradiol (2-ME) is an endogenous metabolite of estradiol with promise for cancer chemotherapy, including advanced prostate cancer. We have focused on events related to cell cycle arrest (G1 and G2/M) and induction of apoptosis in human prostate cancer cells. Treatment with 2-ME increased cyclin B1 protein and its associated kinase activity followed by later inhibition of cyclin A-dependent kinase activity and induction of apoptosis. Similar results were obtained with paclitaxel (taxol), a clinically relevant agent used to treat advanced prostate cancer. Cyclin-dependent kinase inhibitors prevented 2-ME and paclitaxel-mediated increase in cyclin B1-dependent kinase activity and blocked induction of apoptosis. Reduction of X-linked inhibitor of apoptosis (XIAP) protein by 2-ME and paclitaxel correlated with increased apoptosis. Lower doses of 2-ME and paclitaxel resulted in G1 (but not G2/M) cell cycle arrest in the p53 wild type LNCaP cell line, but with minimal induction of apoptosis. We suggest that 2-ME and paclitaxel-mediated induction of apoptosis in prostate cancer cells requires activation of cyclin B1-dependent kinase that arrests cells in G2/M and subsequently leads to the induction of apoptotic cell death.

Keywords: Cyclin B1; Prostate cancer; Mitotic block; Apoptosis; Cyclin A

1. Introduction

One of the more promising emerging chemotherapeutic agents is 2-methoxyestradiol (2-ME), an endogenous metabolite of estradiol [1–4]. 2-ME can inhibit the growth of a variety of cancer cells, including advanced androgen-independent prostate cancer (AI-PC) utilizing a remarkable number of diverse mechanisms that include cell cycle arrest, induction of apoptosis, disruption of microtubules, inhibition of angiogenesis, and increasing oxidative damage [1–6]. What makes 2-ME a promising chemotherapeutic is that it does not harm quiescent or proliferating normal cells and it does not exert significant estrogenic effects from binding estrogen receptors [2,7]. In fact, because of 2-ME's anti-cancer

* Corresponding author: Geriatric Research, Education, and Clinical Center and Research Service, Veterans Affairs Medical Center, GRECC (11-GRC), 1201 NW 16 Street, Miami, FL 33125, USA. Tel.: +1 305 324 4455, ext. 4391.
E-mail address: cperez@med.miami.edu.

0304-3835/$ - see front matter © 2005 Elsevier Ireland Ltd. All rights reserved.
doi:10.1016/j.canlet.2005.01.018

activity without toxicity to normal cells, it is currently in Phase II human trials for breast and prostate cancer [3]. 2-ME's anti-prostate cancer activity, however, is not well understood. A better understanding of the mechanisms of 2-ME's anti-prostate cancer effects will be helpful to better evaluate its clinical potential in managing AI-PC.

One of the proposed mechanisms for 2-ME's anti-cancer effect is the disruption of microtubule function and subsequent block in the G2/M phase of the cell cycle [1,2,4]. We have previously shown that 2-ME inhibits both androgen-dependent LNCaP and androgen-independent DU 145 and PC-3 human prostate cancer cells independent of the expression of androgen receptor and tumor suppressors p53 and Rb [5]. 2-ME blocks LNCaP, DU 145, and PC-3 prostate cancer cells in the G2/M phase of the cell cycle and induces apoptosis [5,6]. Specific mechanisms for 2-ME induced inhibition in prostate cancer cells are proposed to be mediated by activation of c-Jun N-terminal kinase (JNK) and inactivation of the anti-apoptosis proteins Bcl-2/Bcl-xL [8–10], up-regulation of the death receptor 5 and induction of the extrinsic pathway of apoptosis [11], and down-regulation of hypoxia-inducible factor-1 [12]. The effect of 2-ME on the components of the cell cycle, specifically the G2/M cyclins A and B1, and whether these effects are required for induction of apoptosis are not known.

Paclitaxel is a well studied chemotherapeutic agent that stabilizes microtubules and has clinical efficacy in a variety of cancers, including AI-PC [13]. Paclitaxel-mediated microtubule damage activates the mitotic checkpoint and blocks the degradation of cyclin B1, leading to a prolonged activation of cyclin B1-dependent kinase (cdk)1 and mitotic arrest [14–16]. The prolonged activation of cdk1 is required for paclitaxel-mediated apoptosis in the MCF-7 breast cancer cell line, as demonstrated by the use of the chemical inhibitor of cdk1, olomoucine, and anti-sense oligonucleotides specific for cyclin B1 [14]. It appears, however, that the subsequent reduction of cyclin B1-cdk1 activity and exit from the paclitaxel-mediated mitotic block is important for induction of apoptosis [17]. The mechanism proposed is that increased cdk1 activity results in phosphorylation and stabilization of survivin, a member of the inhibitor of apoptosis (IAP) family and a substrate for cdk1 [18]. The subsequent decrease in cyclin B1-cdk1 activity results in a decrease in the levels of survivin and increase in sensitivity to induction of apoptosis. Whether this mechanism is generally applicable to paclitaxel-mediated inhibitory effects in different types of prostate cancer cells is not clear.

To better understand how 2-ME and paclitaxel function as anti-prostate cancer agents, we focused on the effect of these drugs on cyclin A and B1 proteins and their associated kinase activities. We report results demonstrating strong similarities of 2-ME with paclitaxel in regard to an increase in cyclin B1 protein and its associated kinase activity followed by a decrease in cyclin A-dependent kinase activity and induction of apoptosis in prostate cancer cells. Inhibition of cyclin B1-dependent kinase activity blocked subsequent induction of apoptosis by both agents. These results indicated that 2-ME inhibition of prostate cancer cells involves several steps in common with paclitaxel, a clinically relevant chemotherapeutic agent for AI-PC.

2. Materials and methods

2.1. Reagents

2-ME, paclitaxel, dimethylsulfoxide (DMSO), lithium chloride, and propidium iodide (PI) were purchased from Sigma (St Louis, MO, USA). Histone H1 protein was purchased from Roche Applied Sciences (Indianapolis, IN, USA). 4′-6-Diamidino-2-phenylindole (DAPI), purvalanol A, alsterpaullone, PD 98059, caspase-3 substrate (Ac-DEVD-*p*NA) and inhibitor (DEVD-CHO) were purchased from Calbiochem (San Diego, CA, USA). Annexin V-FITC was purchased from Santa Cruz Biotechnology, Santa Cruz, CA, USA).

2.2. Cell culture and treatment with 2-ME and paclitaxel

Human prostate carcinoma cell lines LNCaP-FGC [19], DU 145 [20], and PC-3 [21] were obtained from the American Type Culture Collection (Rockville, MD, USA). Cultures were maintained in RPMI 1640 medium (Invitrogen, Carlsbad, CA, USA) with 5% fetal bovine serum (Hyclone, Logan, UT, USA),

100 U/ml penicillin, 100 μg/ml streptomycin, and 0.25 μg/ml amphotericin (Invitrogen). Prostate cancer cells were treated with different doses of 2-ME (0.5–10 μM), paclitaxel (0.5–50 nM), or DMSO (0.1%) control for varying times (4–72 h). In all the experiments, floating and trypsinized attached cells were pooled for further analysis.

2.3. Three-day cell growth assay for 2-ME and paclitaxel

LNCaP (10,000), DU 145 (2500), and PC-3 (3000) cells were seeded in 96-well plates. The next day, fresh media containing different doses of 2-ME (0.1–50 μM) and paclitaxel (0.1–50 nM) or control (0.1% DMSO) were added and cells incubated for 3 days. The CellTiter Aqueous cell proliferation colorimetric method (Promega, Madison, WI) was used to determine cell viability as per manufacturer's instructions. Cell viability was normalized against the vehicle control and the data expressed as a percentage of control from three independent experiments done in triplicate.

2.4. Flow cytometric analysis

Propidium/hypotonic citrate method [22] was used to study cell cycle distribution of 2-ME and paclitaxel treated prostate cancer cells. After harvesting and washing cells with phosphate-buffered saline (PBS), the cell pellets were resuspended in 0.5 ml of PI staining solution (0.1% sodium citrate, 0.03% NP40, and 50 μg/ml PI), vortexed to release nuclei, and DNA distribution histograms generated by analysis of 10,000 nuclei in a Coulter XL flow cytometer. The percentage of cells in the G1, S, and G2/M DNA content were determined by the ModFit program (Verity Software House, Topsham, ME, USA) from 6 to 8 samples analyzed from at least three independent experiments.

2.5. Western blot analysis

Cell pellets were resuspended in NP40 cell lysis buffer (1% NP-40, 50 mM Tris, pH 8.0, 150 mM NaCl, 2 mM EGTA, 2 mM EDTA, protease inhibitor tablet (Roche Applied Sciences), 50 mM NaF, and 0.1 mM $NaVO_4$), lysed by vortex, left on ice for 30 min, centrifuged, and the protein concentrations of the supernatant determined with the Bio-Rad protein assay (Bio-Rad Laboratories, Hercules, CA, USA). After separation of 25–50 μg protein by SDS-PAGE, proteins were transferred by electrophoresis to Immobilon-P membrane (Millipore Corp, Bedford, MA, USA) and incubated in 5% non-fat dry milk, PBS, and 0.25% Tween-20 for 1 h. Antibodies specific for cyclin B1 (GNS1), cyclin A (H-432), cdk1 (17), cdk2 (D-12), p53 (DO-1), p21 (C-19), survivin (FL-142), IAP-1 (H-83), IAP-2 (H-85), and actin (C-11) (Santa Cruz Biotechnology) were diluted 1/1000 in 5% non-fat dry milk, PBS, and 0.25% Tween-20 and incubated overnight at 4 °C. Similarly, antibodies specific for poly ADP-ribose polymerase (PARP; C2-10), Bcl-xL (polyclonal) (BD Biosciences Pharmingen, San Diego, CA, USA), and XIAP (Cell Signaling Technology, Beverly, MA) were diluted 1/1500. Membranes were washed in PBS and 0.25% Tween-20 (3×10 min) and incubated with horseradish peroxidase-conjugated secondary antibody (anti-mouse IgG1/2a or anti-rabbit; 1/2000 dilution; Santa Cruz Biotechnology) for 1 h, washed in PBS and 0.25% Tween-20, and analyzed by exposure to X-ray film (X-Omat, Eastman Kodak Co, Rochester, NY, USA) using enhanced chemiluminescence plus (ECL plus, Amersham Pharmacia Biotech, Arlington Heights, IL, USA). Goat polyclonal antibodies specific for actin and horseradish peroxidase-conjugated secondary antibody (anti-goat IgG; 1/2000 dilution; Santa Cruz Biotechnology) were used for protein loading controls. Total proteins were stained with Coomassie blue for an additional protein loading control. X-ray films were scanned using an Epson Perfection 2450 Photo scanner and the pixel intensity measured using UN-SCAN-IT digitizing software, version 5.1 (Silk Scientific Corp., Orem, UT, USA). Changes in protein levels of 2-ME and paclitaxel treated cells was determined by normalizing values to actin and comparing to values of control treated cells ($=1.0$) in at least three different samples analyzed from 2 to 5 independent experiments. To determine the overall levels of Bcl-xL and survivin in LNCaP, DU 145, and PC-3 cells, the scanned bands from the same blot were normalized to scanned total protein ($n=6$, two independent experiments).

2.6. Cyclin B1 and A-dependent kinase assay

Four hundred micrograms of total protein were incubated with 2 μg anti-cyclin A or B1 antibody for 3 h on ice, followed by the addition of 20 μl protein A/G-agarose (Santa Cruz Biotechnology), and incubated overnight at 4 °C. with agitation. Immune-complexes were collected by centrifugation, washed 3× with NP40 cell lysis buffer, 3× with kinase buffer (10 mM Tris–HCl [pH 7.5], 150 mM NaCl, 10 mM $MgCl_2$, and 0.5 mM DTT), resuspended in kinase buffer containing 2 μg histone H1 substrate protein, 25 μM ATP, 5 μCi γ^{32}P-ATP, and incubated for 30 min at 30 °C. Reactions were stopped with SDS gel loading buffer, samples electrophoresed on SDS-PAGE, electroblotted to Immobilon P membranes, and analyzed by autoradiography. Coomassie blue staining of membranes revealed similar loading of histone proteins. The histone band was cut out from the paper and ^{32}P measured by scintillation counting. Changes in kinase activity of 2-ME and paclitaxel treated cells was determined by normalizing the ^{32}P-histone values to the scanned H1 protein value and comparing to values of control treated cells (=1.0) in at least three different samples analyzed from 2 to 5 independent experiments.

2.7. p21 immunoprecipitation and cdk2 western blot

Four hundred micrograms of LNCaP total protein were incubated with 2 μg anti-p21 or rabbit IgG antibody for 3 h on ice, followed by the addition of 20 μl protein A/G-agarose, and incubated overnight at 4 °C. with agitation. Immune-complexes were collected by centrifugation, washed 3× with NP40 cell lysis buffer, and analyzed by Western blot using cdk2 antibody.

2.8. Apoptosis assays

For the DAPI staining apoptosis assay, prostate cancer cells were resuspended in 0.6 ml 4% paraformaldehyde/PBS for 15 min, washed with PBS, and resuspended in 0.5 ml of DAPI (1 μg/ml)/PBS for 10 min. Cells were washed with PBS and 10 μl of concentrated cells added on a microscope slide followed by placement of a coverslip. Cells containing densely stained and fragmented chromatin were identified as apoptotic using a Nikon fluorescence microscope with a DAPI filter. The number of apoptotic cells in at least 250 total cells was determined from at least four random microscope fields. Changes in apoptosis from 2-ME and paclitaxel treated prostate cancer cells was determined as percentage of apoptotic cells in at least five different samples from three independent experiments. There was minimal apoptosis detected in control treated cells (<0.5%). For the annexin V apoptosis assay, prostate cancer cells were resuspended in 100 μl annexin binding buffer (10 mM Hepes, pH 7.9; 140 mM NaCl; 2.5 mM $CaCl_2$) followed by the addition of 2.5 μl of annexin V-FITC and 2 μl PI (50 μg/ml) and incubated for 20 min at room temperature. After the addition of 400 μl annexin binding buffer, the cells were read by flow cytometry and the percentage of early apoptotic cells determined by measuring the annexin-FITC positive/PI negative quadrant using WinMDI version 2.8.

2.9. Caspase-3 assay

Prostate cancer cells were resuspended in 50–100 μl ice cold cell lysis buffer (50 mM HEPES, pH 7.4, 100 mM NaCl, 0.1% CHAPS, 1 mM DTT, 0.1 mM EDTA), and incubated 5 min on ice. Cells were centrifuged for 10 min at 4 °C and the supernatant stored at −80 °C. Fifty micrograms of cell extract was added to assay buffer (50 mM HEPES, pH 7.4, 100 mM NaCl, 0.1% CHAPS, 10 mM DTT, 0.1 mM EDTA, 10% glycerol) containing caspase-3 substrate (Ac-DEVD-*p*NA; 200 nM) and incubated at 37 °C. Absorbance at 405 nM was determined using a microtiter plate reader and the changes in caspase-3 activity from 2-ME and paclitaxel treated prostate cancer cells was determined as fold control treated cells (equals 1.0). Addition of caspase-3 inhibitor (DEVD-CHO; 50 nM) was used to confirm specificity.

2.10. Purvalanol A and alsterpaullone cdk inhibitors

The potent cdk inhibitors purvalanol A and alsterpaullone [23,24] were used to investigate the effect on 2-ME and paclitaxel-mediated apoptosis in prostate cancer cells. Dose response experiments determined that 5 μM purvalanol A blocked 2-ME

and paclitaxel-mediated increase in cyclin B1-dependent kinase activity in DU 145 but not LNCaP cells. For alsterpaullone, a dose of 5 μM in LNCaP and 10 μM in PC-3 blocked 2-ME and paclitaxel-mediated increase in cyclin B1-dependent kinase activity. The effect of these doses on 2-ME and paclitaxel-mediated apoptosis was determined using the methods described above.

2.11. Statistical analysis

Statistical differences between 2-ME or paclitaxel-treated and control cells were determined by two-tailed Student's *t*-test with $P < 0.05$ considered significant.

3. Results

3.1. Differential growth inhibition of prostate cancer cells by 2-ME and paclitaxel

Using a 3-day cell growth assay, we showed that androgen-dependent LNCaP cells were more sensitive to inhibition by 2-ME compared to androgen-independent DU 145 and PC-3 prostate cancer cells (Fig. 1). The half-maximal inhibitory concentrations (IC_{50}) with standard deviations in parenthesis were as follows: LNCaP, 1.35 μM (±0.25); DU 145, 2.0 μM (±0.41); and PC-3, 10.4 μM (±2.64). DU 145 cells were more sensitive to inhibition by paclitaxel compared to LNCaP and PC-3 cells. The IC_{50} for paclitaxel treated cells were as follows: DU 145, 1.53 nM (±0.3); LNCaP, 2.6 nM (±0.5); and PC-3, 7.0 nM (±1.8). Subsequent experiments sought to determine why LNCaP and DU 145 cells were more sensitive to inhibition by 2-ME and paclitaxel compared to PC-3 cells.

3.2. Low doses of 2-ME and paclitaxel increase LNCaP cells in the G1 phase of the cell cycle

To investigate the cell cycle effects of 2-ME compared to paclitaxel, we used flow cytometric analysis after treatment of prostate cancer cells with varying doses of 2-ME (0.5–10 μM) and paclitaxel (0.5–50 nM) for 24 h (Fig. 2). Treatment of LNCaP cells with 2 μM 2-ME and 2 nM paclitaxel resulted in a significant (>13%) increase of cells in the G1 and decrease (>30%) in the S phase of the cell cycle. Similar doses of 2-ME and paclitaxel did not cause G1 accumulation in DU 145 (Fig. 2) and PC-3 (result not shown) cells, probably because their G1 cell cycle checkpoints are defective [25,26]. Treatment of all prostate cancer cells with ≥5 μM 2-ME and ≥10 nM paclitaxel resulted in an increase in G2/M with concomitant decrease in G1. These results suggested that lower doses of 2-ME and paclitaxel blocked LNCaP but not DU 145 or PC-3 cells in the G1 phase of the cell cycle.

3.3. Dose-specific changes in cyclins B1 and A in 2-ME and paclitaxel-treated prostate cancer cells

To investigate molecular changes involved in 2-ME and paclitaxel-mediated G1 and G2/M cell

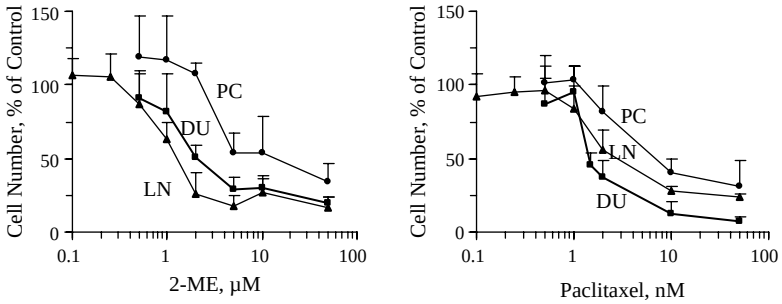

Fig. 1. 2-ME and paclitaxel inhibits growth of human prostate cancer cells in a dose-dependent manner. Androgen-dependent LNCaP (LN, ▲) and androgen-independent DU 145 (DU, ■) and PC-3 (PC, ●) human prostate cancer cell lines were treated with 2-ME (0.1–50 μM), paclitaxel (0.1–50 nM) or vehicle control, as described under Materials and Methods. Cell viability was measured using the CellTiter Aqueous colorimetric method; the data are expressed as percentage of control (mean ± standard deviation) from three independent experiments done in triplicate.

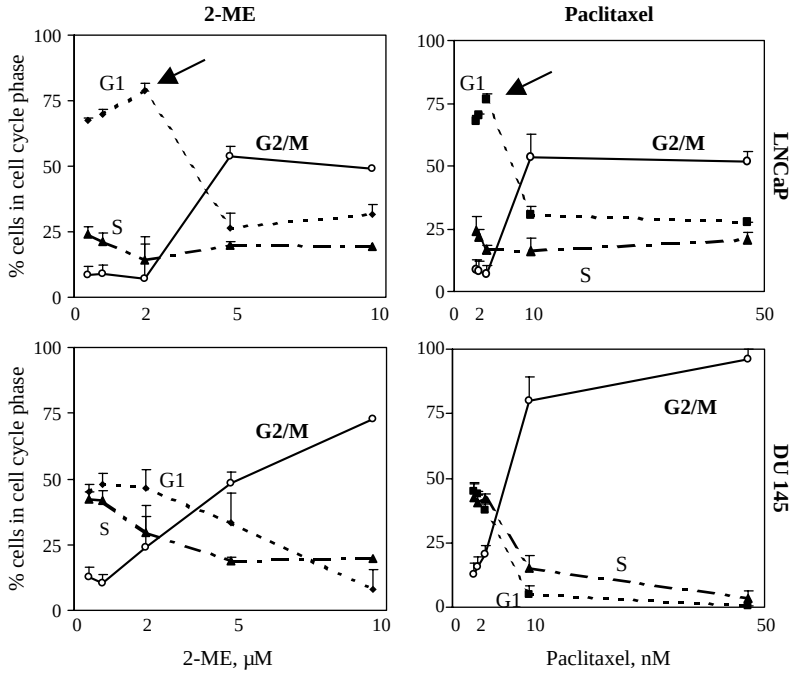

Fig. 2. Flow cytometric analysis of 2-ME and paclitaxel dose response in human prostate cancer cells. LNCaP and DU 145 were treated with varying doses of 2-ME (0.5–10 μM) and paclitaxel (0.5–50 nM) for 24 h and the percentage of cells in the cell cycle phases (G1, S, and G2/M) determined by flow cytometry. In LNCaP, 2 μM 2-ME and 2 nM paclitaxel increased cells in G1 (arrows; $P < 10^{-6}$). Higher doses of 2-ME ($\geq$5 μM) and paclitaxel ($\geq$10 nM) blocked cells in G2/M with concomitant reduction in G1. Results are expressed as means $\pm$ standard deviation (error bars).

cycle arrest in prostate cancer cells, we analyzed expression of cyclins B1 and A by Western blot and kinase assays (Fig. 3A). Cyclin A protein increases during the S and G2 phase of the cell cycle and is believed to be important for DNA replication [27]. The transition from the G2 to the M phase of the cell cycle requires accumulation of cyclin B1 and activation of its associated kinase, cdk1. The end of the G2/M transition and exit from mitosis requires proteolysis of cyclin B1 and reduction of cdk1 activity [28]. Treatment of LNCaP cells with 5 μM 2-ME and 10 nM paclitaxel for 24 h resulted in a 3–4-fold increase of cyclin B1 protein and its associated kinase activity but no increase in cyclin A protein and its associated kinase activity (Fig. 3A). Similar results were obtained in 2-ME and paclitaxel treated DU 145 and PC-3 cells (Fig. 3B). In LNCaP but not in DU 145 and PC-3 cells, treatment with the G1-promoting doses of 2-ME (2 μM) and paclitaxel (2 nM) resulted in a 4–5-fold decrease in cyclin A-dependent kinase activity without any changes in the levels of cyclin A (Fig. 3A) and cdk2 protein (not shown). These results indicated that (1) the G2/M-promoting doses of 2-ME ($\geq$5 μM) and paclitaxel ($\geq$10 nM) increased cyclin B1 protein and kinase activity to similar levels in LNCaP, DU 145, and PC-3 cells and (2) the G1-promoting doses of 2-ME (2 μM) and paclitaxel (2 nM) inhibited cyclin A-dependent kinase only in LNCaP and may explain why LNCaP cells increased in G1 and decreased in S.

3.4. Time-dependent effects of the G2/M-promoting doses of 2-ME and paclitaxel on cell cycle distribution

To analyze the time-dependent effects on the cell cycle after treatment with 2-ME and paclitaxel over 4, 24, 48, and 72 h, we chose the G2/M-promoting dose of 2-ME (5 μM) and paclitaxel (10 nM). After 4 h of 2-ME treatment, there was a significant increase in cells with G2/M DNA content in DU 145 but not in

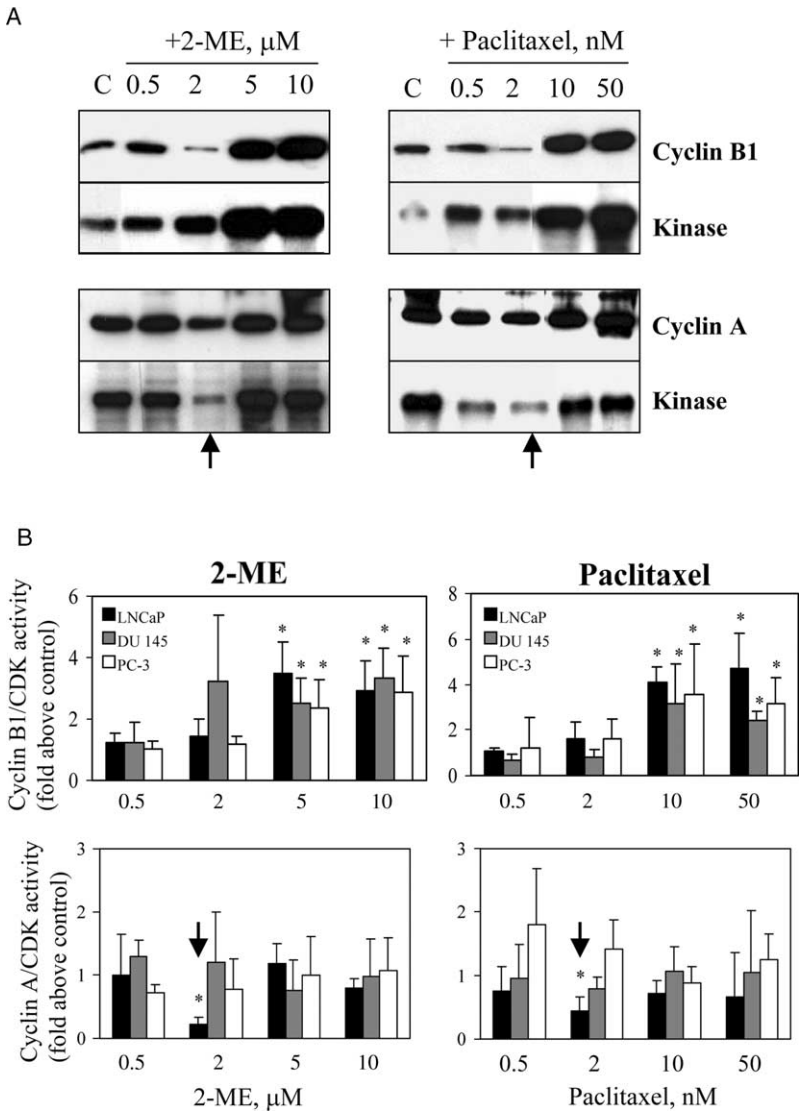

Fig. 3. Effect of G1- and G2/M-promoting doses of 2-ME and paclitaxel on cyclin B1 and A proteins and their associated kinase activities. (A) LNCaP cells were treated with increasing doses of 2-ME (0.5–10 μM) and paclitaxel (0.5–50 nM) for 24 h and the levels of cyclin B1 and A proteins determined by Western blot analysis, normalized to actin protein (not shown), and compared to control (C) treated cells. Cyclin B1 and A proteins were immunoprecipitated and their associated kinase activities (^{32}P-histone) determined from the same lysates. G1-promoting doses of 2-ME (2 μM) and paclitaxel (2 nM) decreased cyclin A-dependent kinase activity (arrow) and the G2/M-promoting doses (5 μM 2-ME and 10 nM paclitaxel) increased cyclin B1-dependent kinase activity. (B) G2/M-promoting doses of 2-ME (5 μM) and paclitaxel (10 nM) resulted in similar increases in cyclin B1-dependent kinase activity in LNCaP, DU 145, and PC-3 cells compared to control treated cells (*, $P < 0.03$). In LNCaP cells, G1-promoting doses of 2-ME (2 μM) and paclitaxel (2 nM) inhibited cyclin A-dependent kinase (arrows). Results are expressed as means (fold control = 1) ± standard deviation (error bars).

LNCaP (Fig. 4). All cells treated with 2-ME and paclitaxel accumulated in G2/M after 24 h with a concomitant decrease in G1. In LNCaP, there was a significant decrease in G2/M after 48 and 72 h treatment with 2-ME and paclitaxel. In DU 145 (Fig. 4) and PC-3 (result not shown), however, cells remained blocked in G2/M after treatment for 48 and 72 h with 2-ME but not paclitaxel. After the initial

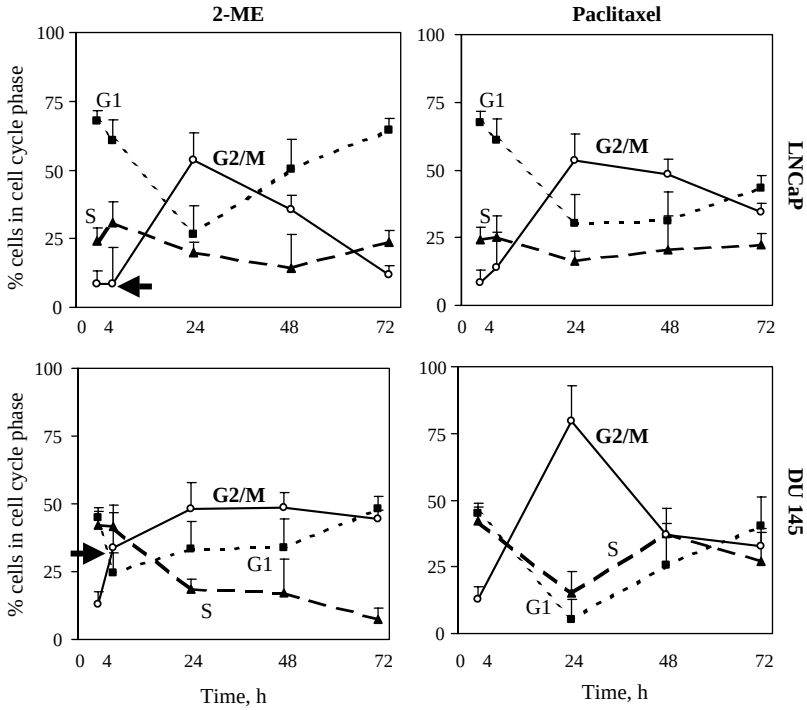

Fig. 4. Changes in cell cycle distribution with time after treatment of prostate cancer cells with 2-ME and paclitaxel. LNCaP and DU 145 cells were treated with 5 μM 2-ME and 10 nM paclitaxel for 4, 24, 48, and 72 h and the percentage of cells in the cell cycle phases (G1, S, and G2/M) analyzed by flow cytometry. In 2-ME treated DU 145 but not LNCaP cells, there was a significant increase in G2/M after 4 h (arrow; $P < 0.03$). At 24 h, all cells showed increase in G2/M with a concomitant reduction in G1. At 48 and 72 h, there was a decrease in G2/M, except with 2-ME treated DU 145 cells. Results are expressed as means ± standard deviation (error bars).

decrease of LNCaP cells in G1 at 24 h, there was a significant increase after 48 and 72 h in 2-ME treated cells. Although these results revealed a common G2/M block at 24 h, there were differences in the cell cycle distribution at 48 and 72 h between 2-ME and paclitaxel-treated prostate cancer cells.

3.5. Changes in cyclins B1 and A before and after 2-ME and paclitaxel-mediated block in G2/M

Since all prostate cancer cells were blocked at G2/M after 24 h treatment with ≥5 μM 2-ME and ≥10 nM paclitaxel, it was not surprising that there was a marked accumulation of cyclin B1 protein (Figs. 2 and 3). However, there was a significant increase in cyclin B1 protein and its associated kinase in LNCaP cells treated with 2-ME after only 4 h, a time when there was no increase in cells with G2/M DNA content (Figs. 4 and 5). This suggested that the increase of cyclin B1 protein and kinase activity was not simply due to increase in the G2/M fraction. In general, the levels of cyclin B1 protein peaked at 24 h and decreased at 48 and 72 h after treatment with 2-ME and paclitaxel (Fig. 5A). Cyclin B1-dependent kinase activity also peaked at 24 h and decreased to control levels by 72 h with the exception of LNCaP cells treated with paclitaxel, in which activity remained significantly elevated. These results indicated that there were differences in the later (>24 h) effects of 2-ME and paclitaxel on cyclin B1-dependent kinase activity after the initial prolonged activation at 24 h. There was a 2–5-fold decrease in cyclin A protein and its associated kinase activity in all prostate cancer cell lines at 48 and 72 h, a time when apoptotic cells were increased (see Fig. 7A).

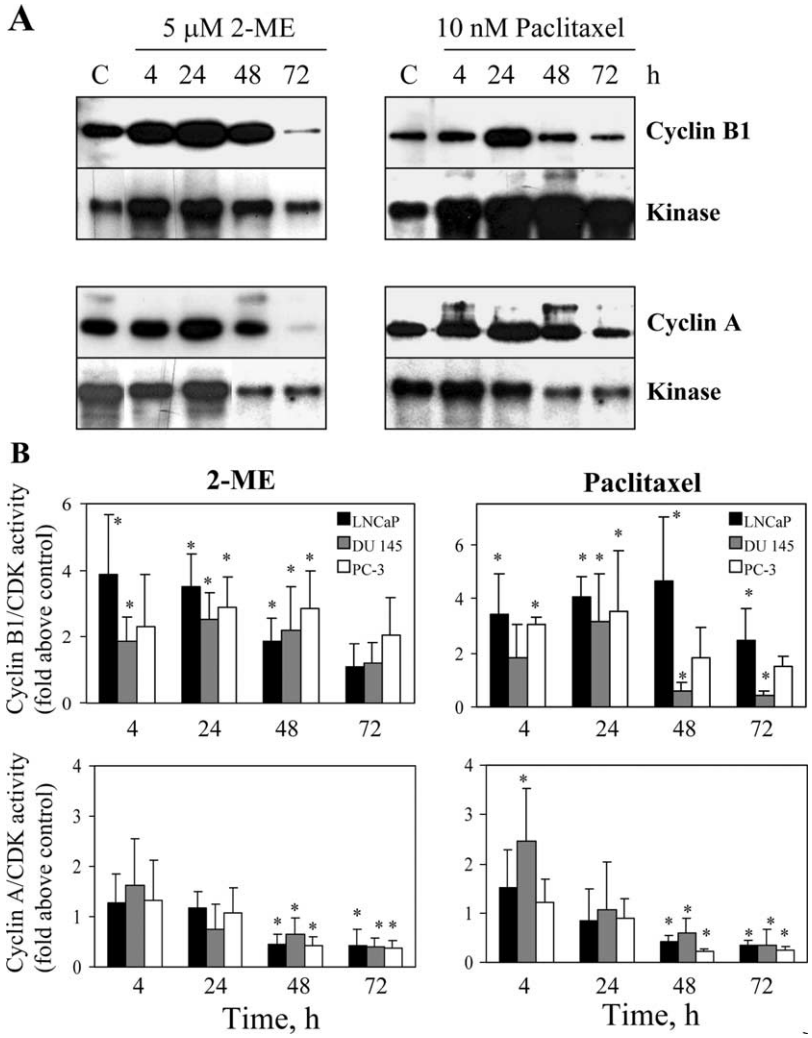

Fig. 5. Changes in cyclin B1 and A proteins and their associated kinase activities with time after treatment of prostate cancer cells with 2-ME and paclitaxel. (A) LNCaP cells were treated with 5 μM 2-ME and 10 nM paclitaxel for 4, 24, 48, and 72 h and the levels of cyclin B1 and A proteins analyzed by Western blot and compared to control (C) treated cells. Cyclin B1 and A proteins were immunoprecipitated and their associated kinase activities (^{32}P-histone) determined from the same lysates. Cyclin B1-dependent kinase activity decreased in 2-ME but not paclitaxel treated LNCaP cells at 48 and 72 h. Cyclin A-dependent kinase activity decreased in both 2-ME and paclitaxel treated LNCaP cells at 48 and 72 h. (B) 2-ME and paclitaxel treatment of LNCaP, DU 145, and PC-3 cells resulted in a peak of cyclin B1-dependent kinase activity at 24 h with subsequent decline at 48 and 72 h. The exception is paclitaxel treated LNCaP cells, which maintained high cyclin B1-dependent kinase activity at 48 and 72 h despite low cyclin B1 protein. There was a greater decrease in cyclin B1-dependent kinase activity in paclitaxel compared to 2-ME treated DU 145 cells (*, $P<0.05$). Cyclin A-dependent kinase activity decreased in all 2-ME and paclitaxel treated prostate cancer cells (*, $P<0.04$) at 48 and 72 h. Results are expressed as means (fold control = 1) ± standard deviation (error bars).

3.6. p53 and p21 proteins are increased in LNCaP cells treated with 2-ME and paclitaxel

To further investigate molecular changes involved in 2-ME and paclitaxel-mediated G1 and G2/M cell cycle arrest in LNCaP cells, we analyzed expression of p53 and p21 by Western blot (Fig. 6). The G1-promoting doses of 2-ME (2 μM) and paclitaxel (2 nM) that decreased cyclin A-dependent kinase activity (see Fig. 3) resulted in a 3–4-fold increase in

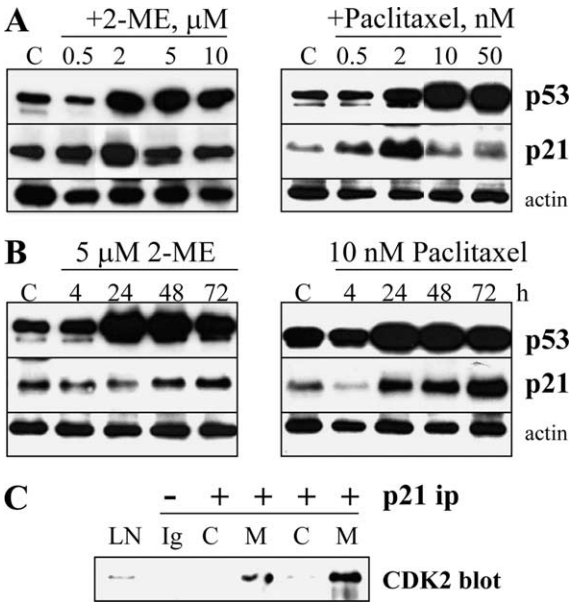

Fig. 6. 2-ME and paclitaxel increased p53 and p21 proteins in LNCaP cells. (A) LNCaP cells were treated with increasing doses of 2-ME (0.5–10 μM) and paclitaxel (0.5–50 nM) for 24 h and the levels of p53 and p21 proteins determined by Western blot, normalized to actin, and compared to control (C) treated cells. p53 increased with 2-ME (≥2 μM) and paclitaxel (≥2 nM), whereas p21 significantly increased with only 2 μM 2-ME and 2 nM paclitaxel ($P<0.05$). (B) LNCaP cells were treated with 5 μM 2-ME and 10 nM paclitaxel for 4, 24, 48, and 72 h and the levels of p53 and p21 proteins analyzed by Western blot. p53 increased at 24 h and remained elevated at 48 and 72 h, whereas p21 increased at 48 and 72 h. (C) Increased association of p21 with cdk2 protein in 2-ME treated LNCaP cells. p21 protein was immunoprecipitated (+ ip) from LNCaP cells treated with 5 μM 2-ME (M) or control (C) for 24 h and samples analyzed by Western blot for cdk2 protein. Duplicate samples from C and M are shown. Positive control was LNCaP (LN) cell total lysate and negative control was immunoprecipitation with non-specific rabbit Ig (-ip).

p53 protein (Fig. 6A); p53 is mutated in DU 145 cells and PC-3 cells and is non-functional [26]. Similarly, p53 protein levels were increased at 24 h (but not at 4 h) using the G2/M-promoting doses of 2-ME (5 μM) and paclitaxel (10 nM) and remained elevated at 48 and 72 h (Fig. 6B). Because p53 is known to increase transcription of the cdk inhibitor p21 gene [29], we also analyzed expression of p21 protein by Western blot. The G1-promoting dose of 2-ME (2 μM) and paclitaxel (2 nM) resulted in a small but significant two-fold increase in p21 protein, whereas the G2/M-promoting doses did not increase p21 (Fig. 6A). There was an increased association of p21 with cdk2 when the G1-promoting dose of 2-ME (2 μM) was utilized (Fig. 6C), suggesting a mechanism for inhibition of cyclin A-dependent kinase and blocking of LNCaP cells in G1. At 48 and 72 h, there was a 2–6-fold increase in p21 protein and this correlated with decreased cyclin A-dependent kinase activity (Figs. 5 and 6). The levels of p21 were very low in DU 145 and PC-3 cells and did not change with 2-ME and paclitaxel treatment (result not shown).

3.7. Increased apoptosis in prostate cancer cells after 2-ME and paclitaxel-mediated mitotic block

To analyze the time of the appearance of apoptotic cells relative to G2/M block, we performed DAPI staining and caspase-3 assays on prostate cancer cells treated with 2-ME (5 μM for LNCaP and DU 145; 10 μM for PC-3) and paclitaxel (10 nM) for 24, 48, and 72 h (Fig. 7A). In LNCaP, there was a significant increase of apoptotic cells from 6, 16, and >25% after 24, 48, and 72 h treatment with 2-ME and paclitaxel, which also corresponded with a significant increase in caspase-3 activity (Fig. 7A). Less apoptotic cells and caspase-3 activity were identified in 2-ME treated DU 145 and PC-3 cells compared to LNCaP cells, probably explaining the differential growth inhibition (LNCaP > DU 145 > PC-3). A difference was observed in paclitaxel treated DU 145 cells, where there were greater number of apoptotic cells (6.5, 25, 27%) compared to 2-ME treated cells (2, 9, 13%). However, there was not a corresponding increase in caspase-3 activity in paclitaxel treated DU 145 cells, possibly due to caspase-independent events or other caspases were more active.

Similar results were obtained in DU145 and PC-3 using annexin V-FITC/PI flow cytometric detection of early apoptotic cells (Fig. 7B). The greater amount of apoptosis measured with annexin V compared to DAPI probably reflected later events in the apoptotic pathway (chromatin fragmentation/condensation) that were inhibited compared to earlier events (annexin V binding). In PC-3 cells (least sensitive to 2-ME and paclitaxel), longer treatment (6 days) was required to obtain increased number of apoptotic cells (8%) (see Fig. 9B). These results indicated that the 2-ME and paclitaxel-mediated induction of apoptosis in prostate cancer cells predominantly occurred after

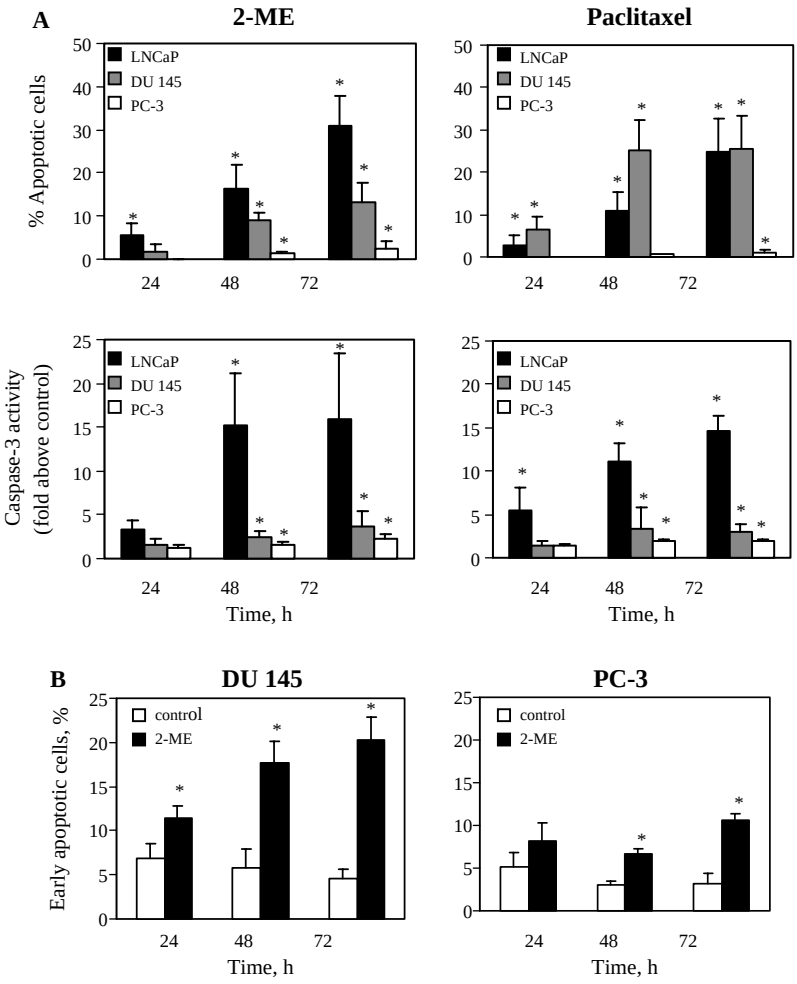

Fig. 7. 2-ME and paclitaxel increased apoptosis and caspase-3 activity in prostate cancer cells at 48 and 72 h. (A) 2-ME and paclitaxel treatment of LNCaP, DU 145, and PC-3 cells resulted in significantly increased apoptotic cells (DAPI) and caspase-3 activity at 48 and 72 h (*, $P<0.04$). Increased apoptotic cells and caspase-3 activity was greatest in LNCaP cells. In DU 145 cells, paclitaxel increased apoptotic cells greater than 2-ME at 48 and 72 h. There was minimal apoptosis (<0.5%) detected by DAPI in the control treated cells (not shown). Caspase-3 results are expressed as means (fold above control = 1) ± standard deviation (error bars). (B) Flow cytometric analysis of annexin V-FITC and PI stained DU 145 and PC-3 cells after treatment with 2-ME (5 μM for DU 145 and 10 μM for PC-3) for 24, 48, and 72 h compared to control cells ($n=6$; *, $P<0.005$). Early apoptotic cells represent the annexinV-FITC positive and PI negative population of cells.

the G2/M cell cycle block at 24 h. In contrast, treatment of LNCaP cells with G1-promoting doses (2 μM 2-ME and 2 nM paclitaxel) resulted in minimal (<1.5%) induction of apoptosis at all time points (not shown). In addition, blocking LNCaP and DU 145 cells in the S phase with 1 μM aphidicolin reduced 2-ME-mediated induction of apoptosis (result not shown), suggesting that G2/M block by 2-ME is important for induction of apoptosis.

3.8. 2-ME and paclitaxel decrease in XIAP correlates with increased apoptosis in prostate cancer cells

To investigate why 2-ME and paclitaxel-treated LNCaP cells undergo apoptosis greater than DU 145 and PC-3 cells, we sought to identify differences in the levels of proteins important in apoptosis by Western blot analysis. Cleavage of the PARP protein, indicative of apoptosis, occurred to a greater extent in 2-ME and

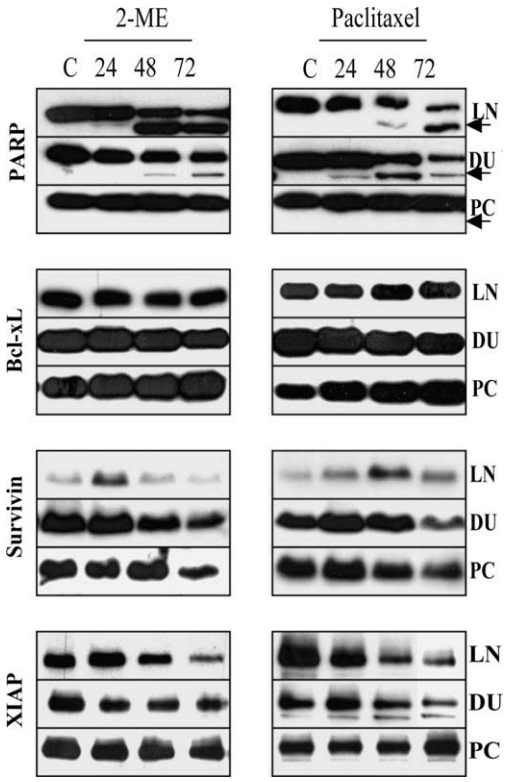

Fig. 8. 2-ME and paclitaxel decrease the levels of IAP protein XIAP at 48 and 72 h. LNCaP (LN), DU 145 (DU), and PC-3 (PC) cells were treated with 5–10 μM 2-ME and 10 nM paclitaxel for 24, 48, and 72 h and the levels of PARP, Bcl-xL, survivin, and XIAP proteins determined by Western blot, normalized to actin (not shown), and compared to control (C) treated cells. There was increased PARP cleavage (arrow) in LNCaP and DU 145 compared to PC-3 cells. There was greater cleavage of PARP in paclitaxel compared to 2-ME treated DU 145 cells. No significant differences were notable in Bcl-xL. Mitotic block and increased cyclin B1-dependent kinase activity resulted in increased survivin, which decreased at 72 h. 2-ME and paclitaxel decreased XIAP in LNCaP cells at 48 and 72 h. Paclitaxel but not 2-ME decreased XIAP in DU 145 cells at 48 and 72 h. There were no differences in XIAP levels in 2-ME treated DU 145 cells and 2-ME and paclitaxel treated PC-3 cells. The overall levels of Bcl-xL and survivin were greater in DU 145 and PC-3 compared to LNCaP cells.

paclitaxel treated LNCaP and DU 145 compared to PC-3 cells (Fig. 8). There were no differences in the levels of the anti-apoptotic protein Bcl-xL. The levels of the anti-apoptotic protein survivin increased when the cyclin B1-cdk1 activity was elevated and subsequently decreased to a level similar to or below that of control cells (Fig. 8). 2-ME and paclitaxel increase in apoptosis in LNCaP (and in paclitaxel treated DU 145) correlated with a 2–3-fold decrease in the levels of XIAP, a member of the IAP family, at 48 and 72 h [30] (Fig. 8). There were no changes in the levels of other IAP family members IAP-1 and IAP-2 (result not shown). Another potential reason for the differential sensitivity to apoptosis may be the 1.5–2-fold higher levels of the Bcl-xL and survivin proteins in DU 145 and PC-3 compared to LNCaP cells, which may have protected these cells from 2-ME and paclitaxel-mediated induction of apoptosis.

3.9. Cyclin-dependent kinase inhibitors block 2-ME and paclitaxel-mediated induction of apoptosis

To investigate whether the increase in cyclin B1-dependent kinase activity was required for 2-ME and paclitaxel-mediated induction of apoptosis, we utilized the potent cdk inhibitors purvalanol A and alsterpaullone [23,24]. Treatment of LNCaP cells with 5 μM alsterpaullone and DU 145 cells with 5 μM purvalanol A for 24 h resulted in an increase in G2/M (result not shown) and blocked the 2-ME and paclitaxel-mediated increase of cyclin B1-dependent kinase activity (Fig. 9A). In addition to inhibiting cyclin B1-dependent kinase activity, alsterpaullone also decreased cyclin A-dependent kinase in control and 2-ME and paclitaxel-treated LNCaP cells. In contrast, purvalanol A, which has a higher specificity for the inhibition of cyclin B1-dependent kinase, increased cyclin A-dependent kinase in control and 2-ME and paclitaxel-treated DU 145 cells (Fig. 9A). At 72 h, alsterpaullone and purvalanol A blocked 2-ME and paclitaxel-mediated induction of apoptosis in LNCaP and DU 145 cells, as determined by DAPI assay, caspase-3 activity, and PARP cleavage (Fig. 9B and C). Because treatment of PC-3 cells with 2-ME and paclitaxel induced minimal apoptosis at 72 h (1–2%; Fig. 7A), we chose treatment for 6 days when apoptosis increased to $>8\%$. The results showed that 10 μM alsterpaulone similarly blocked the 2-ME and paclitaxel increase of apoptosis in PC-3 cells. Kinase inhibitors PD 98059 (20 μM; MAP kinase inhibitor) and lithium chloride (30 mM; glycogen synthase kinase 3β inhibitor) did not significantly block 2-ME-mediated induction of apoptosis in LNCaP and DU 145 cells (result not shown). These results suggested that 2-ME and paclitaxel-mediated increase

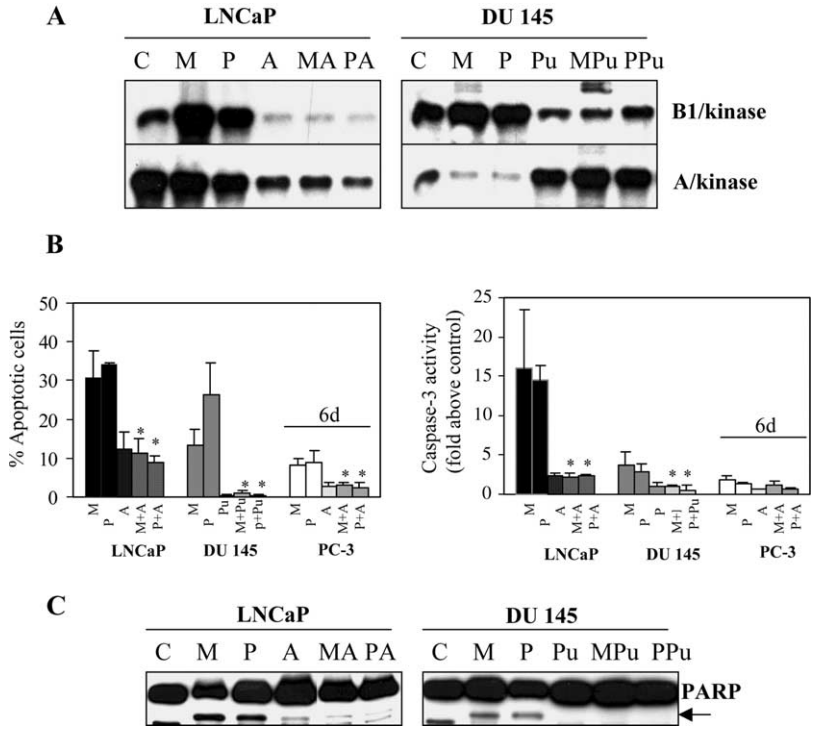

Fig. 9. Inhibition of the 2-ME and paclitaxel-mediated increase of cyclin B1-dependent kinase activity blocked induction of apoptosis. (A) LNCaP and DU 145 cells were treated for 24 h with 5–10 μM 2-ME (M), 10 nM paclitaxel (P), 5 μM alsterpaullone (A, LNCaP), 5 μM purvalanol A (Pu, DU 145), and 2-ME or paclitaxel combined with alsterpaullone (MA, PA) and purvalanol A (MPu, PPu). Cyclin B1 and A proteins were immunoprecipitated and the associated kinase activity (B1/kinase and A/kinase) determined and compared to control (C) treated cells. In LNCaP, alsterpaullone decreased both cyclin B1- and A-dependent kinase activity, whereas in DU 145 purvalanol A decreased cyclin B1-dependent kinase activity with a concomitant increase in cyclin A-dependent kinase activity. (B) Cdk inhibitors alsterpaullone and purvalanol A significantly inhibited 2-ME and paclitaxel-mediated apoptosis in LNCaP, DU 145 (72 h), and PC-3 (6 days) as determined by DAPI staining (left panel) and caspase-3 activity (right panel) (*, $P<0.01$). (C) Western blot showing that alsterpaullone and purvalanol A blocked 2-ME and paclitaxel-mediated cleavage of PARP in LNCaP and DU 145 cells at 72 h. A non-specific band was noted below the cleaved PARP fragment.

in cyclin B1-dependent kinase activity was required for induction of apoptosis in prostate cancer cells.

4. Discussion

We analyzed in human prostate cancer cells the effects of the promising chemotherapeutic drugs 2-ME and paclitaxel on the cyclin proteins important in the G2/M phase of the cell cycle. Our results suggested a requirement for G2/M-promoting doses of 2-ME (5 μM) and paclitaxel (10 nM) to increase cyclin B1-dependent kinase activity in order to induce apoptosis. Furthermore, our results suggested that androgen-dependent LNCaP cells were sensitive to inhibition by 2-ME and paclitaxel because lower drug doses increased p53 and p21 proteins, inhibited cyclin A-dependent kinase activity, and resulted in a G1 block. In addition, G2/M-promoting doses of 2-ME and paclitaxel inhibited cyclin A-dependent kinase activity in all prostate cancer cells at the time apoptosis was increased. However, the differential induction of apoptosis by 2-ME and paclitaxel in prostate cancer cells is correlated with the ability to reduce the levels of XIAP, a member of the IAP family that inhibits caspase activity [30]. Overall, our results indicated that 2-ME has a similar mechanism as paclitaxel in the effects on the cell cycle and induction of apoptosis of human prostate cancer cells.

Similar to paclitaxel treatment of prostate cancer cells, 2-ME increased cyclin B1 protein and blocked cells in mitosis [14–16]. Our results showed that the increase in cyclin B1 protein and kinase activity in LNCaP cells occurred before significant changes in the cell cycle distribution (Figs. 4 and 5). This suggests that it is not just the mitotic spindle checkpoint that increases cyclin B1 protein and kinase activity. Our data agrees with data obtained from paclitaxel treatment of breast and epidermal cancer cells showing that increase of cyclin B1 protein and its associated cdk is required for induction of apoptosis [14,15]. The mechanism proposed for the paclitaxel-mediated increase in cyclin B1 protein is by inhibition of the proteosomal degradation system, which is a key component in the reduction of cyclin B1 protein levels required for metaphase to anaphase transition during mitosis [31]. The end result of increasing cyclin B1 protein is the increase of its associated cdk1 activity, which has been shown to be important in the induction of mitotic catastrophe and many forms of apoptosis [32].

An issue is whether 2-ME and paclitaxel-mediated induction of apoptosis in prostate cancer cells requires the initial increase of cyclin B1-dependent kinase or the subsequent reduction of cyclin B1-dependent kinase activity. The decrease of cyclin B1-dependent kinase activity is proposed to cause apoptosis in sensitive cells by reducing the levels of survivin, a member of the IAP family of proteins and a substrate for cdk1 [17]. Despite the similar decreased levels of cyclin B1-dependent kinase activity in 2-ME treated prostate cancer cells, however, there was a greater induction of apoptosis in LNCaP compared to DU 145 and PC-3 cells (Figs. 5 and 7). In addition, LNCaP cells treated with paclitaxel had elevated cyclin B1-dependent kinase activity at a time when apoptosis was increased. In contrast, DU 145 cells treated with paclitaxel resulted in a faster exit from mitotic block and lower levels of survivin at 72 h, possibly contributing to the greater induction of apoptosis compared to 2-ME treated DU 145 cells (Figs. 4, 7 and 8). These results indicated that decreased cyclin B1-dependent kinase activity and exit from mitotic block varied between 2-ME and paclitaxel treatment of prostate cancer cells. Therefore, we conclude that the initial 2-ME and paclitaxel-mediated increase in cyclin B1-dependent kinase activity is more important than the subsequent decrease in activity for the induction of apoptosis. The substrates for cyclin B1-dependent kinase in addition to survivin that may mediate this effect are yet to be identified.

A common mechanism for chemotherapeutic drug inhibition of cancer cells is the increase in p53 and p21 proteins and block in the G1 phase of the cell cycle [33]. Our studies showed that a similar mechanism was also evident using lower doses of 2-ME and paclitaxel in LNCaP cells, which inhibited cyclin A-dependent kinase activity. Similar results were obtained in p53 wild type lung and breast cancer cell lines treated with 3–6 nM paclitaxel [34]. In order to maximize induction of apoptosis, however, G2/M-promoting doses of 2-ME (5 μM) and paclitaxel (10 nM) that increased cyclin B1-dependent kinase activity were required. In addition, the G2/M-promoting doses of 2-ME (5 μM) and paclitaxel (10 nM) inhibited cyclin A-dependent kinase activity at a time when apoptosis was maximized at 48 and 72 h. An important role for inhibition of cdk2 and induction of apoptosis in cancer but not normal cells was reported [35]. However, a recent report casts doubt on the importance of cdk2 inhibition in cancer therapy [36]. The cdk inhibitor purvalanol A as a single drug inhibited cyclin B1—but not cyclin A-dependent kinase activity in DU 145 cells, resulting in minimal apoptosis. Purvalanol A combined with 2-ME or paclitaxel blocked induction of apoptosis, indicating the importance of increased cyclin B1-dependent kinase activity (Fig. 9). In contrast, alsterpaullone as a single drug inhibited both cyclin B1- and cyclin A-dependent kinase activity and induced apoptosis in LNCaP cells. However, alsterpaullone blocked the 2-ME or paclitaxel-mediated induction of apoptosis (Fig. 9). We suggest that in addition to the early activation of cyclin B1-dependent kinase activity, later inhibition of cyclin A-dependent kinase activity plays an important role in 2-ME and paclitaxel inhibition of prostate cancer cells.

The effects of 2-ME and paclitaxel on cyclin B1- and cyclin A-dependent kinase activity cannot explain the differential induction of apoptosis in prostate cancer cells (LNCaP $\geq$ DU 145 $>$ PC-3). It is likely that the expression of wild type p53 in LNCaP but not in DU 145 and PC-3 cells plays an important role in the greater induction of apoptosis. An important role for p53 in 2-ME-mediated apoptosis has been demonstrated for LNCaP and lung cancer cells [10,37]. The ability of 2-ME

and paclitaxel to decrease the levels of the IAP family member XIAP at 48 and 72 h correlated with increased apoptosis (Figs. 7 and 8). Inhibition of XIAP has been shown to increase apoptosis in cancer cells either directly or indirectly by sensitizing to other chemotherapeutic drugs [38,39]. A predominant role for members of the IAP family in the regulation of the induction of apoptosis in prostate cancer cells has been proposed [40]. Therefore, drugs that decrease the levels of anti-apoptotic proteins like XIAP should shift the overall balance towards apoptosis even in the most resistant AI-PC cells. In addition, higher levels of the anti-apoptotic proteins Bcl-xL and survivin in DU 145 and PC-3 compared to LNCaP may contribute to the differential induction of apoptosis by 2-ME and paclitaxel. Overexpression of Bcl-xL has a well established role as a powerful anti-apoptosis factor in prostate cancer and inhibition of Bcl-xL by anti-sense oligonucleotides can sensitize PC-3 cells to drug-mediated apoptosis [41,42].

In summary, our studies indicate that 2-ME is similar to paclitaxel in the early activation of cyclin B1- and later inhibition of cyclin A-dependent kinase activity and this may be an important mechanism for induction of apoptosis in prostate cancer cells. We are currently investigating in a transgenic mouse model of prostate cancer [43] whether these molecular changes are also occurring in vivo. Anti-cancer chemotherapeutic agents ideally should take advantage of the molecular differences between transformed and normal cells and induce apoptosis only in cancer cells. Two such differences may be the overexpression of cyclin B1 protein in cancer cells [44] and the differential sensitivity of cancer cells to the inhibition of cyclin A-dependent kinase [35]. We suggest that 2-ME and paclitaxel take advantage of these differences to inhibit the growth of prostate cancer cells and induce apoptosis. Given that paclitaxel has an effect on patients with AI-PC as a single drug and in combination with other drugs [45], our results hold promise that 2-ME will have a similar efficacy in AI-PC.

Acknowledgements

We thank Alicia De Las Pozas and Adriana Gomez for excellent technical assistance, Ron Hamelik for help with flow cytometry, and Drs Bernard Roos and Awtar Krishan for review of this manuscript. This work was supported by V.A. Merit Review (026901) and Department of Defense (DAMD17-03-1-0179) to C. Perez-Stable.

References

[1] B.T. Zhu, A.H. Conney, Is 2-methoxyestradiol an endogenous estrogen metabolite that inhibits mammary carcinogenesis?, Cancer Res. 58 (1998) 2269–2277.
[2] V.S. Pribluda, E.R. Gubish, T.M. LaValle, A. Treston, G.M. Swartz, S.J. Green, 2-Methoxyestradiol: an endogenous antiangiogenic and antiproliferative drug candidate, Cancer Met. Rev. 19 (2000) 173–179.
[3] N.J. Lakhani, M.A. Sarkar, J. Venitz, W.D. Figg, 2-Methoxyestradiol, a promising anticancer agent, Pharmacotherapy 23 (2003) 165–172.
[4] S.L. Mooberry, Mechanism of action of 2-methoxyestradiol: new developments, Drug Resist. Update 6 (2003) 355–361.
[5] L.R. Qadan, C.M. Perez-Stable, C. Anderson, G. D'Ippolito, A. Herron, G.A. Howard, B.A. Roos, 2-Methoxyestradiol induces G2/M arrest and apoptosis in prostate cancer, Biochem. Biophys. Res. Commun. 285 (2001) 1259–1266.
[6] A.P. Kumar, G.E. Garcia, T.H. Slaga, 2-methoxyestradiol blocks cell-cycle progression at G(2)/M phase and inhibits growth of human prostate cancer cells, Mol. Carcinog. 31 (2001) 111–124.
[7] T.M. LaValle, X.H. Zhan, C.J. Herbstritt, E.C. Kough, S.J. Green, V.S. Pribluda, 2-Methoxyestradiol inhibits proliferation and induces apoptosis independently of estrogen receptors alpha and beta, Cancer Res. 62 (2002) 3691–3697.
[8] S. Bu, A. Blaukat, X. Fu, N.E. Heldin, M. Landstrom, Mechanisms for 2-methoxyestradiol-induced apoptosis of prostate cancer cells, FEBS Lett. 531 (2002) 141–151.
[9] A. Basu, S. Haldar, Identification of a novel Bcl-xL phosphorylation site regulating the sensitivity of taxol- or 2-methoxyestradiol-induced apoptosis, FEBS Lett. 538 (2003) 41–47.
[10] K. Shimada, M. Nakamura, E. Ishida, M. Kishim, N. Konishi, Roles of p38- and c-jun NH2-terminal kinase-mediated pathways in 2-methoxyestradiol-induced p53 induction and apoptosis, Carcinogenesis 24 (2003) 1067–1075.
[11] T.M. LaVallee, X.H. Zhan, M.S. Johnson, C.J. Herbstritt, G. Swartz, M.S. Williams, et al., 2-Methoxyestradiol up-regulates death receptor 5 and induces apoptosis through activation of the extrinsic pathway, Cancer Res. 63 (2003) 468–475.
[12] N.J. Mabjeesh, D. Escuin, T.M. LaVallee, V.S. Pribluda, G.M. Swartz, M.S. Johnson, et al., 2ME2 inhibits tumor growth and angiogenesis by disrupting microtubules and dysregulating HIF, Cancer Cell 3 (2003) 363–375.
[13] T.H. Wang, H.S. Wang, Y.K. Soong, Paclitaxel-induced cell death: where the cell cycle and apoptosis come together, Cancer 88 (2000) 2619–2628.

[14] S.C. Shen, T.S. Huang, S.H. Jee, M.L. Kuo, Taxol-induced p34cdc2 kinase activation and apoptosis inhibited by 12-*O*-tetradecanoylphorbol-13-acetate in human breast MCF-7 carcinoma cells, Cell Growth Diff. 9 (1998) 23–29.
[15] Y.H. Ling, U. Consol, C. Tornos, M. Andreeff, R. Perez-Soler, Accumulation of cyclin B1, activation of cyclin B1-dependent kinase and induction of programmed cell death in human epidermoid carcinoma KB cells treated with taxol, Int. J. Cancer 75 (1998) 925–932.
[16] R. Panvichian, K. Orth, M.J. Pilat, M.L. Day, K.C. Day, C. Yee, et al., Signaling network of paclitaxel-induced apoptosis in the LNCaP prostate cancer cell line, Urology 54 (1999) 746–752.
[17] D.S. O'Connor, N.R. Wall, A.C. Porter, D.C. Altieri, A p34(cdc2) survival checkpoint in cancer, Cancer Cell 2 (2002) 43–54.
[18] D.S. O'Connor, D. Grossman, J. Plescia, F. Li, H. Zhang, A. Villa, et al., Regulation of apoptosis at cell division by p34cdc2 phosphorylation of survivin, Proc. Natl Acad. Sci. USA 97 (2000) 13103–13107.
[19] J.S. Horoszewicz, S.S. Leong, E. Kawinski, J.P. Kerr, H. Rosenthal, T.M. Chu, et al., LNCaP model of human prostatic carcinoma, Cancer Res. 43 (1983) 1809–1818.
[20] K.R. Stone, D.D. Mickey, H. Wunderli, G.H. Mickey, F. Paulson, Isolation of a human prostate carcinoma cell line (DU 145), Int. J. Cancer 21 (1978) 274–281.
[21] M.E. Kaighn, K.S. Narayan, Y. Ohnuki, J.F. Lechner, L.W. Jones, Establishment and characterization of a human prostatic carcinoma cell line (PC-3), Invest. Urol. 17 (1979) 16–23.
[22] A. Krishan, Rapid DNA content analysis by the propidium iodide–hypotonic citrate method, Methods Cell Biol. 33 (1990) 121–125.
[23] N.S. Gray, L. Wodicka, A.M. Thunnissen, T.C. Norman, S. Kwon, F.H. Espinoza, et al., Exploiting chemical libraries, structure, and genomics in the search for kinase inhibitors, Science 281 (1998) 533–538.
[24] C. Schultz, A. Link, M. Leost, D.W. Zaharevitz, R. Gussio, E.A. Sausville, et al., Paullones, a series of cyclin-dependent kinase inhibitors: synthesis, evaluation of CDK1/cyclin B inhibition, and in vitro antitumor activity, J. Med. Chem. 42 (1999) 2909–2919.
[25] F.H. Sarkar, W. Sakr, Y.W. Li, J. Macoska, D.E. Ball, J.D. Crissman, Analysis of retinoblastoma (RB) gene deletion in human prostatic carcinomas, Prostate 21 (1992) 145–152.
[26] A.G. Carroll, H.J. Voeller, L. Sugars, E.P. Gelmann, p53 oncogene mutations in three human prostate cancer cell lines, Prostate 23 (1993) 123–134.
[27] C.H. Yam, T.K. Fung, R.Y. Poon, Cyclin A in cell cycle control and cancer, Cell Mol. Life Sci. 59 (2002) 1317–1326.
[28] K.L. King, J.A. Cidlowski, Cell cycle regulation and apoptosis, Annu. Rev. Physiol. 60 (1998) 601–617.
[29] W.S. El-Deiry, T. Tokino, V.E. Velculescu, D.B. Levy, R. Parsons, J.M. Trent, et al., WAF1, a potential mediator of p53 tumor suppression, Cell 75 (1993) 817–825.
[30] P. Liston, W.G. Fong, R.G. Korneluk, The inhibitors of apoptosis: there is more to life than Bcl2, Oncogene 22 (2003) 8568–8580.
[31] P. Clute, J. Pines, Temporal and spatial control of cyclin B1 destruction in metaphase, Nat. Cell Biol. 1 (1999) 82–87.
[32] M. Castedo, J.L. Perfettini, T. Roumier, G. Kroemer, Cyclin-dependent kinase-1: linking apoptosis to cell cycle and mitotic catastrophe, Cell Death. Differ. 9 (2002) 1287–1293.
[33] J. Bartek, J. Lukas, Pathways governing G1/S transition and their response to DNA damage, FEBS Lett. 490 (2001) 117–122.
[34] P. Giannakakou, R. Robey, T. Fojo, M.V. Blagosklonny, Low concentrations of paclitaxel induce cell type-dependent p53, p21 and G1/G2 arrest instead of mitotic arrest: molecular determinants of paclitaxel-induced cytotoxicity, Oncogene 20 (2001) 3806–3813.
[35] Y.N. Chen, S.K. Sharma, T.M. Ramsey, L. Jiang, M.S. Martin, K. Baker, et al., Selective killing of transformed cells by cyclin/cyclin-dependent kinase 2 antagonists, Proc. Natl Acad. Sci. 96 (1999) 4325–4329.
[36] O. Tetsu, F. McCormick, Proliferation of cancer cells despite CDK2 inhibition, Cancer Cell 3 (2003) 233–245.
[37] T. Mukhopadhyay, J.A. Roth, Superinduction of wild-type p53 protein after 2-methoxyestradiol treatment of Ad5p53-transduced cells induces tumor cell apoptosis, Oncogene 17 (1998) 241–246.
[38] A.D. Schimmer, K. Welsh, C. Pinilla, Z. Wang, M. Krajewska, M.J. Bonneau, et al., Small-molecule antagonists of apoptosis suppressor XIAP exhibit broad antitumor activity, Cancer Cell 5 (2004) 25–35.
[39] C.P. Ng, A. Zisman, B. Bonavida, Synergy is achieved by complementation with Apo2L/TRAIL and actinomycin D in Apo2L/TRAIL-mediated apoptosis of prostate cancer cells: role of XIAP in resistance, Prostate 53 (2002) 286–299.
[40] J.P. Carson, M. Behnam, J.N. Sutton, C. Du, X. Wang, D.F. Hunt, et al., Smac is required for cytochrome *c*-induced apoptosis in prostate cancer LNCaP cells, Cancer Res. 62 (2002) 18–23.
[41] I. Lebedeva, R. Rando, J. Ojwang, P. Cossum, C.A. Stein, Bcl-xL in prostate cancer cells: effects of overexpression and down-regulation on chemosensitivity, Cancer Res. 60 (2000) 6052–6060.
[42] X. Li, M. Marani, R. Mannucci, B. Kinsey, F. Andriani, I. Nicoletti, et al., Overexpression of BCL-X(L) underlies the molecular basis for resistance to staurosporine-induced apoptosis in PC-3 cells, Cancer Res. 61 (2001) 1699–1706.
[43] C.M. Perez-Stable, G.G. Schwartz, A. Farinas, M. Finegold, L. Binderup, G.A. Howard, B.A. Roos, The Gγ/T-15 transgenic mouse model of androgen-independent prostate cancer: target cells of carcinogenesis and the effect of the vitamin D analogue EB 1089 Cancer Epidemiol, Biomarkers Prev. 11 (2002) 555–563.
[44] H. Kao, J.A. Marto, T.K. Hoffmann, J. Shabanowitz, S.D. Finkelstein, T.L. Whiteside, et al., Identification of cyclin B1 as a shared human epithelial tumor-associated antigen recognized by T cells, J. Exp. Med. 194 (2001) 1313–1323.
[45] D.P. Petrylak, Chemotherapy for androgen-independent prostate cancer, Semin. Urol. Oncol. 20 (2002) 31–35.

Sequential combination of flavopiridol and docetaxel reduces the levels of X-linked inhibitor of apoptosis and AKT proteins and stimulates apoptosis in human LNCaP prostate cancer cells

Adriana Gomez,[3] Alicia de las Pozas,[1] and Carlos Perez-Stable[1,2]

[1]Geriatric Research, Education, and Clinical Center and Research Service, Veterans Affairs Medical Center; [2]Department of Medicine and Sylvester Comprehensive Cancer Center, University of Miami Miller School of Medicine; [3]South Florida Veterans Affairs Foundation, Miami, Florida

Abstract

Clinical trials have shown that chemotherapy with docetaxel combined with prednisone can improve survival of patients with androgen-independent prostate cancer. It is likely that the combination of docetaxel with other novel chemotherapeutic agents would also improve the survival of androgen-independent prostate cancer patients. We investigated whether the combination of docetaxel and flavopiridol, a broad cyclin-dependent kinase inhibitor, can increase apoptotic cell death in prostate cancer cells. Treatment of DU 145 prostate cancer cells with 500 nmol/L flavopiridol and 10 nmol/L docetaxel inhibited apoptosis probably because of their opposing effects on cyclin B1–dependent kinase activity. In contrast, when LNCaP prostate cancer cells were treated with flavopiridol for 24 hours followed by docetaxel for another 24 hours (FD), there was a maximal induction of apoptosis. However, there was greater induction of apoptosis in DU 145 cells when docetaxel was followed by flavopiridol or docetaxel. These findings indicate a heterogeneous response depending on the type of prostate cancer cell. Substantial decreases in X-linked inhibitor of apoptosis (XIAP) protein but not survivin, both being members of the IAP family, were required for FD enhanced apoptosis in LNCaP cells. Androgen ablation in androgen-independent LNCaP cells increased activated AKT and chemoresistance to apoptosis after treatment with FD. The proteasome inhibitor MG-132 blocked FD-mediated reduction of XIAP and AKT and antagonized apoptosis, suggesting that the activation of the proteasome pathway is one of the mechanisms involved. Overall, our data suggest that the docetaxel and flavopiridol combination requires a maximal effect on cyclin B1–dependent kinase activity and a reduction of XIAP and AKT prosurvival proteins for augmentation of apoptosis in LNCaP cells. [Mol Cancer Ther 2006;5(5):1–11]

Introduction

Prostate cancer is the most frequently diagnosed noncutaneous malignancy and the second leading cause of cancer-related deaths among men in the United States (1). The principal therapy for men with advanced disease is androgen ablation, but most of these patients eventually progress to an androgen-independent disease (2). Docetaxel (Taxotere), a semisynthetic derivative of paclitaxel (Taxol) originally derived from the yew tree (3), is a promising anticancer drug shown to inhibit a wide variety of tumor cells, including prostate cancer cells by diverse mechanisms that include cell cycle arrest, induction of apoptosis, stabilization of microtubules, and inhibition of angiogenesis (4, 5). Studies showing that treatment with docetaxel combined with prednisone can improve survival of patients with androgen-independent prostate cancer have been recently reported (6). It is likely that docetaxel combined with other novel chemotherapeutic drugs would also result in improved patient survival. The ability of chemotherapeutic drugs, such as docetaxel, to induce apoptotic cell death in prostate cancer cells is probably one of the chief mechanisms involved in improved survival. However, the precise mechanisms of how docetaxel in combination with other drugs induces apoptosis in prostate cancer cells are not known.

Flavopiridol, a semisynthetic flavonoid derived from an indigenous plant from India, is a broad inhibitor of cyclin-dependent kinases (cdk) and is being tested in clinical trials (7, 8). Treatment of cancer cells with flavopiridol results in a decrease in cyclins D1 and B1 leading to a cell cycle arrest in G_1 and G_2-M phases (9, 10). Flavopiridol also reduces the levels of the antiapoptotic proteins Bcl-2, Bcl-xL, Mcl-1, and X-linked inhibitor of apoptosis (XIAP) and sensitizes cancer cells to apoptosis after subsequent treatment with other chemotherapeutic agents (10–13). However, results from phase II clinical trials of flavopiridol as a single agent have been reported to be unsatisfactory,

Received 11/10/05; revised 2/3/06; accepted 3/2/06.

Grant support: Aventis Pharmaceuticals grant GIA 60025, Veterans Affairs Merit Review grant 026901, and Department of Defense grant DAMD17-03-1-0179 (C. Perez-Stable).

The costs of publication of this article were defrayed in part by the payment of page charges. This article must therefore be hereby marked advertisement in accordance with 18 U.S.C. Section 1734 solely to indicate this fact.

Request for reprints: Carlos Perez-Stable, Geriatric Research, Education, and Clinical Center and Research Service, Veterans Affairs Medical Center, 11-GRC, 1201 Northwest 16 Street, Miami, FL 33125. Phone: 305-324-4455, ext. 4391; Fax: 305-575-3365. E-mail: cperez@med.miami.edu

doi:10.1158/1535-7163.MCT-05-0467

indicating that flavopiridol may work best as an anticancer agent when combined with other agents (14, 15). Whether flavopiridol and docetaxel can enhance apoptotic cell death in prostate cancer cells has not been investigated previously.

One of the proposed mechanisms for the anticancer effect of docetaxel is the stabilization of microtubules, activation of the mitotic checkpoint, and blockade of the degradation of cyclin B1, which leads to a prolonged activation of its associated kinase cdk1, mitotic arrest, and induction of apoptosis (4, 5, 16, 17). An increase in cdk1 activity results in phosphorylation and stabilization of survivin, a member of the IAP family and a substrate for cdk1 (18). Therefore, it has been proposed that the subsequent decrease in cyclin B1-cdk1 activity results in a decrease in the levels of survivin and an increase in sensitivity to induction of apoptosis (19). Preclinical studies in human gastric and breast cancer cell lines have shown that the greatest increase in apoptosis occurs when docetaxel is followed by flavopiridol (16). The hypothesis of this regimen is that flavopiridol treatment after the docetaxel-mediated mitotic block results in the inhibition of cyclin B1-cdk activity, a decrease in phosphorylated survivin, a more rapid exit from mitosis, and an increase in apoptosis. Whether this mechanism is generally applicable to androgen-dependent and androgen-independent prostate cancer cells is not known.

Treatment with single chemotherapeutic agents, such as docetaxel and flavopiridol, will not cure most cancers, including androgen-independent prostate cancer. Therefore, the purpose of the present study was to determine whether the combination of docetaxel and flavopiridol could increase apoptotic cell death in prostate cancer cells. Our results show that in androgen-dependent and androgen-independent LNCaP prostate cancer cells sequential treatment with flavopiridol followed by docetaxel (FD) produces the greatest enhancement of apoptotic cell death. Our data suggest that substantial decreases in XIAP (member of the IAP family; refs. 20, 21) and AKT (prosurvival factor; ref. 22) proteins are important mediators for increased apoptosis in FD-treated LNCaP cells. Because XIAP and AKT activity is up-regulated in most types of cancer, including androgen-independent prostate cancer (22–26), and confers resistance to chemotherapeutic drugs (22, 27, 28), these results suggest that drug combinations that substantially reduce XIAP and AKT proteins will provide the greatest extent of apoptosis.

Materials and Methods

Reagents

Flavopiridol and docetaxel were obtained from Aventis Pharmaceuticals (Bridgewater, NJ). Propidium iodide (PI) and DMSO were purchased from Sigma (St. Louis, MO). Histone H1 protein was purchased from Roche Applied Sciences (Indianapolis, IN). 4′,6-Diamidino-2-phenylindole (DAPI), MG-132, LY 294002, 5,6-dichloro-1-β-D-ribofuranosyl-benzimidazole, alsterpaullone, epoxomicin, and parthenolide were purchased from Calbiochem (San Diego, CA). Annexin V-FITC was purchased from Santa Cruz Biotechnology (Santa Cruz, CA).

Cell Culture

Human prostate carcinoma cell lines LNCaP (29) and DU 145 (30) were obtained from the American Type Culture Collection (Rockville, MD). LN-AI is an androgen-independent derivative of the human prostate cancer cell line LNCaP, which was spontaneously derived in our laboratory (31). These cells express androgen receptor and prostate-specific antigen similar to LNCaP. LNCaP, LN-AI, and DU 145 were maintained in RPMI 1640 (Invitrogen, Carlsbad, CA) with 5% fetal bovine serum (Hyclone, Logan, UT), 100 units/mL penicillin, 100 μg/mL streptomycin, and 0.25 μg/mL amphotericin (Invitrogen). Unlike androgen-dependent LNCaP, the LN-AI cells are able to grow for long-term in RPMI 1640 with 5% charcoal-stripped fetal bovine serum and are called LN-AI/CSS. The normal rat prostate basal epithelial cell line NRP-152 (provided by Dr. David Danielpour) was maintained in HEPES-free DMEM/F12 (1:1, v/v) with 5% fetal bovine serum, antibiotic/antimycotic, 20 ng/mL epidermal growth factor, 10 ng/mL cholera toxin, 5 μg/mL insulin, and 0.1 μmol/L dexamethasone (32). Human mesenchymal stromal cells derived from bone marrow were obtained from Gianluca D'Ippolito and cultured in DMEM (low glucose) with 5% fetal bovine serum and antibiotic/antimycotic (33).

Treatment with Flavopiridol and Docetaxel

For treatment with flavopiridol or docetaxel, 7×10^5 LNCaP cells, 5×10^5 LN-AI, 10×10^5 LN-AI/CSS, 3×10^5 DU 145 cells, 1×10^5 NRP-152 cells, and 2×10^5 mesenchymal stromal cells were seeded per 6-cm dish and allowed to attach overnight. The next day, fresh medium containing different doses of flavopiridol (10–500 nmol/L), docetaxel (2–50 nmol/L), or DMSO (0.1%) control was added and the cells were cultured for varying times (24–72 hours). For the sequential combinations of flavopiridol and docetaxel, after 24 hours treatment with 500 nmol/L flavopiridol or 10 nmol/L docetaxel, floating cells were removed, centrifuged, resuspended in the appropriate medium containing flavopiridol, docetaxel, or DMSO, added back to the attached cells, and incubated for an additional 24 hours. In all the experiments, floating and trypsinized attached cells were pooled for further analysis. Similar experiments were conducted using alsterpaullone (5 μmol/L), LY 294002 (20 μmol/L), MG-132 (5 μmol/L), and epoxomicin (1 μmol/L).

Flow Cytometric Analysis

Propidium/hypotonic citrate method (34) was used to study cell cycle distribution of flavopiridol- and docetaxel-treated prostate cancer cells. After harvesting and washing cells with PBS, the cell pellets were resuspended in 0.5 mL PI staining solution (0.1% sodium citrate, 0.03% NP40, 50 μg/mL PI) and vortexed to release nuclei, and DNA distribution histograms were generated by analysis of 10,000 nuclei in a Coulter XL flow cytometer. The percentage of

cells in the G_1, S, and G_2-M DNA content was determined by the ModFit program (Verity Software House, Topsham, ME) from six to eight samples analyzed from at least three independent experiments.

Western Blot Analysis

Cell pellets were resuspended in NP40 cell lysis buffer [1% NP40, 50 mmol/L Tris (pH 8.0), 150 mmol/L NaCl, 2 mmol/L EGTA, 2 mmol/L EDTA, protease inhibitor tablet, 50 mmol/L NaF, 0.1 mmol/L $NaVO_4$], lysed by vortex, left on ice for 30 minutes, and centrifuged, and the protein concentrations of the supernatant were determined with the Bio-Rad protein assay. After separation of 25 to 50 μg protein by SDS-PAGE, proteins were transferred by electrophoresis to Immobilon-P membrane and incubated in 5% nonfat dry milk, PBS, and 0.25% Tween 20 for 1 hour. Antibodies specific for cyclin B1 (GNS1), cyclin A (H-432), survivin (FL-142), Mcl-1 (S-19; Santa Cruz Biotechnology), poly(ADP-ribose polymerase) (PARP; C2-10), Bcl-xL (polyclonal; BD Biosciences PharMingen, San Diego, CA), XIAP, cleaved caspase-3, phosphorylated AKT (Ser^{473}; 587F11), and AKT (9272; Cell Signaling Technology, Beverly, MA) were diluted 1:1,000 to 1:3,000 in 5% nonfat dry milk, PBS, and 0.25% Tween 20 and incubated overnight at 4°C. Membranes were washed in PBS and 0.25% Tween 20 and incubated with the appropriate horseradish peroxidase–conjugated secondary antibody (1:1,000 dilution; Santa Cruz Biotechnology) for 1 hour, washed in PBS and 0.25% Tween 20, and analyzed by exposure to X-ray film using Enhanced Chemiluminescence Plus (Amersham Pharmacia Biotech). Phosphorylated AKT blots were stripped and reprobed with AKT antibody. Antibodies specific for α-tubulin (TU-02; 1:5,000 dilution; Santa Cruz Biotechnology) were used as protein loading controls. Total proteins were stained with Coomassie blue for an additional protein loading control. Changes in protein levels were determined as described previously (35) from at least four different samples analyzed from two to three independent experiments.

Cyclins B1– and A–Dependent Kinase Assay

Total protein (400 μg) was incubated with 2 μg anti–cyclin B1 (H-433; Santa Cruz Biotechnology) or cyclin A antibody for 3 hours on ice followed by the addition of 20 μL protein A/G-agarose (Santa Cruz Biotechnology) and incubation overnight at 4°C. with agitation. Immune complexes were collected by centrifugation, washed thrice with NP40 cell lysis buffer, thrice with kinase buffer [10 mmol/L Tris-HCl (pH 7.5), 150 mmol/L NaCl, 10 mmol/L $MgCl_2$, 0.5 mmol/L DTT], resuspended in kinase buffer containing 2 μg histone H1 substrate protein, 25 μmol/L ATP, 5 μCi [γ^{32}P]ATP, and incubated for 30 minutes at 30°C. Reactions were stopped with SDS gel loading buffer, samples were electrophoresed on SDS-PAGE, electroblotted to Immobilon P membranes, and analyzed by autoradiography. Coomassie blue staining of membranes revealed similar loading of histone proteins. Changes in kinase activity were determined as described previously (35) from at least four different samples analyzed from two independent experiments.

Apoptosis Assays

For the DAPI staining apoptosis assay, cells were resuspended in 0.6 mL of 4% paraformaldehyde/PBS for 15 minutes, washed with PBS, and resuspended in 0.5 mL DAPI (1 μg/mL)/PBS for 10 minutes. Cells were washed with PBS and 10 μL concentrated cells were added on a microscope slide followed by placement of a coverslip. Cells containing densely stained and fragmented chromatin were identified as apoptotic using a Nikon fluorescence microscope with a DAPI filter. The number of apoptotic cells in at least 200 total cells was determined from at least four random microscope fields. Changes in apoptosis from flavopiridol- and docetaxel-treated cells were determined as percentage of apoptotic cells in at least five different samples from three independent experiments. Only minimal apoptosis was detected in control-treated cells (<0.5%). For the Annexin V apoptosis assay, LN-AI and DU 145 prostate cancer cells were resuspended in 100 μL Annexin V binding buffer [10 mmol/L HEPES (pH 7.9), 140 mmol/L NaCl, 2.5 mmol/L $CaCl_2$] followed by the addition of 2.5 μL Annexin V-FITC and 2 μL PI (50 μg/mL) and incubated for 20 minutes at room temperature. After the addition of 400 μL Annexin V binding buffer, the cells were read by flow cytometry and the percentage of early apoptotic cells was determined by measuring the Annexin V-FITC–positive/PI-negative quadrant using WinMDI version 2.8.

RNase Protection Assay

RNA from prostate cancer cells sequentially treated with flavopiridol and docetaxel was isolated using QIAshredder and RNeasy miniprep kit (Qiagen, Inc., Valencia, CA). The hAPO-5c human apoptosis multiprobe template set (BD Biosciences PharMingen) was used for T7 RNA polymerase (Ambion, Austin, TX) synthesis of ^{32}P-labeled antisense RNA probes specific for XIAP, survivin, and glyceraldehyde-3-phosphate dehydrogenase. Total RNA (10 μg) was hybridized to antisense RNA probes at 56°C overnight followed by digestion with RNase mixture (Ambion) at 30°C for 45 minutes. RNase digestion products were analyzed by electrophoresis on 5% polyacrylamide-urea gels followed by autoradiography.

Transfection of XIAP Small Interfering RNA

LN-AI/CSS cells (2×10^5) were seeded in 12-well plates and transfected the next day with 200 nmol/L small interfering RNA (siRNA) SMART pool specific for XIAP and siCONTROL nontargeting pool (Dharmacon, Lafayette, CO) using Oligofectamine (Invitrogen) following the manufacturer's instructions. After 72 hours, cells were harvested and analyzed for expression of XIAP by Western blot as described above. Subsequently, LN-AI/CSS cells were transfected with XIAP and control siRNA for 24 hours followed by treatment with FD with or without 20 μmol/L LY 294002 for an additional 48 hours. The numbers of apoptotic cells were determined by DAPI staining as described above. Changes in apoptosis were determined in at least eight different samples analyzed from three independent experiments.

Statistical Analysis

Statistical differences between drug-treated and control cells were determined by two-tailed Student's t test with $P < 0.05$ considered significant.

Results

To evaluate the effect of flavopiridol and docetaxel as single drugs and in combination, we used various human prostate cancer cell lines (LNCaP, LN-AI, LN-AI/CSS, and DU 145), a nontransformed rat prostate cell line (NRP-152), and a primary human mesenchymal stromal cell line. These cells provide useful *in vitro* models of the different stages of progression of human prostate cancer, from normal nontransformed to androgen-independent prostate cancer compared with a primary nontransformed nonprostate cell.

G_1 and G_2-M Cell Cycle Effects of Flavopiridol- and Docetaxel-Treated Prostate Cancer Cells

To evaluate the cell cycle effects of flavopiridol and docetaxel on LNCaP and DU 145 prostate cancer cells, we did flow cytometric analysis after treatment with varying doses of flavopiridol (10–500 nmol/L) and docetaxel (0.5–50 nmol/L) for 24 hours (Fig. 1). The treatment of LNCaP and DU 145 cells with increasing doses of flavopiridol (≥50–100 nmol/L) results in an increase in cells in G_1 and G_2-M with a decrease in S phase (Fig. 1). These results reflect the ability of flavopiridol to inhibit multiple cdks important in the G_1 and G_2-M phases of the cell cycle. Flow cytometric analysis of LNCaP and DU 145 cells treated with varying doses of docetaxel (2–50 nmol/L) shows that

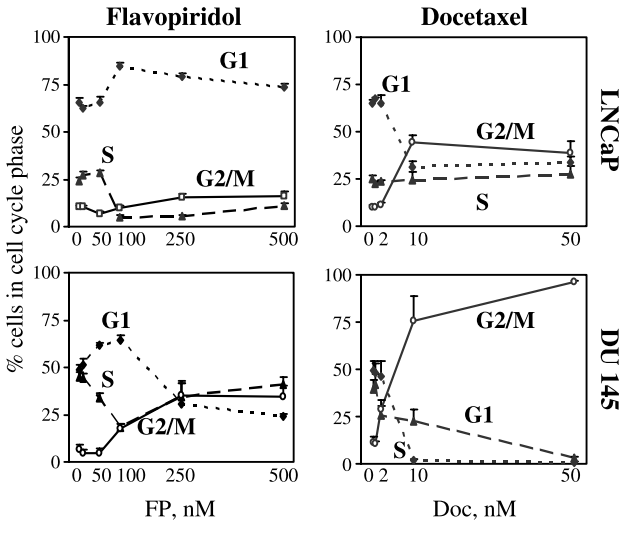

Figure 1. Flow cytometric analysis of flavopiridol and docetaxel dose responses in human prostate cancer cells. LNCaP and DU 145 cells were treated with varying doses of flavopiridol (*FP*; 10–500 nmol/L) and docetaxel (*Doc*; 0.5–50 nmol/L) for 24 h and the percentage of cells in the cell cycle phases (G_1, S, and G_2-M) was determined by flow cytometry. Increasing doses of flavopiridol (≥50–100 nmol/L) resulted in increased LNCaP and DU 145 cells in G_1 and G_2-M with decreased S phase. Docetaxel doses ≥10 nmol/L resulted in increased G_2-M and decreased G_1 in LNCaP and DU 145 cells. *Columns,* mean of three independent experiments done in duplicate; *bars,* SD.

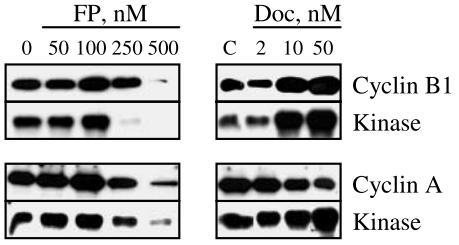

Figure 2. Opposite effects of flavopiridol and docetaxel on cyclin B1–dependent kinase activity. DU 145 cells were treated with increasing doses of flavopiridol (50–500 nmol/L) and docetaxel (2–50 nmol/L) and the levels of cyclins B1 and A proteins were determined by Western blot analysis, normalized to tubulin protein (data not shown), and compared with control (*C*)–treated cells. Cyclins B1 and A proteins were immunoprecipitated and their associated kinase activities ([^{32}P]histone) were determined from the same lysates. Flavopiridol in doses of ≥250 nmol/L decreased both cyclins B1– and A–dependent kinases, whereas docetaxel in doses ≥10 nmol/L increased cyclin B1– but not cyclin A–dependent kinase activity.

≥10 nmol/L docetaxel results in an increase in G_2-M and a decrease in G_1. As expected, these results are similar to those after treatment with 10 nmol/L paclitaxel (35) and indicate that docetaxel blocks prostate cancer cells in the G_2-M phase of the cell cycle.

Opposite Effects of Flavopiridol and Docetaxel on Cyclin B1–Dependent Kinase Activity

To evaluate molecular changes involved in the mediated effects on the cell cycle in LNCaP and DU 145 cells by flavopiridol and docetaxel, we analyzed the expression of cyclins B1 and A proteins by Western blot and kinase analysis (Fig. 2). Cyclin A protein increases during the S and G_2 phase of the cell cycle and is believed to be important for DNA replication (36). The transition from the G_2 to the M phase of the cell cycle requires an accumulation of cyclin B1 and activation of its associated kinase, cdk1. The end of the G_2-M transition and exit from mitosis requires the proteolysis of cyclin B1 and a reduction of cdk1 activity (37). Increased doses of flavopiridol (≥250 nmol/L) decrease both cyclins B1 and A proteins and their associated kinase activities in DU 145 cells (Fig. 2). In contrast, the treatment of DU 145 cells with the G_2-M-promoting doses of docetaxel (≥10 nmol/L) for 24 hours results in an increase in cyclin B1 protein and kinase activity but not cyclin A protein and kinase activity (Fig. 2). Similar results were obtained in flavopiridol- and docetaxel-treated LNCaP cells (data not shown). These results indicate that (*a*) flavopiridol inhibits both cyclins B1– and A–dependent cdk activity probably explaining the G_1 and G_2-M effects on the cell cycle and (*b*) docetaxel increases cyclin B1–dependent kinase activity, which correlates with increased G_2-M.

Differential Induction of Apoptosis by Flavopiridol and Docetaxel in Prostate Cancer Cells

The induction of apoptosis is a requirement for the effect of chemotherapeutic drugs on prostate cancer cells (38). To measure the induction of apoptosis by flavopiridol and docetaxel, we did a DAPI staining assay in LNCaP, LN-AI,

LN-AI/CSS, DU 145, NRP-152, and mesenchymal stromal cells treated with 500 nmol/L flavopiridol and 10 nmol/L docetaxel for 72 hours (Fig. 3A and B). We selected these doses because of the increased effect on cyclin B1–dependent kinase (Fig. 2), which was shown previously to be important in the induction of apoptosis (35). The results indicate that both flavopiridol- and docetaxel-mediated apoptosis was greatest in LN-AI (38–49%) followed by LNCaP (14–25%) cells. A removal of androgens results in a decrease in flavopiridol- and docetaxel-mediated apoptosis in LN-AI/CSS (8–10%) compared with LN-AI cells. The levels of apoptosis in DU 145 (5–12%) are similar to those in LN-AI/CSS cells. Flavopiridol induces a similar degree of apoptosis in nontumorigenic NRP-152 and mesenchymal stromal cells (9%) compared with LN-AI/CSS and DU 145 cells, whereas docetaxel induces less apoptosis in NRP-152 and mesenchymal stromal cells (2–5%) compared with prostate cancer cells. These results indicate that flavopiridol and docetaxel are most effective in producing apoptosis in LN-AI cells and that the removal of androgens reduces the ability of flavopiridol and docetaxel to produce apoptosis in LN-AI/CSS cells.

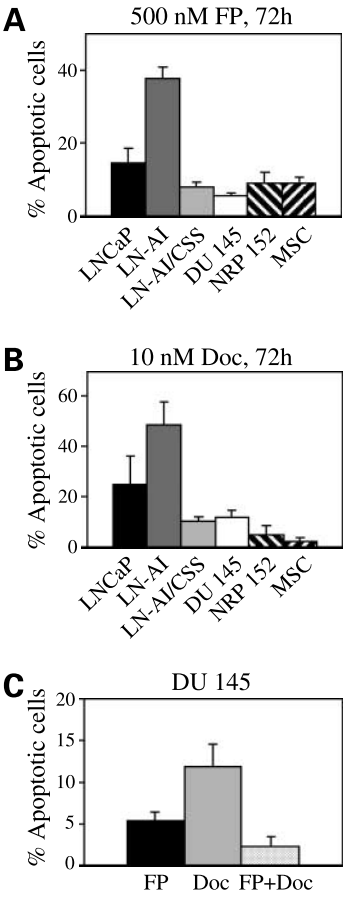

Figure 3. Induction of apoptosis by flavopiridol and docetaxel as single drugs and in combination. **A,** percentage of apoptotic cells were determined by DAPI in LNCaP, LN-AI, LN-AI/CSS, and DU 145 prostate cancer cells treated with 500 nmol/L flavopiridol for 72 h and compared with treatment of nontransformed NRP-152 and mesenchymal stromal cells. **B,** percentage of apoptotic cells after treatment for 72 h with 10 nmol/L docetaxel. Flavopiridol and docetaxel as single drugs were most effective in inducing apoptosis in LN-AI cells and removal of androgens reduced their ability to induce apoptosis in LN-AI/CSS cells. There was minimal apoptosis (<0.5%) detected by DAPI in the control-treated cells (data not shown). **C,** treatment of DU 145 cells with the combination of 500 nmol/L flavopiridol and 10 nmol/L docetaxel added simultaneously for 72 h (*FP + Doc*) results in less apoptosis (DAPI) compared with each drug alone (*FP* and *Doc*). *Columns,* mean of three independent experiments ($n = 6$); *bars,* SD. *, $P < 0.001$.

Treatment with Flavopiridol and Docetaxel Antagonizes Induction of Apoptosis

If the effect of flavopiridol and docetaxel on cyclin B1–dependent kinase activity is important for induction of apoptosis, then it can be predicted from the previous results (Fig. 2) that treatment with flavopiridol (inhibits cyclin B1–dependent kinase) and docetaxel (increases cyclin B1–dependent kinase) should antagonize each other and result in less than additive induction of apoptosis. The treatment of DU 145 cells with 500 nmol/L flavopiridol and 10 nmol/L docetaxel for 72 hours results in only 2% apoptosis, which is a decrease from flavopiridol (5%) and docetaxel (12%) alone (Fig. 3C). This result was confirmed by Western blot showing less cleaved PARP (signifying apoptosis) in the flavopiridol and docetaxel combination compared with docetaxel alone (data not shown). In LNCaP cells, treatment with flavopiridol and docetaxel results in no additional apoptosis above each drug alone (data not shown). These results indicate that simultaneous treatment of prostate cancer cells with flavopiridol and docetaxel results in antagonism with respect to induction of apoptosis probably due to opposing effects on cyclin B1–dependent kinase activity.

Flavopiridol followed by Docetaxel Produces the Greatest Induction of Apoptosis in LNCaP cells

We used the DAPI apoptosis assay in LNCaP cells to identify the sequential combination of flavopiridol and docetaxel that can induce apoptosis to a greater extent than each drug alone (Fig. 4). Previous studies have shown that docetaxel followed by flavopiridol (DF) was more effective in inducing apoptosis in gastric cancer cells (16). Our results indicate that the best sequence for induction of apoptosis is 500 nmol/L flavopiridol for 24 hours followed by 10 nmol/L docetaxel for 24 hours. Similar results with the FD sequence were obtained in LN-AI and LN-AI/CSS cells, although there was less apoptosis in LN-AI/CSS (10%) compared with LN-AI (46%) cells (data not shown). In DU 145 cells, the DF sequence (9%) induces greater apoptosis compared with the FD sequence (2%). However, there was no additional apoptosis in DF-treated DU 145 cells compared with docetaxel followed by docetaxel (DD)–treated cells (Fig. 4). In LN-AI cells, a greater apoptosis in the FD sequence compared with the DF sequence was confirmed by flow cytometry using the Annexin V-FITC/PI assay, whereas in DU 145 cells there was no difference in any sequence of flavopiridol and docetaxel (Fig. 4B).

Interestingly, when flavopiridol was followed by vehicle control in LNCaP, LN-AI, and LN-AI/CSS cells, there was

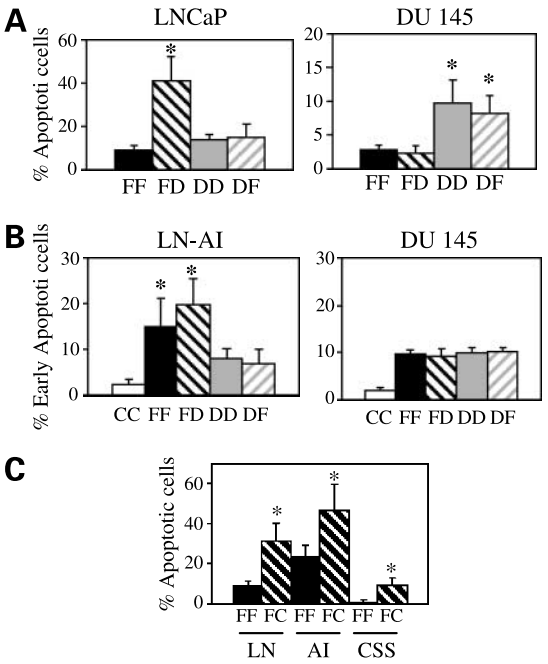

Figure 4. Heterogeneous apoptosis response to the sequential combinations of flavopiridol and docetaxel in prostate cancer cells. **A,** percentage of apoptotic cells determined by DAPI showing that flavopiridol followed by docetaxel was more effective in inducing apoptosis in LNCaP cells compared with flavopiridol followed by flavopiridol (*FF*) and docetaxel followed by docetaxel (*DD*) or flavopiridol (*DF*). *Columns,* mean of three to six independent experiments (n = 6–11); *bars,* SD. *, $P < 1 \times 10^{-5}$. In contrast, the DD and DF sequence was more effective to induce apoptosis in DU 145 cells compared with the FF and FD sequence. *Columns,* mean of three independent experiments (n = 5–7); *bars,* SD. *, $P < 0.001$. There was minimal apoptosis (<0.5%) detected by DAPI in the control-treated cells (data not shown). **B,** flow cytometric analysis of Annexin V-FITC– and PI-stained LN-AI and DU 145 cells after treatment with FF, FD, DD, and DF and compared with control (*CC*)–treated cells. Early apoptotic cells represent the Annexin V-FITC–positive and PI-negative population of cells. In LN-AI cells, there were more early apoptotic cells in FF and FD compared with DD- and DF-treated cells. *Columns,* mean of three independent experiments (n = 6); *bars,* SD. *, $P < 0.01$. In DU 145 cells, there were no differences in early apoptotic cells in any of the sequence combinations. *Columns,* mean of three independent experiments (n = 6); *bars,* SD. **C,** percentage of apoptotic cells determined by DAPI showing that treatment of LNCaP (*LN*), LN-AI (*AI*), and LN-AI/CSS (*CSS*) cells with flavopiridol followed by vehicle control (*FC*) was more effective in inducing apoptosis than continuous treatment (*FF*). *Columns,* mean of three independent experiments (n = 6); *bars,* SD. *, $P < 0.005$.

a greater induction of apoptosis compared with sequential use of flavopiridol (FF; Fig. 4C). Similar results were obtained when LNCaP cells were treated with the cdk inhibitor alsterpaullone (5 μmol/L; ref. 39) for 24 hours followed by vehicle control for 24 hours (data not shown), suggesting that increased apoptosis was due to inhibition of cdk activity by flavopiridol. In contrast, the treatment of LNCaP cells with the cdk9 inhibitor 5,6-dichloro-1-β-D-ribofuranosyl-benzimidazole (75 μmol/L; required for transcription elongation; ref. 40) for 24 hours followed by vehicle control or 5,6-dichloro-1-β-D-ribofuranosyl-benzimidazole resulted in low apoptosis (data not shown). These results indicate that the optimal sequence combination in LNCaP cells is flavopiridol followed by docetaxel and that a continuous treatment of LNCaP cells with flavopiridol for 48 hours is less effective in inducing apoptosis compared with a 24-hour treatment followed by no drug.

Increased Apoptosis Is Correlated with Decreased XIAP but Not Survivin Protein

To investigate in LNCaP cells why the FD sequence induced greater apoptosis than the DF, FF, and DD sequences, we sought to identify the differences in the levels of proteins important for apoptosis by Western blot analysis. The results in LNCaP and LN-AI cells show that FD treatment contained more cleaved (activated) caspase-3 and PARP (Fig. 5) compared with the DF, FF, and DD sequences. There was much less cleaved caspase-3 in LN-AI/CSS compared with LN-AI cells using the FD sequence. In DU 145 cells, there was a greater cleaved capsase-3 in the DD and DF sequence compared with the FF and FD sequence. These results correlate with those obtained with the apoptosis assays (Fig. 4). There were no significant differences in the levels of the antiapoptotic protein Bcl-xL in any drug sequence.

In contrast, all of the FF- and DF-treated cells show a substantial reduction in the antiapoptotic protein Mcl-1 compared with FD and DD sequence (Fig. 6); however, these results did not correlate with greater apoptosis in the FD sequence. The FD sequence reduces the levels of XIAP and survivin, members of the IAP family (20, 21), in LNCaP, LN-AI, and LN-AI/CSS compared with DU 145 cells (Fig. 6). However, the FD sequence decreases XIAP to a greater extent in LNCaP (7-fold) and LN-AI (10-fold) compared with LN-AI/CSS (3-fold) cells and this correlates with increased apoptosis. In DU 145, there was a 2-fold decrease in XIAP protein in DD- and DF-treated cells. These results suggest that the greatest levels of apoptosis induced by the FD sequence may require a substantial decrease in XIAP protein.

Reduction of XIAP Protein by siRNA Increases Apoptosis in FD-Treated LN-AI/CSS Cells

To determine if a reduction of XIAP protein can increase FD-mediated apoptosis in LN-AI/CSS cells, we used siRNA specific for XIAP. The results show that XIAP siRNA caused a 7-fold decrease in XIAP protein in LN-AI/CSS cells compared with cells transfected with control siRNA (Fig. 7A). Subsequently, LN-AI/CSS cells were transfected with XIAP and control siRNA for 24 hours followed by treatment with FD for an additional 48 hours and the effect on apoptosis was determined by DAPI staining. The results indicate that in the presence of XIAP siRNA there was a small but significant increase in apoptotic LN-AI/CSS cells compared with control siRNA transfected cells (Fig. 7B). This suggests that lowering XIAP protein levels sensitizes prostate cancer cells to FD treatment.

Decrease in XIAP Protein Is Not Due to Decreased mRNA

One of the mechanisms proposed for flavopiridol inhibition of cancer cells is its ability to inhibit cdk7 and

cdk9, which are required for phosphorylation of RNA polymerase II and transcription elongation (40). We therefore did RNase protection assay using the hAPO-5c human apoptosis multiprobe template set to determine whether the FD-mediated decrease in XIAP protein was due to a decrease in mRNA. The results show that this treatment of LNCaP, LN-AI, LN-AI/CSS, and DU 145 cells with FD did not reduce the levels of XIAP mRNA compared with control-treated cells (Fig. 8). In contrast, FD treatment of LNCaP, LN-AI, and LN-AI/CSS but not DU 145 cells results in a decrease in survivin mRNA, which may explain the decrease in survivin protein. In addition, there was a decrease in mRNA for XIAP in FF- and DF-treated cells, which possibly corresponds to a decrease in XIAP protein. These results indicate that decreased XIAP protein in FD-treated LNCaP and LN-AI cells was due to post-transcriptional mechanisms and not to decreased XIAP mRNA.

FD Treatment Decreases Total AKT Protein in LN-AI Cells

To investigate molecular changes possibly involved in the reduction of XIAP protein in FD-treated LNCaP cells, we analyzed the expression of activated and total AKT by Western blot. In addition to phosphorylation and inactivation of the proapoptotic protein Bad (22), AKT has recently been shown to phosphorylate and stabilize XIAP (41).

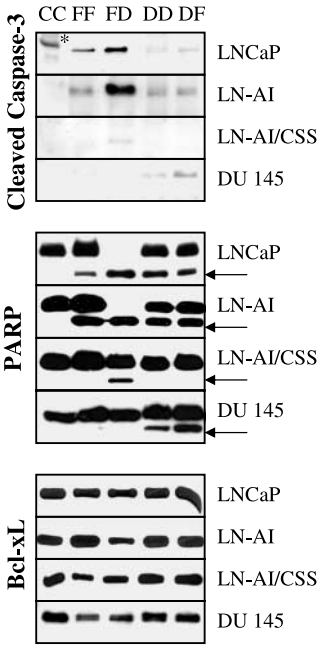

Figure 5. FD treatment of LNCaP cells increases markers of apoptosis. LNCaP, LN-AI, LN-AI/CSS, and DU 145 cells were treated with FF, FD, DD, and DF and the levels of cleaved caspase-3, cleaved PARP (*arrow*), and total Bcl-xL proteins were determined by Western blot, normalized to tubulin (data not shown), and compared with control-treated cells. There was increased cleaved caspase-3 and PARP in LNCaP and LN-AI compared with LN-AI/CSS and DU 145 cells. No significant differences in the levels of Bcl-xL were observed for any of the drug sequences. *Asterisk,* nonspecific band.

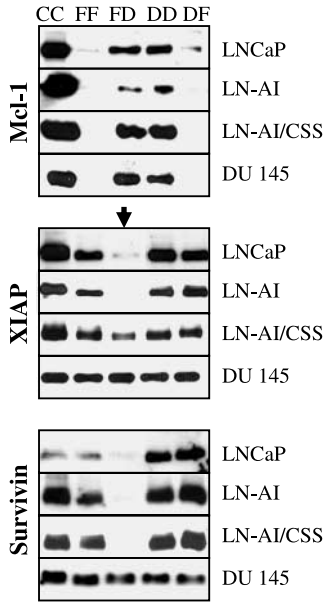

Figure 6. Loss of XIAP but not survivin protein correlates with increased apoptosis in FD-treated LNCaP cells. LNCaP, LN-AI, LN-AI/CSS, and DU 145 cells were treated with FF, FD, DD, and DF and the levels of the antiapoptotic proteins Mcl-1, XIAP, and survivin were determined by Western blot, normalized to tubulin (data not shown), and compared with control-treated cells. Loss of Mcl-1 in FF- and DF-treated cells did not result in increased apoptosis compared with FD- and DD-treated cells. There was a greater decrease in XIAP protein in FD-treated LNCaP and LN-AI cells compared with LN-AI/CSS cells (*arrow*), which correlates with increased apoptosis. However, loss of survivin protein in FD-treated LN-AI/CSS cells did not result in increased apoptosis. In DU 145 cells, there was little change in XIAP or survivin protein in any sequence combination.

Results indicate that LN-AI/CSS cells contain a higher level of activated (phosphorylated at Ser^{473}) AKT compared with LN-AI cells (Fig. 9A). Because activated AKT has been shown to protect cells from apoptosis (22), this may explain why LN-AI/CSS cells are more resistant to apoptosis induced by FD treatment compared with LN-AI cells. We then analyzed the levels of activated and total AKT in FD-treated LN-AI compared with LN-AI/CSS cells (Fig. 9B). The results show that FD treatment greatly reduces the levels of total AKT protein (and therefore activated AKT) in LN-AI cells with few changes in LN-AI/CSS cells. Interestingly, the treatment of LN-AI but not LN-AI/CSS cells with FF results in a 5-fold increase in activated AKT compared with control-treated cells. Inhibition of AKT activity with the phosphatidylinositol 3-kinase inhibitor LY 294002 (20 μmol/L inhibits Ser^{473} phosphorylated AKT) increases apoptosis (Fig. 9C) and decreases XIAP protein levels (data not shown) in FF- and FD-treated LN-AI/CSS cells. Finally, the combination of a reduction in XIAP protein with siRNA and an inhibition of AKT activity with LY 294002 cause a greater increase in apoptosis than a reduction of XIAP or a decrease in AKT activity alone (Fig. 9D). Overall, these results suggest that (*a*) an increase in activated AKT in LN-AI/CSS cells may explain its greater resistance to apoptosis; (*b*) FD treatment reduces

total AKT protein levels in LN-AI but not LN-AI/CSS cells, possibly explaining differentially decreased XIAP and increased apoptosis; and (*c*) a reduction of XIAP protein and an inhibition of AKT activity greatly increases apoptosis in FD-treated LN-AI/CSS cells.

Inhibition of the Proteasome Pathway Antagonizes FD-Induced Apoptosis

A possible mechanism explaining FD decrease in XIAP protein without a reduction in XIAP mRNA may be the increased degradation by the ubiquitin-proteasome pathway (42). To address this hypothesis, we treated LNCaP cells with flavopiridol (500 nmol/L), proteasome inhibitor MG-132 (5 μmol/L), and combination of flavopiridol and MG-132 for 24 hours. The results show that MG-132 blocks the ability of flavopiridol to reduce the protein levels of cyclin B1 and Mcl-1 (Fig. 10A). This suggests that flavopiridol activates the proteasome pathway to decrease these proteins. The addition of MG-132 (5 μmol/L) in the FD sequence combination results in lesser cleavage of PARP in LNCaP cells, which correlates with a block in FD-mediated decrease in XIAP and AKT (Fig. 10B). Conversely, FD lowers cleavage of PARP mediated by MG-132, suggesting antagonism relative to proteasome degradation activity. MG-132 also blocks FD-mediated apoptosis as determined by DAPI staining (data not shown). Similar results were obtained using the proteasome inhibitor epoxomicin (1 μmol/L; data not shown). In addition, treatment of LNCaP cells with FD and the nuclear factor-κB inhibitor parthenolide (20 μmol/L) had no effect on apoptosis, suggesting that an inhibition of nuclear factor-κB activity was not important for the ability of MG-132 to block FD-mediated apoptosis (data not shown). These results suggest that FD increases the degradation of cyclin B1, XIAP, and AKT proteins by stimulating the proteasome pathway and this augments apoptosis in LNCaP cells.

Discussion

We analyzed in human prostate cancer cells whether the combination of flavopiridol and docetaxel can enhance apoptosis more than either drug alone. Our results indicate

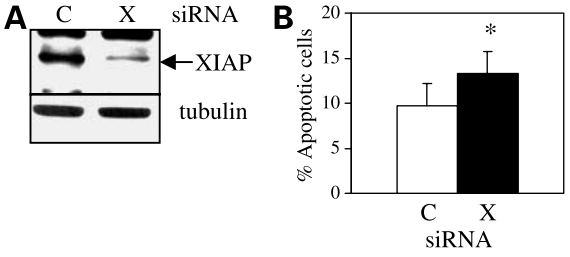

Figure 7. Decrease in XIAP protein by siRNA increases FD-mediated apoptosis in LN-AI/CSS cells. **A,** Western blot showing that treatment of LN-AI/CSS cells with 200 nmol/L XIAP (*X*) siRNA for 72 h reduced XIAP protein levels compared with control (*C*) siRNA-treated cells. There was no change in tubulin protein levels. **B,** percentage of apoptotic cells determined by DAPI showing that transfection of LN-AI/CSS cells with XIAP siRNA increases apoptosis in FD-treated cells compared with control siRNA-transfected cells. *Columns,* mean of three independent experiments ($n = 7$); *bars,* SD. *, $P < 0.02$.

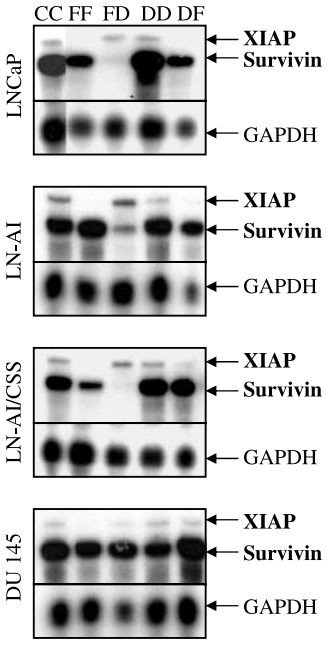

Figure 8. Reduced XIAP protein in FD-treated LNCaP and LN-AI prostate cancer cells are not due to decreased mRNA. RNase protection assay of human XIAP and survivin mRNA was done with 10 μg total RNA from FF-, FD-, DD-, and DF-treated LNCaP, LN-AI, LN-AI/CSS, and DU 145 cells and compared with control-treated cells using the hAPO-5c human apoptosis multiprobe template set. Glyceraldehyde-3-phosphate dehydrogenase (*GAPDH*) was used as an internal RNA control. Results show that survivin but not XIAP mRNA was reduced in FD-treated LNCaP, LN-AI, and LN-AI/CSS cells. Autoradiograms were exposed for 18 h (XIAP and survivin) or 3 h (glyceraldehyde-3-phosphate dehydrogenase) using two intensifying screens. Similar results were obtained from another independent experiment.

that the sequential addition of flavopiridol followed by docetaxel was required for maximal induction of apoptosis in LNCaP cells. The opposing effects on cyclin B1–dependent kinase activity by flavopiridol (a decrease) and docetaxel (an increase) likely plays an important role in the requirement for a sequential combination regimen and an induction of apoptosis. Our data also suggest that the FD-mediated decrease in XIAP and AKT proteins, both being IAPs, is an important factor for increased apoptosis in LNCaP and LN-AI compared with LN-AI/CSS and DU 145 prostate cancer cells. A possible mechanism for flavopiridol-mediated decrease in XIAP, AKT, cyclin B1, and Mcl-1 proteins may be the activation of the proteasome pathway of protein degradation. Overall, our data suggest that the sequential regimen of flavopiridol and docetaxel that leads to the greatest decrease in XIAP and AKT protein also results in the greatest increase in apoptosis.

The deregulated increase of cyclin B1–dependent kinase activity by docetaxel is an important mechanism for the induction of apoptosis in prostate cancer cells (35, 43). However, it is not clear if an inhibition of cyclin B1–dependent kinase activity by flavopiridol is also important for induction of apoptosis. Our data show that when flavopiridol and docetaxel were added simultaneously

there was an antagonism of apoptosis compared with either drug alone (Fig. 3C). This suggests that inhibition by flavopiridol of cyclin B1–dependent kinase activity is important for the induction of apoptosis in prostate cancer cells. Therefore, to maximize apoptosis, flavopiridol and docetaxel should not be added simultaneously because of their opposing effects on cyclin B1–dependent kinase activity.

In contrast to results in gastric cancer cell lines (16), our results show that in LNCaP cells treatment with FD is more effective than that with DF in inducing apoptosis (Fig. 4). Flavopiridol can decrease proteins that inhibit apoptosis, such as Bcl-2, Bcl-xL, Mcl-1, and XIAP (10–13). Therefore, it is possible that in LNCaP an initial treatment with flavopiridol decreases IAPs and sensitizes cells for subsequent treatment with docetaxel. In contrast to LNCaP cells, DF is more effective for induction of apoptosis than FD in DU 145 cells as determined by DAPI and greater cleavage of caspase-3 and PARP (Figs. 4 and 5). However, overall apoptosis in DF-treated DU 145 cells were not different from that in DD-treated cells (Fig. 4). Therefore, the FD or DF sequence that optimally induces apoptosis may depend on the type of prostate cancer cells (i.e., androgen-dependent or androgen-independent) as well as on the expression of androgen receptor or p53 proteins. Because prostate cancers growing *in vivo* consist of a heterogeneous mixture of different cell types (44, 45), our results suggest that either the FD or the DF sequence regimen may work in inhibiting tumor growth and inducing apoptosis. In fact, we have shown in the Gγ/T-15 transgenic mouse model of androgen-independent prostate cancer (31) that DF or FD treatment can inhibit the growth of primary and metastatic prostate tumors more effectively than either drug alone by increasing apoptotic cell death.[4]

In addition to inhibition of cyclin B1–dependent kinase activity and a decrease in IAPs, another potential mechanism for flavopiridol is its ability to inhibit transcription elongation (40). It is thought that blocking transcription results in a loss of mRNAs with short half-lives (e.g., Mcl-1 and cyclin D1) and therefore a loss of protein (9, 46). Our results show that FD treatment of LNCaP cells did not decrease XIAP mRNA (Fig. 8) and therefore cannot be an explanation for decreased XIAP protein (Fig. 6). FD treatment results in decreased mRNA for survivin and therefore is a likely explanation for decreased survivin protein in LNCaP cells (Figs. 6 and 8). However, decreased

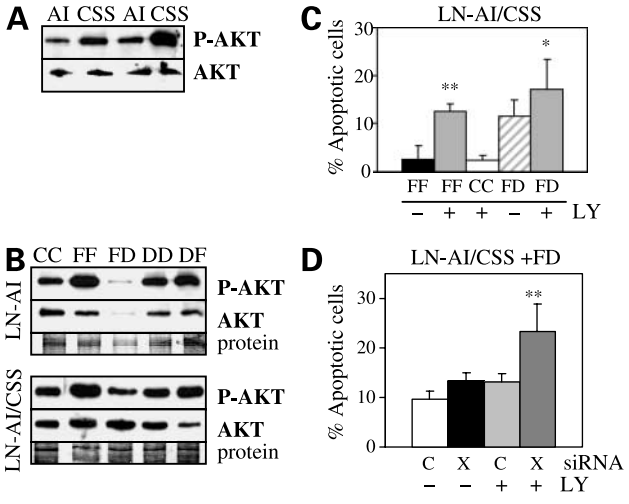

Figure 9. Reduction of total AKT protein in FD-treated LN-AI cells correlated with increased apoptosis. **A,** levels of activated AKT (*P-AKT*; phosphorylated at Ser^{473}) and total AKT in duplicate samples of LN-AI and LN-AI/CSS cells were determined by Western blot. Results show a greater activated AKT in LN-AI/CSS cells compared with LN-AI cells. **B,** LN-AI and LN-AI/CSS cells were treated with FF, FD, DD, and DF and the levels of P-AKT and total AKT was determined by Western blot, normalized to total protein, and compared with control-treated cells. Results show that FD treatment reduced total AKT protein levels in LN-AI but not LN-AI/CSS cells. P-AKT was higher in FF-treated LN-AI compared with control cells. **C,** percentage of apoptotic cells determined by DAPI indicating that phosphatidylinositol 3-kinase inhibitor LY 294002 (*LY*; 20 μmol/L) increases apoptosis in FF- and FD-treated LN-AI/CSS cells compared with FF-, FD-, and LY-treated cells. *Columns,* mean of four independent experiments ($n = 5–8$); *bars,* SD. *, $P < 0.03$; **, $P < 2 \times 10^{-5}$. **D,** percentage of apoptotic cells determined by DAPI showing that reduction of XIAP with siRNA and inhibition of AKT activity with LY 294002 increases apoptosis in FD-treated LN-AI/CSS cells more than reduction in XIAP or inhibition of AKT activity alone. *Columns,* mean of three independent experiments ($n = 6–7$); *bars,* SD. **, $P < 0.0002$.

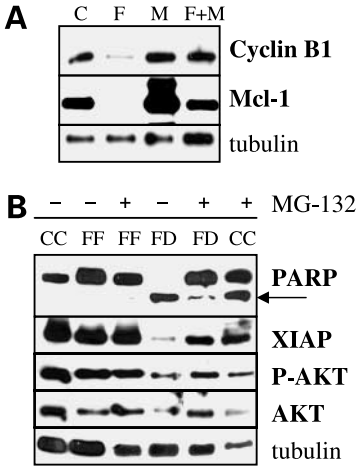

Figure 10. Inhibition of proteasome activity blocks FD-mediated apoptosis in LNCaP cells. **A,** LNCaP cells were treated with 500 nmol/L flavopiridol (*F*), 5 μmol/L MG-132 (*M*), and flavopiridol + MG-132 (*F + M*) for 24 h and the levels of cyclin B1 and Mcl-1 were determined by Western blot, normalized to tubulin, and compared with control-treated cells. Results show that inhibition of proteasome activity by MG-132 blocked the ability of flavopiridol to reduce cyclin B1 and Mcl-1 proteins. **B,** LNCaP cells were treated with FF and FD (±5 μmol/L MG-132) and the levels of cleaved PARP, XIAP, activated AKT, and total AKT were determined by Western blot, normalized to tubulin, and compared with control-treated cells ±5 μmol/L MG-132. Results show that treatment with MG-132 blocks the ability of FD treatment to cleave PARP and decrease XIAP and total AKT proteins.

[4] T. Reiner, A. de las Pozas, and C. Perez-Stable. Sequential combinations of flavopiridol and docetaxel inhibit prostate tumors, induce apoptosis, and decreases angiogenesis in the Gγ/T-15 transgenic mouse model of prostate cancer, submitted for publication 2006. Q8

survivin protein does not seem to play a major role in FD-mediated induction of apoptosis because there is less apoptosis in LN-AI/CSS compared with LN-AI cells despite that both have decreased survivin protein and mRNA (Figs. 6 and 8). XIAP protein was higher in FD-treated LN-AI/CSS compared with LN-AI and LNCaP cells and a reduction of XIAP protein with siRNA increased apoptosis (Fig. 7), suggesting a more important role for XIAP. A recent report shows that lowering XIAP protein can sensitize prostate cancer cells to a variety of chemotherapeutic agents (27). In addition, treatment of LN-AI cells with the transcription inhibitor 5,6-dichloro-1-β-D-ribofuranosyl-benzimidazole (75 μmol/L) did not result in increased apoptosis (data not shown), indicating that the ability of flavopiridol to inhibit transcription is not required for induction of apoptosis in FD-treated LN-AI cells.

Another potential mechanism for FD-mediated apoptosis is the differential effect on the prosurvival AKT protein in LN-AI compared with LN-AI/CSS cells (Fig. 9). Our results show that the greater resistance to apoptosis in LN-AI/CSS compared with LN-AI cells was possibly due to higher levels of activated AKT (Fig. 9A). It has been shown previously that androgen ablation can increase AKT activation in LNCaP cells and support survival and proliferation in conditions of androgen deprivation (47). Treatment with FD reduces total AKT protein levels in LN-AI but not LN-AI/CSS cells possibly by increased proteasome degradation of AKT. This may be an explanation why FD treatment induced greater apoptosis in LN-AI compared with LN-AI/CSS cells. Because activated AKT has recently been shown to phosphorylate and stabilize XIAP (41), lower AKT protein (and therefore reduced activated AKT) in FD-treated LN-AI and LNCaP cells may be another explanation for lower XIAP protein. In addition, our results suggest that a 24-hour treatment with flavopiridol followed by no drug is more effective in inducing apoptosis than a continuous 48-hour treatment (Fig. 4C) possibly because of the effect on total AKT protein, which is higher in continuous compared with noncontinuous treatment (Fig. 9B; data not shown). The addition of the phosphatidylinositol 3-kinase inhibitor LY 294002 enhanced apoptosis in FD-treated LN-AI/CSS cells, especially when XIAP protein was reduced with siRNA (Fig. 9C and D), further suggesting the importance of decreasing AKT activity to augment apoptotic cell death. Drug combinations that reduce XIAP protein and activated AKT are more likely to increase apoptosis (22), especially in prostate cancer cells, such as LNCaP, which has a mutated PTEN and a constitutively active AKT (48). However, this strategy may not be effective in prostate cancer cells, such as DU 145, in which PTEN is not mutated and AKT is not constitutively active (49).

A potential explanation for decreased XIAP protein without decreased mRNA in FD-treated LNCaP and LN-AI cells is the activation of the proteasome degradation pathway by flavopiridol. Our results show that the proteasome inhibitor MG-132 can block the ability of flavopiridol to decrease cyclin B1 and Mcl-1 proteins in LNCaP cells (Fig. 10A). This suggests that flavopiridol can decrease these proteins using the proteasome pathway. In FD-treated LNCaP cells containing MG-132, there was less PARP cleavage and higher levels of XIAP and AKT proteins, implying an antagonism between proteasome inhibition and FD treatment (Fig. 10B). These results are in contrast to synergistic induction of apoptosis in leukemic cells treated with flavopiridol and MG-132, which is associated with disruption of the nuclear factor-κB pathway (50). Thus, treatment strategies that are synergistic in one type of tumor may be antagonistic in another type of tumor.

In summary, our studies suggest that the FD sequence combination in LNCaP and LN-AI prostate cancer cells results in the activation of the proteasome pathway, degradation of prosurvival proteins XIAP and AKT, and induction of apoptosis. The FD sequence induces less apoptosis in the LN-AI/CSS cells possibly because of the failure to substantially decrease XIAP and AKT proteins. However, in the DU 145 cells, the DF and DD sequence combinations are more effective than the FD and FF regimens, suggesting a heterogeneous response depending on the type of prostate cancer cell. Phase I clinical trials on the DF sequence in patients with lung cancer have shown few responses, although there was some disease stabilization (8). Because of the heterogeneous nature of prostate cancers, we suggest that the efficacy of the DF or FD sequence may depend on the relative levels of the different types of prostate cancer cells, such as LNCaP (sensitive to FD) and DU 145 (sensitive to DF), present in tumors.

Acknowledgments

We thank Dr. Andrew Schally (Veterans Affairs Medical Center, New Orleans, LA) and Dr. Diana Brassard (Aventis Pharmaceuticals) for review of this article, Dr. Gianluca D'Ippolito for mesenchymal stromal cells, and Dr. David Danielpour for NRP-152 cells.

References

1. Jemal A, Murray T, Ward E, et al. Cancer statistics. CA Cancer J Clin 2005;55:10 – 30.

2. So A, Gleave M, Hurtado-Col A, Nelson C. Mechanisms of the development of androgen independence in prostate cancer. World J Urol 2005;23:1 – 9.

3. Bissery MC, Nohynek G, Sanderink GJ, Lavelle F. Docetaxel (Taxotere®): a review of preclinical and clinical experience. Part I. Preclinical experience. Anticancer Drugs 1995;6:339 – 55.

4. Pienta KJ. Preclinical mechanisms of action of docetaxel and docetaxel combinations in prostate cancer. Semin Oncol 2001;28:3 – 7.

5. Herbst RS, Khuri FR. Mode of action of docetaxel—a basis for combination with novel anticancer agents. Cancer Treat Rev 2003;29:407 – 15.

6. Tannock IF, de Wit R, Berry WR, et al. Docetaxel plus prednisone or mitoxantrone plus prednisone for advanced prostate cancer. N Engl J Med 2004;351:1502 – 12.

7. Zhai S, Senderowicz AM, Sausville EA, Figg WD. Flavopiridol, a novel cyclin-dependent kinase inhibitor, in clinical development. Ann Pharmacother 2002;36:905 – 11.

8. Shapiro GI. Preclinical and clinical development of the cyclin-dependent kinase inhibitor flavopiridol. Clin Cancer Res 2004;10:4270 – 5s.

9. Carlson B, Lahusen T, Singh S, et al. Down-regulation of cyclin D1 by transcriptional repression in MCF-7 human breast carcinoma cells induced by flavopiridol. Cancer Res 1999;59:4634 – 41.

10. Wittmann S, Bali P, Donapaty S, et al. Flavopiridol down-regulates

antiapoptotic proteins and sensitizes human breast cancer cells to epothilone B-induced apoptosis. Cancer Res 2003;63:93 – 9.

11. Kitada S, Zapata JM, Andreeff M, Reed JC. Protein kinase inhibitors flavopiridol and 7-hydroxy-staurosporine down-regulate anti-apoptosis proteins in B-cell chronic lymphocytic leukemia. Blood 2000; 96:393 – 7.

12. Gojo I, Zhang B, Fenton RG. The cyclin-dependent kinase inhibitor flavopiridol induces apoptosis in multiple myeloma cells through transcriptional repression and down-regulation of Mcl-1. Clin Cancer Res 2002;8: 3527 – 38.

13. Ma Y, Cress WD, Haura EB. Flavopiridol-induced apoptosis is mediated through up-regulation of E2F1 and repression of Mcl-1. Mol Cancer Ther 2003;2:73 – 81.

14. Schwartz GK, Ilson D, Saltz L, et al. Phase II study of the cyclin-dependent kinase inhibitor flavopiridol administered to patients with advanced gastric carcinoma. J Clin Oncol 2001;19:1985 – 92.

15. Liu G, Gandara DR, Lara PN, Jr., et al. A phase II trial of flavopiridol (NSC #649890) in patients with previously untreated metastatic androgen-independent prostate cancer. Clin Cancer Res 2004;10:924 – 8.

16. Motwani M, Rizzo C, Sirotnak F, She Y, Schwartz GK. Flavopiridol enhances the effect of docetaxel *in vitro* and *in vivo* in human gastric cancer cells. Mol Cancer Ther 2003;2:549 – 55.

17. Castedo M, Perfettini JL, Roumier T, Kroemer G. Cyclin-dependent kinase-1: linking apoptosis to cell cycle and mitotic catastrophe. Cell Death Differ 2002;9:1287 – 93.

18. O'Connor DS, Grossman D, Plescia J, et al. Regulation of apoptosis at cell division by p34cdc2 phosphorylation of survivin. Proc Natl Acad Sci U S A 2000;97:13103 – 7.

19. O'Connor DS, Wall NR, Porter AC, Altieri DC. A p34(cdc2) survival checkpoint in cancer. Cancer Cell 2002;2:43 – 54.

20. Liston P, Fong WG, Korneluk RG. The inhibitors of apoptosis: there is more to life than Bcl2. Oncogene 2003;22:8568 – 80.

21. Schimmer AD. Inhibitor of apoptosis proteins: translating basic knowledge into clinical practice. Cancer Res 2004;64:7183 – 90.

22. Kim D, Dan HC, Park S, et al. AKT/PKB signaling mechanisms in cancer and chemoresistance. Front Biosci 2005;10:975 – 87.

23. Tamm I, Kornblau SM, Segall H, et al. Expression and prognostic significance of IAP-family genes in human cancers and myeloid leukemias. Clin Cancer Res 2000;6:1796 – 803.

24. Krajewska M, Krajewski S, Banares S, et al. Elevated expression of inhibitor of apoptosis proteins in prostate cancer. Clin Cancer Res 2003;9: 4914 – 25.

25. Malik SN, Brattain M, Ghosh PM, et al. Immunohistochemical demonstration of phospho-Akt in high Gleason grade prostate cancer. Clin Cancer Res 2002;8:1168 – 71.

26. Kreisberg JI, Malik SN, Prihoda TJ, et al. Phosphorylation of Akt (Ser^{473}) is an excellent predictor of poor clinical outcome in prostate cancer. Cancer Res 2004;64:5232 – 6.

27. Amantana A, London CA, Iversen PL, Devi GR. X-linked inhibitor of apoptosis protein inhibition induces apoptosis and enhances chemotherapy sensitivity in human prostate cancer cells. Mol Cancer Ther 2004;3: 699 – 707.

28. McManus DC, Lefebvre CA, Cherton-Horvat G, et al. Loss of XIAP protein expression by RNAi and antisense approaches sensitizes cancer cells to functionally diverse chemotherapeutics. Oncogene 2004;23: 8105 – 17.

29. Horoszewicz JS, Leong SS, Kawinski E, et al. LNCaP model of human prostatic carcinoma. Cancer Res 1983;43:1809 – 18.

30. Stone KR, Mickey DD, Wunderli H, Mickey GH, Paulson DF. Isolation of a human prostate carcinoma cell line (DU 145). Int J Cancer 1978;21: 274 – 81.

31. Perez-Stable CM, Schwartz GG, Farinas A, et al. The Gγ/T-15 transgenic mouse model of androgen-independent prostate cancer: target cells of carcinogenesis and the effect of the vitamin D analog EB 1089. Cancer Epidemiol Biomarkers Prev 2002;11:555 – 63.

32. Danielpour D, Kadomatsu K, Anzano MA, Smith JM, Sporn MB. Development and characterization of nontumorigenic and tumorigenic epithelial cell lines from rat dorsal-lateral prostate. Cancer Res 1994;54: 3413 – 21.

33. D'Ippolito G, Schiller PC, Ricordi C, Roos BA, Howard GA. Age-related osteogenic potential of mesenchymal stromal stem cells from human vertebral bone marrow. J Bone Miner Res 1999;14:1115 – 22.

34. Krishan A. Rapid DNA content analysis by the propidium iodide-hypotonic citrate method. Methods Cell Biol 1990;33:121 – 5.

35. Perez-Stable C. 2-Methoxyestradiol and paclitaxel have similar effects on the cell cycle and induction of apoptosis in prostate cancer cells. Cancer Lett. In press 2005.

36. Yam CH, Fung TK, Poon RY. Cyclin A in cell cycle control and cancer. Cell Mol Life Sci 2002;59:1317 – 26.

37. King KL, Cidlowski JA. Cell cycle regulation and apoptosis. Annu Rev Physiol 1998;60:601 – 17.

38. Bruckheimer EM, Kyprianou N. Apoptosis in prostate carcinogenesis. A growth regulator and a therapeutic target. Cell Tissue Res 2000;301: 153 – 62.

39. Schultz C, Link A, Leost M, et al. Paullones, a series of cyclin-dependent kinase inhibitors: synthesis, evaluation of CDK1/cyclin B inhibition, and *in vitro* antitumor activity. J Med Chem 1999;42:2909 – 19.

40. Chao SH, Price DH. Flavopiridol inactivates P-TEFb and blocks most RNA polymerase II transcription *in vivo*. J Biol Chem 2001;276:31793 – 9.

41. Dan HC, Sun M, Kaneko S, et al. Akt phosphorylation and stabilization of X-linked inhibitor of apoptosis protein (XIAP). J Biol Chem 2004;279: 5405 – 12.

42. Voorhees PM, Dees EC, O'Neil B, Orlowski RZ. The proteasome as a target for cancer therapy. Clin Cancer Res 2003;9:6316 – 25.

43. Shen SC, Huang TS, Jee SH, Kuo ML. Taxol-induced p34cdc2 kinase activation and apoptosis inhibited by 12-*O*-tetradecanoylphorbol-13-acetate in human breast MCF-7 carcinoma cells. Cell Growth Differ 1998;9:23 – 9.

44. Roudier MP, True LD, Higano CS, et al. Phenotypic heterogeneity of end-stage prostate carcinoma metastatic to bone. Hum Pathol 2003;34: 646 – 53.

45. Shah RB, Mehra R, Chinnaiyan AM, et al. Androgen-independent prostate cancer is a heterogeneous group of diseases: lessons from a rapid autopsy program. Cancer Res 2004;64:9209 – 16.

46. Yang T, Buchan HL, Townsend KJ, Craig RW. MCL-1, a member of the BLC-2 family, is induced rapidly in response to signals for cell differentiation or death, but not to signals for cell proliferation. J Cell Physiol 1996;166:523 – 36.

47. Murillo H, Huang H, Schmidt LJ, Smith DI, Tindall DJ. Role of PI3K signaling in survival and progression of LNCaP prostate cancer cells to the androgen refractory state. Endocrinology 2001;142:4795 – 805.

48. Carson JP, Kulik G, Weber MJ. Antiapoptotic signaling in LNCaP prostate cancer cells: a survival signaling pathway independent of phosphatidylinositol 3′-kinase and Akt/protein kinase B. Cancer Res 1999;59:1449 – 53.

49. Nesterov A, Lu X, Johnson M, Miller GJ, Ivashchenko Y, Kraft AS. Elevated AKT activity protects the prostate cancer cell line LNCaP from TRAIL-induced apoptosis. J Biol Chem 2001;276:10767 – 74.

50. Dai Y, Rahmani M, Grant S. Proteasome inhibitors potentiate leukemic cell apoptosis induced by the cyclin-dependent kinase inhibitor flavopiridol through a SAPK/JNK- and NF-κB-dependent process. Oncogene 2003;22: 7108 – 22.

Sequential Combinations of Flavopiridol and Docetaxel Inhibit Prostate Tumors, Induce Apoptosis, and Decrease Angiogenesis in the Gγ/T-15 Transgenic Mouse Model of Prostate Cancer

Teresita Reiner[2], Alicia de las Pozas[1], and Carlos Perez-Stable[1, 2]

[1]Geriatric Research, Education, and Clinical Center and Research Service, VA Medical Center, Miami, Florida; [2]Department of Medicine and Sylvester Comprehensive Cancer Center, University of Miami Miller School of Medicine, Miami Florida

Request for reprints: Carlos Perez-Stable, Veterans Affairs Medical Center, GRECC (11-GRC), 1201 NW 16 Street, Miami, FL 33125. Phone: (305) 324-4455, extension 4391. E-mail: cperez@med.miami.edu.

Running Title: Combination Chemotherapy in Prostate Cancer

Grant support: Sanofi-Aventis Pharmaceuticals (GIA 60025), VA Merit Review (026901), and Department of Defense (DAMD17-03-1-0179) (C. Perez-Stable).

ABSTRACT

BACKGROUND. We investigated whether sequential combinations of flavopiridol and docetaxel can increase apoptotic cell death and inhibit the growth of primary and metastatic prostate tumors in the Gγ/T-15 transgenic mouse model of androgen-independent prostate cancer (AI-PC).

METHODS. Gγ/T-15 transgenic males were treated with flavopiridol, docetaxel, flavopiridol followed by docetaxel (FD), or docetaxel followed by flavopiridol (DF) every 3 days for two weeks. Primary and metastatic prostate tumors were weighed and the differences between mice treated with drugs and control were determined. Immunostaining for activated caspase-3, PCNA, and CD-31 was done to evaluate the differences in apoptosis, proliferation, and angiogenesis. Western blot was performed for quantitative measurements of activated caspase-3, XIAP, survivin, Bcl-xL, and Bcl-2.

RESULTS. Docetaxel was slightly more effective than flavopiridol in inhibiting primary prostate tumors, but neither drug alone inhibited metastases. The DF combination resulted in the greatest inhibition of primary prostate tumors (61%) and the FD combination provided the greatest suppression of metastases (96%) compared to control mice. Both the DF and FD regimens increased apoptosis and decreased angiogenesis more than either drug alone. The greatest effect on inhibition of primary prostate tumors in DF-treated mice was correlated with decreases in XIAP and Bcl-xL proteins, whereas the greatest effect on metastases in FD-treated mice was associated with an increase in activated caspase-3.

CONCLUSIONS. Both the DF and FD sequence combinations were effective in inhibiting AI-PC in the Gγ/T-15 transgenic mice. An increase in apoptosis and a decrease in angiogenesis resulted in the greatest inhibition of prostate cancers.

Key Words: Prostate Cancer; Transgenic Mice; Metastases; Apoptosis; Angiogenesis

INTRODUCTION

Prostate cancer is the most frequently diagnosed non-cutaneous cancer and the second leading cause of cancer-related deaths among men in the United States [1]. The principal therapy for men with advanced disease is androgen ablation, but most of these patients eventually progress to an androgen-independent disease [2]. Studies showing that treatment with docetaxel combined with prednisone can improve survival of patients with androgen-independent prostate cancer (AI-PC) have been recently reported [3]. It is likely that docetaxel combined with other novel chemotherapeutic drugs might also result in improved patient survival. Determining the efficacy of docetaxel combinations in preclinical animal models of prostate cancer is necessary before doing clinical trials. However, although traditional animal models based on prostate cancer cell lines xenografted subcutaneously into immunocompromised mice frequently respond to anti-cancer drugs, these drugs often do not show activity in clinical trials [4].

Targeting of oncogenes like SV40 T antigen (Tag) to the prostate has resulted in the development of animal models of prostate cancer that represent a more natural history of tumor development, i.e., the cancer originates from normal cells in their natural microenvironment and progresses through multiple stages, as in the case of human prostate cancer [5,6]. The TRAMP and LADY models (probasin/Tag) have been used by a variety of investigators to study the molecular events in the carcinogenesis of the prostate and in the preclinical testing of new therapies [7-16]. We have developed a unique transgenic mouse model of AI-PC (Gγ/T-15) that targets a subset of basal epithelial cells by using the human fetal Gγ-globin promoter linked to Tag [17-19]. The progression of prostate cancer in the Gγ/T-15 transgenic mice is similar to progression in humans, i.e., it originates from high-grade prostate intraepithelial neoplasia (PIN) and progresses to advanced metastatic carcinomas. We have utilized the Gγ/T-15 transgenic mice to test the efficacy against prostate cancer using EB 1089 (a less calcemic and more potent analog of 1,25-dihydroxyvitamin D_3) [19] and 2-methoxyestradiol, an estrogen metabolite [20]. It remains to be determined whether the outcome of drug efficacy in transgenic mouse models will be more predictive of clinical outcome and therefore reduce the clinical failure rates of novel chemotherapeutic drugs and their combinations.

Docetaxel (taxotere), a semi-synthetic derivative of paclitaxel (taxol) that is derived from the yew tree [21], is a promising anti-cancer drug shown to inhibit a wide variety of tumor cells including prostate cancer cells by diverse mechanisms that include cell cycle arrest, induction of apoptosis, stabilization of microtubules, and inhibition of angiogenesis [22,23]. Flavopiridol, a semisynthetic flavonoid derived from an indigenous plant from India, is a broad inhibitor of cyclin-dependent kinases (cdk) and it is being tested in clinical trials [24,25]. However, results of Phase II clinical trials of flavopiridol as a single agent have been reported to be unsatisfactory, indicating that flavopiridol may work best as an anti-cancer agent when combined with other agents [26,27]. Studies in a preclinical model of xenografted human gastric cancer cells have shown that the greatest increase in apoptosis occurs when docetaxel is followed by flavopiridol [28]. Whether flavopiridol and docetaxel can enhance apoptotic cell death in a transgenic mouse model of prostate cancer has not been previously investigated.

Treatment with single chemotherapeutic agents like flavopiridol and docetaxel will not cure most cancers, including AI-PC. We have recently reported that the human prostate cancer cell lines LNCaP and DU 145 show a heterogeneous response to the sequential combination of flavopiridol and docetaxel [29]. The purpose of the present study was to determine whether the combination of flavopiridol and docetaxel could inhibit the growth of primary and metastatic

prostate tumors in the Gγ/T-15 transgenic mice better than either drug alone. Our results show that the sequences of flavopiridol followed by docetaxel (FD) or docetaxel followed by flavopiridol (DF) produce greater apoptosis and inhibit angiogenesis better than either drug alone, leading to a significant inhibition of primary and metastatic prostate tumors. Our findings suggests that both flavopiridol and docetaxel sequence combinations should provide greater efficacy against prostate cancer than either drug alone.

MATERIALS AND METHODS

Reagents

Flavopiridol and docetaxel were obtained from Sanofi-Aventis Pharmaceuticals (Bridgewater, NJ). Flavopiridol was resuspended in PBS at 3 mg/ml, dissolved by adjusting the pH to 3.25, aliquoted, and stored at −20°C. Docetaxel was dissolved in ethanol, Tween 80 (Sigma, St. Louis, MO., USA), PBS (1:1:18, v/v/v) (final concentration of docetaxel was 1.5 mg/ml), and it was stored at −20 °C. Vehicle controls (PBS for flavopiridol and ethanol/Tween 80/PBS for docetaxel) were stored at +4°C.

Treatment of Gγ/T-15 Transgenic Males with Flavopiridol and Docetaxel

We utilized the Gγ/T-15 transgenic mouse model of AI-PC [17-19] to evaluate the antitumor effects of flavopiridol and docetaxel in vivo as single drugs and in sequence-specific combinations (flavopiridol followed by docetaxel [FD] and docetaxel followed by flavopiridol [DF]). Transgenic mice (CBA x C57) were identified by DNA slot blot analysis as previously described [17,18]. These mice, bred to homozygosity, begin to develop prostate tumors at 13 weeks of age, an earlier time than in hemizygous mice (16 weeks). Homozygous male transgenic mice were palpated 3 times per week in the urogenital region starting at 13 weeks to detect prostate tumor mass. Mice with palpable prostate tumors were randomly divided into experimental and control groups and injected i.p. every 3 days with 0.1 ml of flavopiridol (F, 10 mg/kg; n=7), docetaxel (D, 5 mg/kg; n=7), or the appropriate vehicle controls (PBS, n=7; ethanol/Tween 80/PBS, n=7) for two weeks (5 injections). Treatment with higher doses of docetaxel (15 and 30 mg/kg) resulted in deaths before the 2 week period. For sequence-specific combinations, mice with palpable prostate tumors were injected i.p. with flavopiridol followed by docetaxel 24 hours later (FD; n=9), docetaxel followed by flavopiridol 24 hours later (DF; n=10), or the appropriate vehicle controls (PBS followed by ethanol/Tween 80/PBS, n=6; ethanol/Tween 80/PBS followed by PBS, n=6). This regimen was repeated a total of 5 times over two weeks. On day 15, mice were anesthetized, blood collected by cardiac puncture, and serum stored at −80°C. Primary prostate tumors and visible metastases to the pelvic lymph nodes were removed and their weights determined. A portion of primary prostate tumor was stored at −80°C for Western blot analysis and another portion was fixed overnight in formalin for histology (H&E) and immunohistochemistry. Statistical differences between drug and control (combined controls, n=26) primary and metastatic prostate tumor weights were determined by two-tailed Student-s *t*-test, with $P<0.05$ considered significant. All animal studies were carried out with the approval of the Institutional Animal Care and Use Committee of the Miami VA Medical Center (AAALAC accredited) and conducted in accordance with the NIH Guidelines for the Care and Use of Laboratory Animals.

Change in Body Weight and Serum Chemistries

The body weights for the drug-treated and control mice were determined at the end of the

study. Serum from transgenic mice with prostate tumors treated with drugs and controls were analyzed for albumin, alanine aminotransferase (ALT) (markers of liver function), aspartate aminotransferase (AST, marker of soft tissue damage), lactate dehydrogenase (LDH), creatine phosphokinase (CPK) (markers of cardiac and skeletal muscle damage), and alkaline phosphatase (ALKP, marker of kidney, intestine, liver, and bone damage) using a Vitros 250 chemistry analyzer (Ortho Clinical Diagnostics, Rochester, NY). Bile acids (liver function) were measured by radioimmunoassay (MP Biomedicals, Orangeburg, NY).

Histology and Immunohistochemistry

After fixation of primary prostate tumor overnight in 10% buffered formalin, samples were dehydrated, embedded in paraffin, sectioned at 5 μm, and baked at 55°C overnight. Control and drug-treated prostate tumor sections were stained with H&E. For immunostaining, endogenous peroxides were blocked using 3% H_2O_2 in methanol for 5 minutes. Antigen retrieval was done by incubating sections in hot 10 mM citrate buffer (pH 6.0) for 20 minutes. Immunostaining for PCNA was performed using a 1/100 dilution of mouse monoclonal antibody to PCNA (PC10; Santa Cruz Biotechnology, Santa Cruz, CA) and the Vector Mouse on Mouse (M.O.M.) Peroxidase Kit (Vector Laboratories, Burlingame, CA) following the manufacturer=s instructions. Immunostaining for cleaved caspase-3 (Cell Signaling Technology, Beverly, MA) and Ki67 (NCL-Ki67p; Vision BioSystems Inc., Norwell, MA) was performed using a 1/100 dilution of rabbit polyclonal antibody and a 1/100 dilution of biotinylated goat anti-rabbit IgG secondary antibody (Vector Laboratories). Specific color was developed with the Vector ABC kit and 3,3=-diaminobenzidine (DAB) substrate kit (Vector Laboratories) and the sections were counterstained with hematoxylin, dehydrated, and glass cover slipped. For the negative controls, we used the same concentration of mouse and rabbit IgG (Santa Cruz Biotechnology) instead of specific primary antibodies, which resulted in no immunostaining. For the TUNEL (terminal deoxynucleotidyl transferase [TdT]-mediated deoxyuridinetriphosphate [dUTP] nick end-labeling) technique, we used hot citrate antigen retrieval and the In Situ Cell Death Detection Kit, POD (Roche Applied Sciences, Indianapolis, IN) following the manufacturer=s instructions.

Western Blot Analysis

Total protein lysates from prostate tumors was prepared by resuspending frozen tissues in NP40 cell lysis buffer (1% NP-40, 50 mM Tris, pH 8.0, 150 mM NaCl, 2 mM EGTA, 2 mM EDTA, protease inhibitor tablet, 50 mM NaF, and 0.1 mM $NaVO_4$), lysed in a glass homogenizer, left on ice for 30 minutes, and centrifuged. The protein concentrations of the supernatant were determined with the Bio-Rad protein assay. After separation of 50-100 μg protein by SDS-PAGE, proteins were transferred by electrophoresis to Immobilon-P membrane and incubated in 5% nonfat dry milk, PBS, and 0.25% Tween-20 for 1 hour. Antibodies specific for cleaved caspase-3, XIAP (Cell Signaling Technology), Bcl-xL (polyclonal; BD Biosciences Pharmingen, San Diego, CA), survivin (FL-142), and Bcl-2 (N-19) (Santa Cruz Biotechnology) were diluted 1/3,000 in 5% nonfat dry milk, PBS, and 0.25% Tween-20 and incubated overnight at 4°C. Membranes were washed in PBS and 0.25% Tween-20 and incubated with the appropriate horseradish peroxidase-conjugated secondary antibody (1/3,000 dilution; Santa Cruz Biotechnology) for 1 hour, washed in PBS and 0.25% Tween-20, and analyzed by exposure to X-ray film using enhanced chemiluminescence plus (ECL plus, Amersham Pharmacia Biotech, Arlington Heights, IL USA). Antibodies specific for β-tubulin (TU-02; 1;3,000 dilution; Santa Cruz Biotechnology) were used as protein loading controls. X-ray films were scanned using an

Epson Perfection 2450 Photo scanner and the pixel intensity measured using UN-SCAN-IT digitizing software, version 5.1 (Silk Scientific Corp, Orem, UT USA). The changes in cleaved caspase-3, XIAP, survivin, Bcl-xL, and Bcl-2 protein levels in drug-treated and control prostate tumors were determined by normalizing the values to tubulin from the same Western blot.

Blood Vessel Density

Sections of prostate tumor were processed as described above and immunostained for CD-31 (PECAM) using a 1/50 dilution of goat polyclonal antibody (M20; Santa Cruz Biotechnology) and a 1/100 dilution of biotinylated rabbit anti-goat IgG secondary antibody (Vector Laboratories). Specific color was developed as described above. Blood vessel density was determined by counting the number of CD-31 positive vessels from four random high powered fields (x400) of each section. Four to five tumors were analyzed for each group.

Statistical Analysis

Statistical differences between drug-treated and control prostate tumors were determined by two-tailed Student-s *t*-test with $P<0.05$ considered significant.

RESULTS

Primary and Metastatic Prostate Tumors in Gγ/T-15 Transgenic Mice

The Gγ/T-15 transgenic mice contain the human fetal Gγ-globin promoter linked to SV40 T antigen, which targets a subset of basal epithelial cells present in the normal prostate. These mice develop AI-PC and metastasis to the pelvic lymph nodes [17-19]. At between 13 to 26 weeks of age, >75% of the transgenic males develop palpable primary prostate tumors. The peak of tumor incidence occurs at 19 weeks and the weights of the palpable prostate tumors range from 0.1 to 0.2 grams. After a period of 2-3 weeks, the primary prostate tumors grow rapidly and metastasize to the pelvic lymph nodes to form visible lesions (Fig. 1). Using the Gγ/T-15 transgenic mouse system, we previously determined the anti-tumor efficacy of vitamin D analog EB 1089 [19] and 2-methoxyestradiol [20].

Flavopiridol and Docetaxel as Single Chemotherapeutic Drugs in Gγ/T-15 Mice

We used the Gγ/T-15 mice to test the efficacy of flavopiridol and docetaxel as single chemotherapeutic drugs and in combination. Gγ/T-15 males with palpable prostate tumors were treated every three days with flavopiridol (F, 10 mg/kg), docetaxel (D, 5 mg/kg), or the appropriate controls for a period of two weeks. The primary and metastatic prostate tumors were weighed and the results are shown in Fig. 2. Treatment of mice with flavopiridol caused a 16% decrease in the weights of primary prostate tumors compared to control mice (n=7; $P=0.33$) and treatment with docetaxel resulted in a 32% decrease in the weights of primary prostate tumors (n=7; $P=0.09$). Neither drug decreased the weights of metastatic prostate tumors compared to control mice. Although inhibition of primary tumors by single drugs was not statistically significant, there was a trend for docetaxel to be more effective than flavopiridol, similar to what is observed in the treatment of human AI-PC [30]

Flavopiridol and Docetaxel Sequence Combinations Inhibit Primary and Metastatic Prostate Tumors in Gγ/T-15 Mice

We have shown that the simultaneous addition of flavopiridol and docetaxel to human DU 145 prostate cancer cells results in antagonism with respect to induction of apoptosis, compared to each drug alone [29]. Therefore, a sequential addition of flavopiridol and docetaxel

is required for maximal induction of apoptosis. Our in vitro data indicate that treatment of human LNCaP prostate cancer cells with flavopiridol for 24 hours followed by docetaxel for another 24 hours (FD) induces apoptosis more effectively than docetaxel followed by flavopiridol (DF). In contrast, the DF sequence is more effective to induce apoptosis compared to the FD sequence in the DU 145 prostate cancer cells [29]. The results show that the DF sequence decreases the weights of primary prostate tumors in Gγ/T-15 mice by 61% compared to control mice (n=10; $P<0.0003$) and the FD sequence reduces primary prostate tumors by 43% (n=9; $P<0.02$). Although the average weights of the primary prostate tumors were smaller in the DF sequence compared to the FD sequence, the differences were not significant ($P=0.08$). There was a significant difference between DF (but not FD) treatment and the single drug treatments with flavopiridol and docetaxel ($P<0.04$).

Only 1 of 9 FD treated mice (11%) developed metastatic prostate tumors, resulting in a 96% decrease in tumor weights compared with control mice ($P<0.05$). In DF treated mice, 5/10 (50%) developed metastatic prostate tumors, but the overall average tumor weights were not significantly different from control mice ($P=0.20$). Metastatic prostate tumors developed in 93% of control mice (24/26) and 86% of F and D treated mice (12/14). Overall, the results in the Gγ/T-15 mice indicate that: 1) the DF sequence was more effective in inhibiting primary prostate tumors; 2) the FD sequence more effectively suppressed metastatic prostate tumors; and 3) both the DF and FD sequences had greater efficacy against prostate cancer compared with single drugs alone.

Treatment with Flavopiridol and Docetaxel is Not Toxic in Gγ/T-15 Mice

To determine in the Gγ/T-15 mice if treatment with flavopiridol, docetaxel, and their sequence combinations is toxic, we measured the body weights and serum chemistry, and compared these values to those in control mice. There were no significant differences in final body weights in drug-treated compared to control mice (not shown). In addition, serum chemistry measuring soft tissue damage (liver, muscle, and kidney) shows no significant differences between drug-treated and control mice (Table 1). One significant difference was lower serum alkaline phosphatase in mice treated with flavopiridol, possibly due to a specific effect on the alkaline phosphatase gene or the tissues synthesizing alkaline phosphatase (liver, bone, etc). Overall, these results indicate that treatment of the Gγ/T-15 mice with flavopiridol, docetaxel, and their sequence combinations does not result in acute toxicity. However, differences in pharmacokinetics between mice and humans make it difficult to extrapolate these toxicity results clinically.

Increase in Apoptosis without a Decrease in Cell Proliferation in Gγ/T-15 Prostate Tumors Treated with FD and DF

We investigated whether the decrease in the weights of the primary prostate tumors in the FD and DF treatment groups were due to increases in apoptosis and/or decreases in cell proliferation. Immunostaining for the DNA proliferation marker PCNA revealed no obvious differences between drug-treated and control prostate tumors (Fig. 3). A prostate duct embedded within the control tumor showed no immunostaining for PCNA. Similar results were also obtained by immunostaining for the proliferation marker Ki67 (not shown). Results with the in situ TUNEL peroxidase method showed a greater number of apoptotic cells in the DF compared to the control tumors (Fig. 3). Finally, a greater number of cells in FD-treated Gγ/T-15 prostate tumors were immunostained by an antibody specific for the cleaved and activated form of

caspase-3 (Fig. 3). Overall, these results suggest that the FD and DF-treated primary prostate tumors were smaller because there was greater apoptosis without significant changes in cell proliferation.

Decreases in XIAP and Bcl-xL Proteins in DF-treated Gγ/T-15 Prostate Tumors

To further investigate why the FD and DF-treated Gγ/T-15 primary prostate tumors had decreased weights compared to controls, we sought to identify by Western blot analysis the differences in the levels of proteins important in apoptosis (Figs. 4 and 5). The results showed a 6.5- and 2.1-fold greater level of cleaved caspase-3 in FD and DF treated prostate tumors, respectively, compared to control prostate tumors. In F- and D-treated prostate tumors, there was a 1.7 and 1.4-fold increase in cleaved capsase-3 compared to control prostate tumors. The levels of cleaved caspase-3 detected by Western blot correlated with the levels identified by immunohistochemistry.

XIAP is a member of the IAP family that binds caspase-3, inhibits its activity, and blocks apoptosis [31,32]. Prostate tumors treated with D and DF showed a small but consistent decrease (27 and 29%; $P<0.05$) in total XIAP protein, whereas there was a 58% increase in F- ($P<0.01$) and no change in FD-treated prostate tumors (Figs. 4 and 5). There were no significant changes in the levels of survivin, which is also a member of the IAP family [31,32], in any treatment groups (not shown). We also measured the levels of Bcl-xL and Bcl-2, anti-apoptotic members of the Bcl-2 family that increase with progression of prostate cancer [32]. F- and DF-treated prostate tumors show a small but consistent decrease (18 and 22%; $P<0.02$) in total Bcl-xL protein, whereas there were no significant changes in prostate tumors treated with D and FD. There were no significant modifications in Bcl-2 protein in any treatment group (not shown). Overall, these results suggest that the inhibition of the growth of primary prostate tumors induced by the DF regimen correlates with lower levels of XIAP and Bcl-xL proteins and the inhibition of the growth of metastases in the FD combination can be correlated with higher levels of activated (cleaved) caspase-3 in primary prostate tumors.

Inhibition of Angiogenesis in DF- and FD-treated Gγ/T-15 Prostate Tumors

We investigated whether treatment of Gγ/T-15 mice with F, D, FD, and DF results in the inhibition of angiogenesis by immunostaining for CD31 (PECAM) (Fig. 6). Results show that treatment with F and D as single drugs significantly inhibited the number of blood vessels compared to control prostate tumors (F, 6.0 ± 1.9 and D, 7.1 ± 2.3 versus control, 14 ± 4.8 CD31 positive blood vessels per high powered field; $P<6 \times 10^{-5}$). Treatment with FD and DF also inhibited the number of blood vessels compared to controls (FD, 4.0 ± 1.3; DF, 4.7 ± 1.6; $P<5 \times 10^{-7}$). There were significantly fewer blood vessels in FD-treated compared to F- and D-treated prostate tumors ($P<0.002$). In DF-treated prostate tumors, there were significantly less blood vessels compared to D-treated ($P< 0.006$) but not compared to F-treated ($P=0.06$) prostate tumors. These results indicate that the combination of FD and DF inhibits angiogenesis more than each drug alone.

DISCUSSION

We evaluated in the Gγ/T-15 transgenic mouse model of AI-PC whether the combination of flavopiridol and docetaxel can inhibit the growth of primary and metastatic prostate tumors better than either drug alone. Our results indicate that the regimen docetaxel followed by

flavopiridol (DF) is more effective in inhibiting primary prostate tumors and that the flavopiridol followed by docetaxel (FD) sequence is better at decreasing metastases (Fig. 2). An increase in apoptosis is a likely reason for smaller prostate tumors in the FD and DF regimens (Fig. 3). The highest levels of cleaved (activated) caspase-3 in the FD group could be correlated with a reduction in metastases and a decrease in the anti-apoptosis proteins XIAP and the Bcl-xL in the DF group correlated with smaller primary prostate tumors (Figs. 4 and 5). There was a better inhibition of angiogenesis in the FD- and DF treated groups compared to single drugs (Fig. 6). Overall, our results indicate that in the Gγ/T-15 transgenic mice both sequence combinations of flavopiridol and docetaxel are more effective in reducing primary and metastatic prostate tumors than either drug alone.

There is a strong probability that docetaxel combined with other chemotherapeutic drugs would result in an improved inhibition of prostate cancer cell growth. A previous study using the subcutaneous xenografts of MKN-74 human gastric cancer cells in nude mice showed that the DF regimen is more effective than FD in decreasing tumor growth [28]. These results are similar to the flavopiridol and paclitaxel or epothilone B regimens in gastric and breast cancer cell lines in vitro, i.e., paclitaxel or epothilone B followed by flavopiridol can increase apoptosis more than the inverse sequence combination [33,34]. In contrast, our in vitro studies show that the LNCaP prostate cancer cells are more sensitive to the FD regimen, whereas the DU 145 prostate cancer cells are more sensitive to the DF sequence combination [29]. These results suggest a heterogeneous response to the DF or FD combination sequence depending on the type of prostate cancer cell. In the Gγ/T-15 transgenic mouse prostate tumors, the expression of Tag results in the inactivation of p53 and Rb, a cellular phenotype similar to that in DU 145 cells [36]. Although Gγ/T-15 prostate tumors are poorly differentiated, these tumors express androgen receptors (AR), similarly to LNCaP cells [19]. It is likely that in Gγ/T-15 prostate tumors, a heterogeneous mixture of prostate cancer cells like DU 145 (sensitive to DF) and LNCaP (sensitive to FD) is present. This offers an explanation why both sequence combinations have efficacy against prostate cancer. This heterogeneous mixture of cancer cells is most likely absent in xenograft models of cancer cell lines grown in vitro.

The induction of apoptosis is a requirement for the effect of chemotherapeutic drugs on prostate cancer cells [37]. Our results in the Gγ/T-15 mice demonstrate that the greatest efficacy against prostate cancer occurs when apoptosis increases in the FD and DF regimens (Figs 4 and 5). Although the FD and DF sequence combinations inhibit proliferation of prostate cancer cells and have an effect on the cell cycle in vitro [29], neither sequence combination had a significant effect on cell proliferation in Gγ/T-15 prostate tumors (Fig. 3). Most anticancer drugs appear to exert their therapeutic effect by decreasing proliferation and increasing apoptosis [38]. Anticancer regimens like FD and DF that are not dependent on a significant decrease in cell proliferation to increase apoptosis in vivo may have a therapeutic advantage in slow growing tumors like prostate cancer [39]. In addition, there is a correlation with an increase in activated caspase-3 and a decrease in metastases in the FD treatment group (Figs. 2-4). This suggests that chemotherapy that increases apoptosis will result in a decrease in metastases [40]. Transgenic models of prostate cancer like Gγ/T-15 are more useful in testing the effect of combination chemotherapy on metastases, compared to subcutaneous xenograft models, which rarely metastasize.

We have recently shown that a substantial decrease in XIAP, but not in survivin protein,

both being members of the Inhibitor of Apoptosis (IAP) family, correlates with enhancement of apoptosis by FD in LNCaP prostate cancer cells [29]. In the Gγ/T-15 mice, the D and DF regimens show a small, but significant decrease in total XIAP protein in primary prostate tumors (Figs. 4 and 5), whereas there were no significant changes in survivin protein in any treatment group (not shown). XIAP is upregulated in most types of cancer, including AI-PC, and confers resistance to chemotherapeutic drugs [41,42]. Targeted downregulation of XIAP increases the sensitivity of cancer cells, including that of AI-PC cells, to a variety of chemotherapeutic drugs [41-44]. The combination of chemotherapeutic drugs that results in the greatest decrease in XIAP protein may lead to the highest efficacy against prostate cancer. However, the greatest decrease of XIAP protein in single DF-treated mice did not always correlate with an increase in activated caspase-3 or with the smallest prostate tumors, suggesting that other factors are also important in mediating the effect against prostate cancer.

Flavopiridol reduces the levels of the anti-apoptotic proteins Bcl-2 and Bcl-xL and sensitizes cancer cells to apoptosis after subsequent treatment with other chemotherapeutic agents [35]. Our results show that treatment of Gγ/T-15 mice with F and DF results in a small, but significant decrease in Bcl-xL (but not Bcl-2) proteins in primary prostate tumors (Figs. 4 and 5). However, similarly to results with XIAP, a decrease in Bcl-xL protein in single DF-treated mice did not always correlate with higher cleaved caspase-3 and smaller prostate tumors, suggesting that other factors may be important. Our results do not provide a specific mechanism to distinguish the differential effects of the DF and FD regimens on primary and metastatic prostate tumors. The molecular identification of the factors that mediate the inhibition of primary and metastatic prostate tumors in FD- and DF-treated Gγ/T-15 mice could be better addressed by gene expression microarray studies.

The inhibition of angiogenesis is an important mechanism in increasing the anticancer efficacy of chemotherapeutic drugs [45]. In Gγ/T-15 mice, both flavopiridol and docetaxel as single drugs significantly inhibited angiogenesis compared to controls (Fig. 6). These results support previous results showing that flavopiridol and docetaxel can inhibit angiogenesis and suggest that this may be an important mechanism for inhibiting tumor growth [46,47]. However, the inhibition of angiogenesis without an increase in apoptosis did not result in a significant reduction in the weights of primary and metastatic prostate tumors in flavopiridol and docetaxel treated Gγ/T-15 mice. The FD and DF regimens increase apoptosis and further inhibit angiogenesis, resulting in a significant reduction in the weights of primary and metastatic prostate tumors. These results suggest that drug combinations that increase apoptosis and decrease angiogenesis to the greatest extent will provide the greatest antitumor effect.

Two of the features of cancer that are essential for the progressive growth and expansion of solid tumors are the evasion of apoptosis and the formation of new blood vessels by angiogenesis [48]. Our results in the Gγ/T-15 transgenic mouse model of AI-PC indicate that either the FD or DF regimen can simultaneously increase apoptosis and inhibit angiogenesis, providing the greatest efficacy against prostate cancer.

ACKNOWLEDGEMENTS

We thank Drs. Andrew Schally and Diana Brassard for the review of this manuscript and helpful suggestions. We also thank Carolyn Cray for assistance and advice on the chemistry of

mouse serum. This research was supported by grants from Sanofi-Aventis Pharmaceuticals, VA Merit Review, and the Department of Defense, all to C. Perez-Stable.

REFERENCES

1. Jemal A, Murray T, Ward E, Samuels A, Tiwari R, Ghafoor A, Feuer EJ, Thun MJ. Cancer Statistics, 2005. CA Cancer J Clin 2005;55:10-30.
2. So A, Gleave M, Hurtado-Col A, Nelson C. Mechanisms of the development of androgen independence in prostate cancer. World J Urol 2005;23:1-9.
3. Tannock IF, de Wit R, Berry WR, Horti J, Pluzanska A, Chi KN, Oudard S, Theodore C, James ND, Turesson I, Rosenthal MA, Eisenberger MA; TAX 327 Investigators. Docetaxel plus prednisone or mitoxantrone plus prednisone for advanced prostate cancer. N Engl J Med 2004;351:1502-1512.
4. Johnson JI, Decker S, Zaharevitz D, Rubinstein LV, Venditti JM, Schepartz S, Kalyandrug S, Christian M, Arbuck S, Hollingshead M, Sausville EA. Relationships between drug activity in NCI preclinical in vitro and in vivo models and early clinical trials. Br J Cancer 2001;84:1424-1431.
5. Abate-Shen C, Shen MM. Mouse models of prostate carcinogenesis. Trends Genet 2002;18:S1-5.
6. Kasper S. Survey of genetically engineered mouse models for prostate cancer: analyzing the molecular basis of prostate cancer development, progression, and metastasis. J Cell Biochem 2005;94:279-297.
7. Greenberg NM, DeMayo F, Finegold MJ, Medina D, Tilley WD, Aspinall JO, Cunha GR, Donjacour AA, Matusik RJ, Rosen JM. Prostate cancer in a transgenic mouse. Proc Natl Acad Sci 1995;92:3439-3443.
8. Kasper S, Sheppard PC, Yan Y, Pettigrew N, Borowsky AD, Prins GS, Dodd JG, Duckworth ML, Matusik RJ. Developmental progression and androgen-dependence of prostate tumors in probasin-large T antigen transgemc mice: a model for prostate cancer. Lab Invest 1998;78:319-333.
9. Polnaszek N, Kwabi-Addo B, Peterson LE, Ozen M, Greenberg NM, Ortega S, Basilico C, Ittmann M. Fibroblast growth factor 2 promotes tumor progression in an autochthonous mouse model of prostate cancer. Cancer Res 2003;63:5754-5760.
10. Pflug BR, Pecher SM, Brink AW, Nelson JB, Foster BA. Increased fatty acid synthase expression and activity during progression of prostate cancer in the TRAMP model. Prostate 2003;57:245-254.
11. Huss WJ, Hanrahan CF, Barrios RJ, Simons JW, Greenberg NM. Angiogenesis and prostate cancer: identification of a molecular progression switch. Cancer Res 2001;61:2736-2743.
12. Klezovitch O, Chevillet J, Mirosevich J, Roberts RL, Matusik RJ, Vasioukhin V. Hepsin promotes prostate cancer progression and metastasis. Cancer Cell 2004;6:185-195.
13. Man S, Bocci G, Francia G, Green SK, Jothy S, Hanahan D, Bohlen P, Hicklin DJ, Bergers G, Kerbel RS. Antitumor effects in mice of low-dose (metronomic) cyclophosphamide administered continuously through the drinking water. Cancer Res 2002;62:2731-2735.
14. Huss WJ, Barrios RJ, Greenberg NM. SU5416 selectively impairs angiogenesis to induce prostate cancer-specific apoptosis. Mol Cancer Ther 2003;2:611-616.

15. Huss WJ, Lai L, Barrios RJ, Hirschi KK, Greenberg NM. Retinoic acid slows progression and promotes apoptosis of spontaneous prostate cancer. Prostate 2004;61:142-152.
16. Gupta S, Adhami VM, Subbarayan M, MacLennan GT, Lewin JS, Hafeli UO, Fu P, Mukhtar H. Suppression of prostate carcinogenesis by dietary supplementation of celecoxib in transgenic adenocarcinoma of the mouse prostate model. Cancer Res 2004;64:3334-3343.
17. Perez-Stable C, Altman NH, Brown J, Cray C, Harbison M, Roos BA. Prostate, adrenocortical, and brown adipose tumors in fetal globin/T antigen transgenic mice. Lab Invest 1996;74:363-373.
18. Perez-Stable C, Altman NH, Mehta PP, Deftos LJ, Roos BA. Prostate cancer progression, metastasis, and gene expression in transgenic mice. Cancer Res 1997;57:900-906.
19. Perez-Stable CM, Schwartz GG, Farinas A, Finegold M, Binderup L**,** Howard GA, Roos BA. The Gγ/T-15 transgenic mouse model of androgen-independent prostate cancer: target cells of carcinogenesis and the effect of the vitamin D analog EB 1089. Cancer Epi Bio Prev 2002;11: 555-563.
20. Qadan LR, Perez-Stable CM, Anderson C, D'Ippolito G, Herron A, Howard GA, Roos BA. 2-Methoxyestradiol induces G2/M arrest and apoptosis in prostate cancer. Biochem Biophys Res Commun 2001;285:1259-1266.
21. Bissery MC, Nohynek G, Sanderink GJ, Lavelle F. Docetaxel (Taxotere7): a review of preclinical and clinical experience. Part I: preclinical experience. Anticancer Drugs 1995; 6:339-355.
22. Pienta KJ. Preclinical mechanisms of action of docetaxel and docetaxel combinations in prostate cancer. Semin Oncol 2001;28:3-7.
23. Herbst RS, Khuri FR. Mode of action of docetaxel - a basis for combination with novel anticancer agents. Cancer Treat Rev 2003;29:407-415.
24. Zhai S, Senderowicz AM, Sausville EA, Figg WD. Flavopiridol, a novel cyclin-dependent kinase inhibitor, in clinical development. Ann Pharmacother 2002;36: 905-911.
25. Shapiro GI. Preclinical and clinical development of the cyclin-dependent kinase inhibitor flavopiridol. Clin Cancer Res 2004;10:4270s-4275s.
26. Schwartz GK, Ilson D, Saltz L, O'Reilly E, Tong W, Maslak P, Werner J, Perkins P, Stoltz M, Kelsen D. Phase II study of the cyclin-dependent kinase inhibitor flavopiridol administered to patients with advanced gastric carcinoma. J Clin Oncol 2001;9:1985-1992.
27. Liu G, Gandara DR, Lara PN Jr, Raghavan D, Doroshow JH, Twardowski P, Kantoff P, Oh W, Kim K, Wilding G. A Phase II trial of flavopiridol (NSC #649890) in patients with previously untreated metastatic androgen-independent prostate cancer. Clin Cancer Res 2004;10:924-928.
28. Motwani M, Rizzo C, Sirotnak F, She Y, Schwartz GK. Flavopiridol enhances the effect of docetaxel in vitro and in vivo in human gastric cancer cells. Mol Cancer Ther 2003;2:549-555.
29. Gomez A, de las Pozas A, Perez-Stable C.Sequential combination of flavopiridol and docetaxel reduces the levels of XIAP and AKT proteins and stimulates apoptosis in human LNCaP prostate cancer cells. Mol. Cancer Therapeutics 2006, in press.
30. Logothetis CJ. Docetaxel in the integrated mangement of prostate cancer. Current applications and future promise. Oncology (Huntingt.) 2002;16:63-72.

31. Liston P, Fong WG, Korneluk RG. The inhibitors of apoptosis: there is more to life than Bcl2. Oncogene 2003;22:8568-8580.
32. Schimmer AD. Inhibitor of apoptosis proteins: translating basic knowledge into clinical practice. Cancer Res 2004;64:7183-7190.
33. Krajewska M, Krajewski S, Epstein JI, Shabaik A, Sauvageot J, Song K, Kitada S, Reed JC. Immunohistochemical analysis of bcl-2, bax, bcl-X, and mcl-1 expression in prostate cancers. Am J Pathol 1996;148:1567-1576.
34. Motwani M, Delohery TM, Schwartz GK. Sequential dependent enhancement of caspase activation and apoptosis by flavopiridol on paclitaxel-treated human gastric and breast cancer cells. Clin Cancer Res 1999;5:1876-1883.
35. Wittmann S, Bali P, Donapaty S, Nimmanapalli R, Guo F, Yamaguchi H, Huang M, Jove R, Wang HG, Bhalla K. Flavopiridol down-regulates antiapoptotic proteins and sensitizes human breast cancer cells to epothilone B-induced apoptosis. Cancer Res 2003;63:93-99.
36. Webber MM, Bello D, Quader S. Immortalized and tumorigenic adult human prostatic epithelial cell lines: characteristics and applications. Part 3. Oncogenes, suppressor genes, and applications. Prostate 1997;30:136-142.
37. Bruckheimer EM, Kyprianou N. Apoptosis in prostate carcinogenesis. A growth regulator and a therapeutic target. Cell Tissue Res 2000;301:153-162.
38. Klein S, McCormick F, Levitzki A. Killing time for cancer cells. Nat Rev Cancer 2005; 5:573-580.
39. Berges RR, Vukanovic J, Epstein JI, CarMichel M, Cisek L, Johnson DE, Veltri RW, Walsh PC, Isaacs JT. Implication of cell kinetic changes during the progression of human prostatic cancer. Clin. Cancer Res 1995;1:473-480.
40. Chan DC, Earle KA, Zhao TL, Helfrich B, Zeng C, Baron A, Whitehead CM, Piazza G, Pamukcu R, Thompson WJ, Alila H, Nelson P, Bunn PA Jr. Exisulind in combination with docetaxel inhibits growth and metastasis of human lung cancer and prolongs survival in athymic nude rats with orthotopic lung tumors. Clin Cancer Res 2002;8:904-912.
41. Tamm I, Kornblau SM, Segall H, Krajewski S, Welsh K, Kitada S, Scudiero DA, Tudor G, Qui YH, Monks A, Andreeff M, Reed JC. Expression and prognostic significance of IAP-family genes in human cancers and myeloid leukemias. Clin Cancer Res 2000;6:1796-1803.
42. Krajewska M, Krajewski S, Banares S, Huang X, Turner B, Bubendorf L, Kallioniemi OP, Shabaik A, Vitiello A, Peehl D, Gao GJ, Reed JC. Elevated expression of inhibitor of apoptosis proteins in prostate cancer. Clin Cancer Res 2003;9:4914-4925.
43. Amantana A, London CA, Iversen PL, Devi GR. X-linked inhibitor of apoptosis protein inhibition induces apoptosis and enhances chemotherapy sensitivity in human prostate cancer cells. Mol Cancer Ther 2004;3:699-707.
44. McManus DC, Lefebvre CA, Cherton-Horvat G, St-Jean M, Kandimalla ER, Agrawal S, Morris SJ, Durkin JP, Lacasse EC. Loss of XIAP protein expression by RNAi and antisense approaches sensitizes cancer cells to functionally diverse chemotherapeutics. Oncogene 2004;23:8105-8117.
45. Neri D, Bicknell R. Tumour vascular targeting. Nat Rev Cancer 2005;5:436-446.
46. Rapella A, Negrioli A, Melillo G, Pastorino S, Varesio L, Bosco MC. Flavopiridol inhibits vascular endothelial growth factor production induced by hypoxia or picolinic acid in human

neuroblastoma. Int J Cancer 2002;99:658-664.
47. Sweeney CJ, Miller KD, Sissons SE, Nozaki S, Heilman DK, Shen J, Sledge GW Jr. The antiangiogenic property of docetaxel is synergistic with a recombinant humanized monoclonal antibody against vascular endothelial growth factor or 2-methoxyestradiol but antagonized by endothelial growth factors. Cancer Res 2001;61:3369-3372.
48. Hanahan D, Weinberg RA. The hallmarks of cancer. Cell 2000;100:57-70.

Table I. Serum chemistry from Gγ/T-15 transgenic males treated with flavopiridol (F), docetaxel (D), flavopiridol followed by docetaxel (FD), docetaxel followed by flavopiridol (DF), and vehicle controls.

Mice + Drug	N[1]	Albumin g/dL	AST U/L	LDH U/L	CPK U/L	ALKP U/L	ALT U/L	Bile Acids μmol/L
Controls	19	2.23 (0.49)[2]	377 (213)	8335 (5563)	3911 (3961)	58.8 (16.7)	63.9 (31.9)	7.5 (8.65)
F, 10mg/kg	7	1.86 (0.45)	273 (167)	6425 (2597)	2224 (2563)	*42.3 (12.4)	78.9 (80.7)	5.89 (4.18)
D, 5mg/kg	7	1.9 (0.47)	372 (149)	5868 (3084)	3354 (2582)	63.7 (25.6)	70.4 (29.6)	4.93 (3.26)
FD	8	2.45 (0.64)	337 (188)	6251 (1764)	4034 (4890)	47.1 (34.3)	65.8 (34.5)	4.13 (1.64)
DF	8	2.05 (0.59)	294 (131)	7700 (6608)	4110 (4309)	46.8 (18)	61.5 (29)	17.9 (25.3)

[1] Numbers of mice.

[2] Numbers in parenthesis refers to standard deviations.

* $P<0.03$.

Figure 1

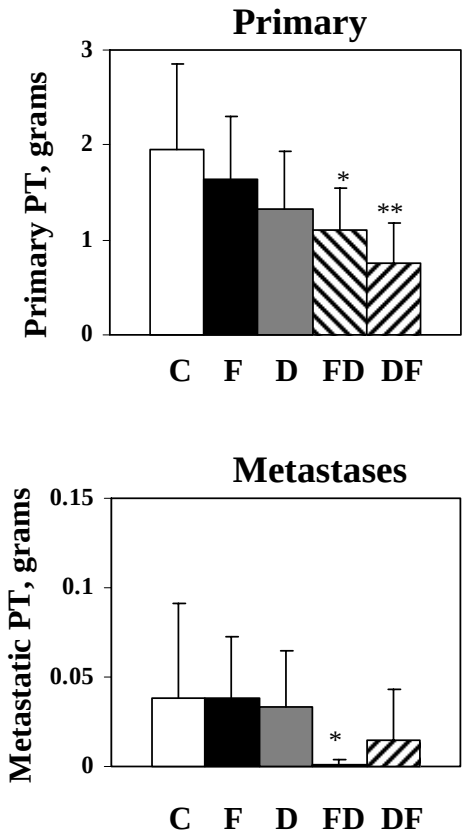
Primary
Primary PT, grams
3
2
1
0
*
**
C
F
D
FD
DF
Metastases
Metastatic PT, grams
0.15
0.1
0.05
0
*
C
F
D
FD
DF

Figure 2

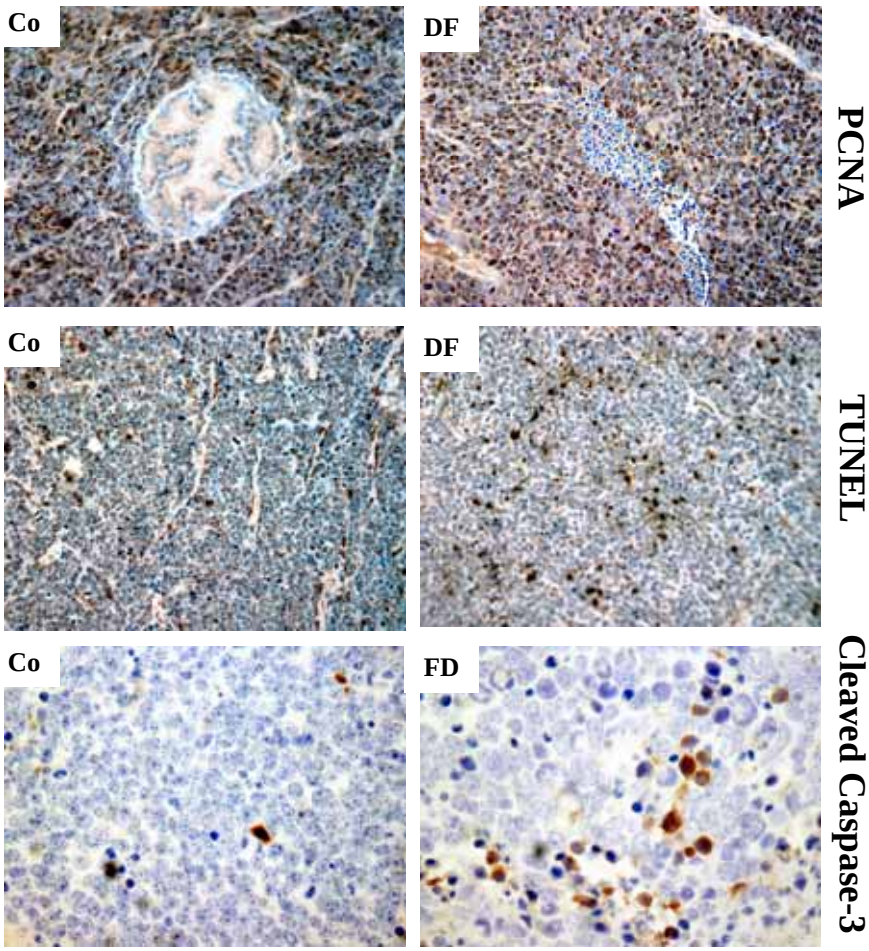

Figure 3

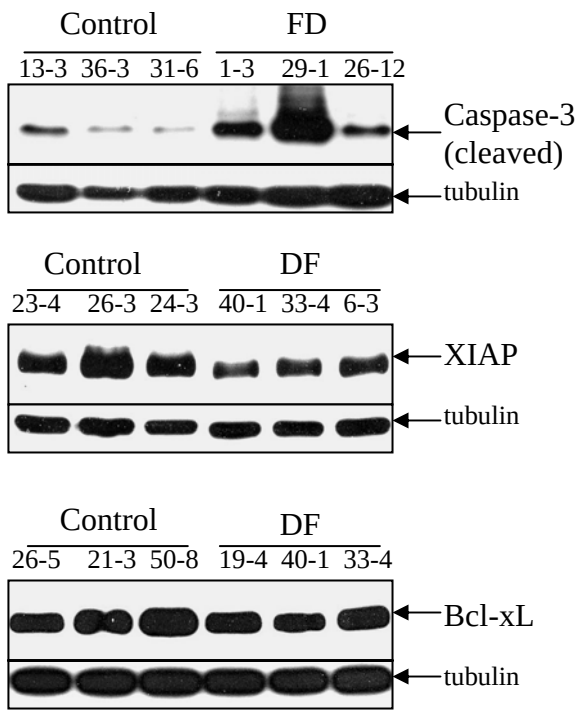
Control
FD
13-3 36-3 31-6 1-3 29-1 26-12
Caspase-3
(cleaved)
tubulin
Control
DF
23-4 26-3 24-3 40-1 33-4 6-3
XIAP
tubulin
Control
DF
26-5 21-3 50-8 19-4 40-1 33-4
Bcl-xL
tubulin

Figure 4

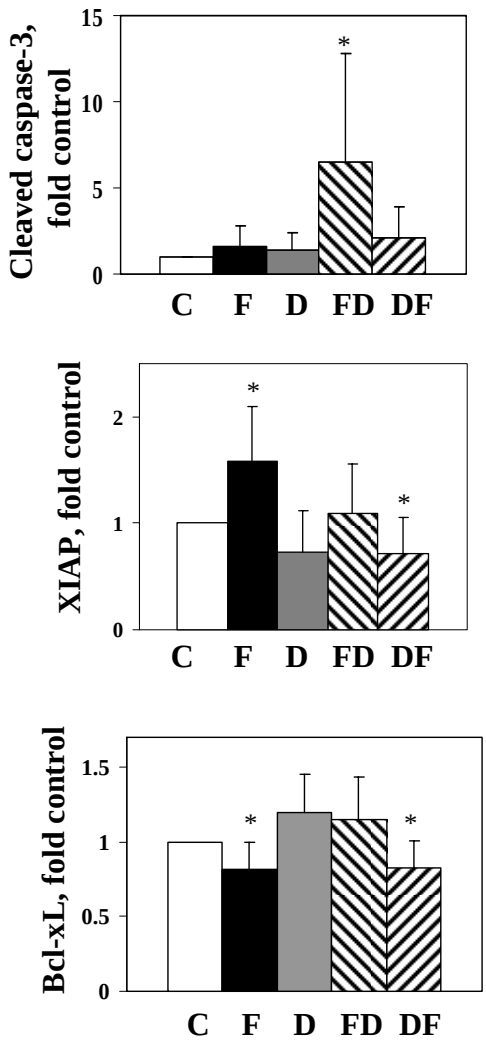
Cleaved caspase-3, fold control
15
10
5
0
*
C F D FD DF
XIAP, fold control
2
1
0
*
*
C F D FD DF
Bcl-xL, fold control
1.5
1
0.5
0
*
*
C F D FD DF

Figure 5

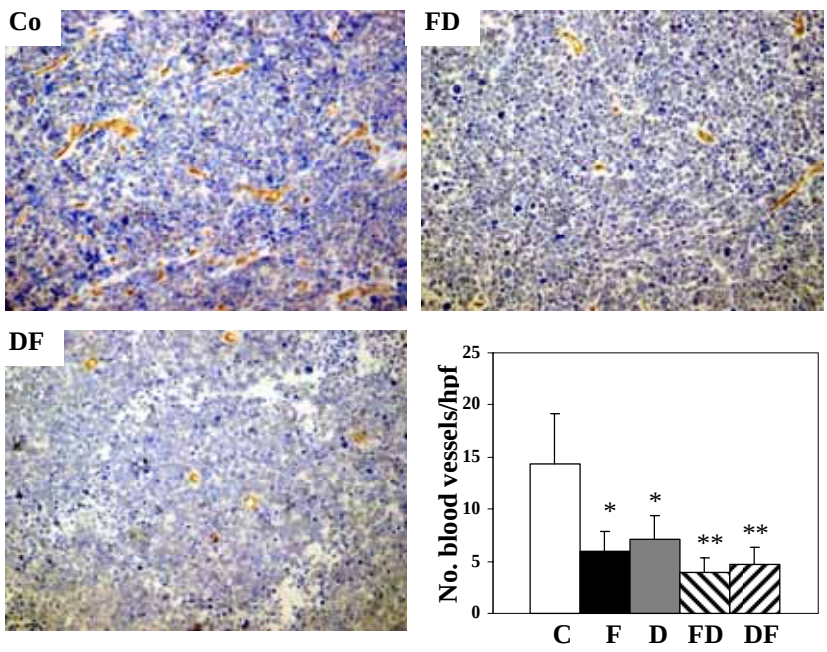

Figure 6